Investigating the roles of the JC virus agnogene and regulatory region using a naturally occurring, pathogenic viral isolate

Investigating the roles of the JC virus agnogene and regulatory region using a naturally occurring, pathogenic viral isolate

A dissertation presented

by

Laura Christine Ellis

to

The Division of Medical Sciences

in partial fulfillment of the requirements

for the degree of

Doctor of Philosophy

in the subject of

Virology

Harvard University

Cambridge, Massachusetts

April 2014

Dissertation Advisor: Dr. Igor Koralnik Laura Christine Ellis

Investigating the roles of the JC virus agnogene and regulatory region using a naturally occurring, pathogenic viral isolate

Abstract

Progressive Multifocal Leukoencephalopathy (PML) is caused by lytic infection of oligodendrocytes by JC Virus (JCV). JCV Encephalopathy (JCVE) is a newly identified disease characterized by JCV infection of cortical pyramidal neurons. JCV_{CPN} was isolated from the brain of a JCVE patient. JCV_{CPN} contains a unique 143 base pair deletion in the agnogene and has an archetype-like regulatory region (RR), of the type typically found in the kidneys. In this dissertation, we studied the JCV_{CPN} virus to better understand the role of the agnogene and the RR in JCV replication. We used kidney, glial and neuronal cell lines to compare the replication of JCV_{CPN} to the prototype virus JCV_{Mad-1}. JCV_{CPN} was able to replicate viral DNA in all cell lines tested, but was unable to establish the high level of infection seen with JCV_{Mad-1}. Levels of VP1 capsid protein were undetectable in JCV_{CPN} transfected cells, and few infectious virions were produced. JCV_{CPN} did not have a replication advantage in the neuronal cell line tested. To determine if the agnogene deletion or the archetype-like RR was responsible for the observed phenotype of JCV_{CPN}, we generated a series of chimeric viruses between JCV_{CPN} and JCV_{Mad-1}. We found that the phenotype of JCV_{CPN} was due predominantly to the deletion in the agnogene, in particular the loss of the DNA and not the lack of a

full length agnoprotein. To further study the role of the agnogene DNA in JCV replication, we introduced a series of small agnogene deletions into a virus with a start codon mutation which prevents agnoprotein expression. We characterized the replication of these additional mutants and found that nucleotides 376-396 are crucial for the expression of VP1 capsid protein. Previous studies have provided evidence for the binding of host cell proteins to the agnogene DNA. We used DNA-Immunoprecipitations with the agnogene to identify candidate binding proteins, but were unable to confirm any candidate proteins as binding specifically to the JCV agnogene. Studying this naturally occurring pathogenic variant of JCV provided a valuable tool for understanding the functions of the agnogene and RR form in JCV replication.

ACKNOWLEDGMENTS

There are many people who I need to thank for support and encouragement throughout my time in graduate school.

First, thank you to my advisor Igor Koralnik, for supporting me throughout my dissertation research and for valuable discussion and advice.

I also need to thank my dissertation advisory committee, Jim DeCaprio, Dana Gabuzda and Fred Wang, for helpful advice, discussions and intellectual input.

Thank you to the past and present members of the Koralnik lab: Shruti Agnihotri, Stephanie Batson, Evelyn Bord, Tom Broge, Spyridon Chalkias, Xin Dang, Sarah Gheuens, Michael Khoury, Gabriel Lerner, Matt McKenzie, Liz Norton, Sabrina Tan and Chris Wuthrich. You offered helpful and interesting conversations, both scientific and otherwise, and made the lab a fun place to work. A special thanks to Liz, for helping with protocol troubleshooting and sample processing.

Thank you to the Virology Program and my fellow Virology graduate students, in particular my Vironaut cohort, for support and friendship. You've made my time here at Harvard a lot of fun.

Thank you to my previous mentors, Brian Murphy, Ann-Marie Cruz, Anne Fausto-Sterling, Jürgen Kreyling and Randy Morse, for getting me started and supporting me early in my research career.

A big thanks to my friends here in Boston for filling my free time with fun activities. To Kevin McCarthy and Victor Lum for being great roommates. To my climbing partners and friends for great times on the cliffs and elsewhere. To Erik Guldbech for being supportive and encouraging, and for going on awesome adventures with me.

Finally, I need to thank my family. To my parents for unconditional love, support and encouragement throughout my entire education, and for getting me interested in science. Thanks Mom, for the encouragement throughout my years here, and for all the food and baked goods! To my sister, Karen, and brother, Joe, for being the best siblings anyone could ask for.

TABLE OF CONTENTS

FIGURES AND TABLES

CHAPTER 1: INTRODUCTION

JC VIRUS

The human polyomavirus JC Virus (JCV) is in the polyomaviridae family, and is the etiological agent of Progressive Multifocal Leukoencephalopathy (PML). Polyomaviruses are small non-enveloped DNA viruses with a circular double stranded DNA genome. This family also includes the human polyomavirus BK Virus (BKV), which causes BKV nephropathy, and Simian Virus 40 (SV40). JCV is 75% homologous to BKV and 69% homologous to SV40 (1). Since 2007, numerous new polyomaviruses have been discovered in humans, non-human primates and other species. In 2007, KI polyomavirus (KIPyV) and WU polyomavirus (WUPyV) were isolated from respiratory tract samples (2, 3). In 2008, Merkel cell polyomavirus (MCPyV) was isolated from a human Merkel cell carcinoma (4). Since then, HPyV6, HPyV7, Trichodysplasia spinulosa-associated virus (TSPyV), HPyV9, HPyV10, MWPyV, MxPyV, and Saint Louis polyomavirus (STLPyV) have been isolated from human samples (5-11). Some of these viruses, such as JCV, BKV, MCPyV and TSPyV, have been associated with human diseases (4, 6, 12). Others have not, and may be non-pathogenic. This family of viruses will certainly continue to grow as new viruses and associated diseases are identified.

Genome Organization, Proteins and Virion Structure

The first full JCV sequence was published in 1984 (1). This sequence was named Mad-1, after Madison, Wisconsin, where it was isolated. It is the most commonly used prototype JCV strain in *in vitro* studies. The genome of JCV_{Mad-1} is 5,130 nucleotides long, and contains three regions (Figure 1.1). The early region

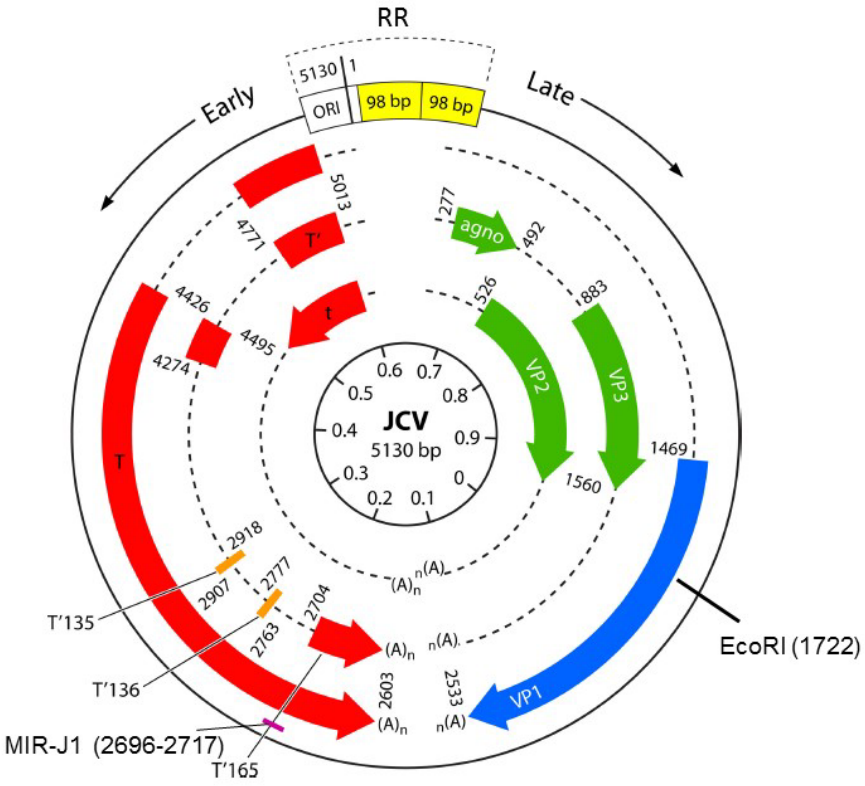

Figure 1.1 Schematic of JCV genome organization. This diagram shows the JCV_{Mad-1} genome. The early region is transcribed in the counter clockwise direction and encodes the Large T Ag, small t ag and T' proteins T'135, T'136 and T'165. The late region is transcribed in the clockwise direction and encodes the structural proteins VP1, VP2 and VP3 and the agnoprotein. The RR contains the origin of replication (ORI) and early and late promoters. The location of the JCV miRNA MIR-J1 is indicated. The unique EcoRI site used for cloning is indicated at 1722. (Adapted from Ferenzy et al. 2012 (14)).

encodes the early regulatory proteins, Large T Antigen (T Ag) and small t antigen (t ag). Three additional T forms, T'135, T'136 and T'165 have been identified as being expressed from alternatively spliced early transcripts (13). The late region encodes the structural proteins VP1, VP2 and VP3, as well as the agnoprotein, which was named due to the unknown nature of its function. Finally, the regulatory region (RR) contains the origin of replication and the promoters for the early and late transcripts. The early and late coding regions are highly conserved and the RR is hypervariable (14, 15).

Large T Ag is a multifunctional phosphoprotein that is involved in numerous processes important for viral replication. Large T Ag is involved in the modulation of both viral DNA replication initiation and activation of late gene transcription through interactions with host cell proteins (16-19). Large T Ag can bind to the JCV origin of replication, which activates replication of the viral genome (20, 21). It has a helicase domain which acts to unwind the viral genome during replication (20). Large T Ag autoregulates its own expression by binding to the RR and down regulating early gene expression (21). It has the ability to transform cells by altering cell cycle regulation (20). Large T Ag can bind to the host cell protein Rb, which induces expression of the S phase cellular genes required for viral replication (22). SV40 Large T Ag can substitute for JCV Large T Ag during replication in cell culture. Many of the JCV-permissive cell lines are transformed with SV40 Large T Ag. Small t ag promotes the expression of host cell genes involved in cell survival and promotes entry into S phase of the cell cycle (23).

The structural proteins VP1, VP2 and VP3 are expressed from the late region of the virus, and form the capsid of the viral particle. VP1 capsid proteins form pentamers, each of which is associated with one monomer of either VP2 or VP3 (24). Seventy-two of these pentamers make up the viral capsid, which contains the viral genome packaged as a mini-chromosome on host-cell histones (Figure 1.2A) (14, 24). JCV virions have a T=7 icosahedral symmetry and are 42 nm in diameter (Figure 1.2B) (24). VP2 and VP3 have been shown to be essential for JCV propagation, and likely play a role in virion assembly (25, 26). In addition to the capsid proteins, the agnoprotein is expressed from the leader region of the late transcript (27). It is a multifunctional,

auxiliary protein which plays a role in viral processes, such as regulation of DNA replication and gene expression, and alters host cell processes (27).

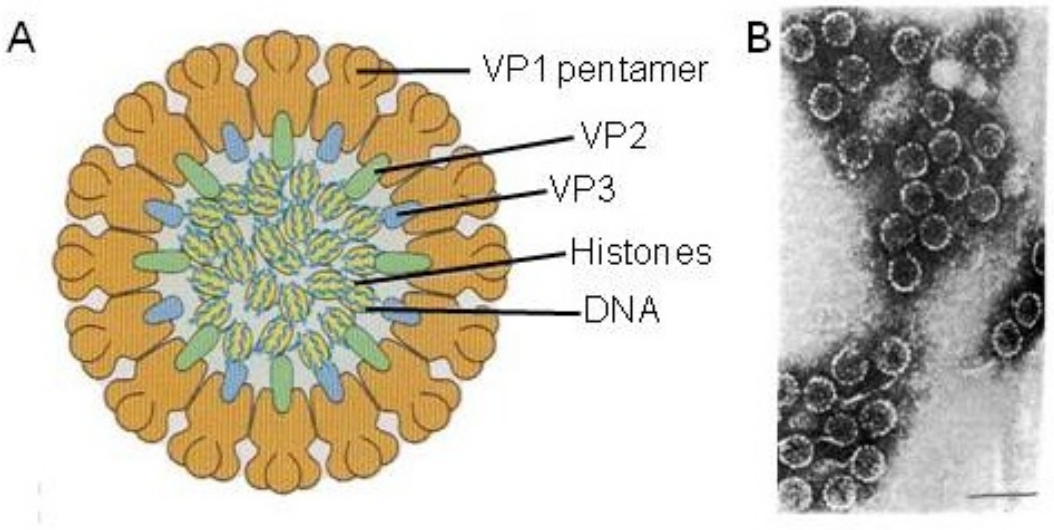

Figure 1.2 The JCV virion. (A) The JCV virion is made up of 72 pentamers of VP1, each of which is associated with one monomer of VP2 or VP3. The DNA genome is packaged as a mini-chromosome on host cell histones. (Adapted from Flint et al. 2004 (31)). (B) Negative Stain of JCV virions in primary human fetal glial cells. Bar is 100nm. (Adapted from Padgett et al. 1971 (47)).

Replication Cycle

JCV infection begins with binding of the virion to receptors on the cell surface (Figure 1.3). The 2,6-linked glycan, lactoseries tetrasaccharide c (LSTc) acts as the attachment factor for JCV (28). The JCV cellular receptor is the serotonin receptor 5HT-2α, which facilitates JCV entry (29, 30). Following receptor binding, JCV is internalized through clathrin-mediated endocytosis. The virion is then trafficked to the early endosome, the late endosome and finally the endoplasmic reticulum (ER) (14). From the ER, the virus enters the cytoplasm and then the nucleus (14, 31). The virus then uncoats, and the early coding region is transcribed leading to the production of Large T Ag and small t ag. Large T Ag activates replication of the viral genomic DNA

and transcription of the late coding region, leading to the production of the structural proteins VP1, VP2 and VP3 and the agnoprotein. The structural proteins are transported into the nucleus where they encapsidate viral genomes to form mature viral particles. These virions then exit the nucleus and are released from the cell (14).

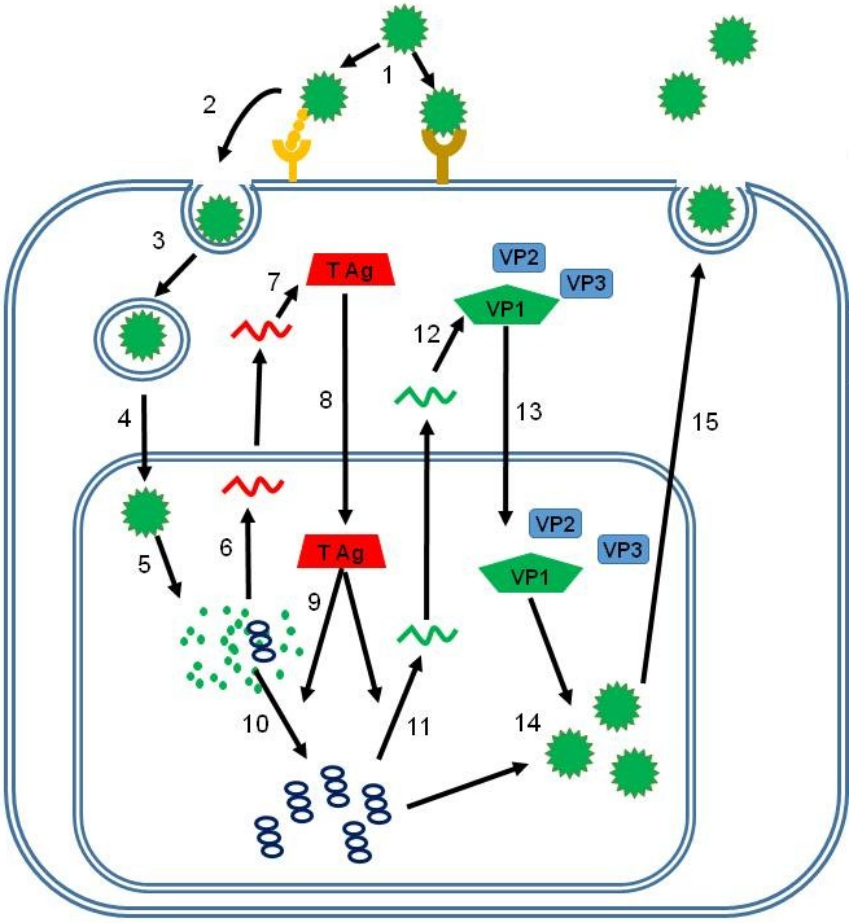

Figure 1.3 JCV Replication Cycle. JCV binds to the 5HT-2α receptor and the attachment factor LSTc (1) and enters the cell through clathrin-mediated endocytosis (2). The virus is trafficked through the early endosome, late endosome and endoplasmic reticulum (3). The virus enters the nucleus (4) and uncoats (5). Early mRNA is transcribed from the viral DNA and transported into the cytoplasm (6). Large T Ag and small t ag are translated from the early transcript (7). Large T Ag is transported to the nucleus where it actives viral DNA replication and production of the late transcript (9-11). The late transcript is transported into the cytoplasm and VP1, VP2 and VP3 are produced (12). The capsid proteins are transported into the nucleus (13) and viral particles are formed (14). These virions are released from the nucleus and the cell (15).

JCV Tropism and RR Variation

Polyomaviruses exhibit highly species and tissue-specific patterns of infection. Much of this specificity is due to variations in the structure of the RR of the viruses. JCV exhibits tropism for kidney epithelial cells and oligodendrocytes (32). More recently, JCV has been found to also infect neurons (33, 34).

The RR of JCV is hypervariable and can display unique changes in each individual (35). The sequence elements which make up different forms of the RR can be defined as 6 blocks of sequences, called A-F (Figure 1.4) (35-38). Analysis of the sequence of different forms of the RR from individuals has led to hypotheses on how the virus emerges from latency and becomes pathogenic. The kidneys and urine usually contain JCV with a well conserved, non-pathogenic RR which is called the "archetype" (Figure 1.4) (39). This form contains one copy of each of the elements A-F. The 23-base pair (bp) B block and 66-bp D block are also referred to as the 23-bp insert and 66-bp insert, respectively. Some forms of the RR may be classified as "archetype-like" when they have only one copy of the A, C and E blocks, but also have mutations in these blocks or the insert blocks B and D. The JCV RR detected in the brain and the cerebrospinal fluid (CSF) of PML patients usually has duplications, tandem repeats, and deletions, and has been called "rearranged" compared to the archetype (Figure 1.4). The prototype rearranged strain is Mad-1, which contains 2 repeats of a 98-bp element made up of the A, C and E blocks followed by one F block (37, 38).

The RR controls transcription of both the early and late genes, and contains binding sites for host cell transcription factors. The expression of both the early and late

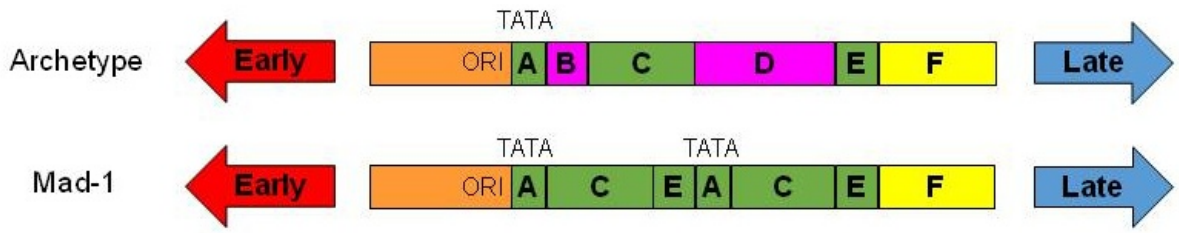

Figure 1.4 Schematic of Mad-1 versus Archetype RR. The JCV RR can be divided into 6 blocks (A-F). Archetype is usually found in the kidneys and urine, and is made up of one copy each of Blocks A-F. Mad-1 is the prototype rearranged form, which is generally found in the brain and CSF of PML patients and is made up of 2 repeats Blocks A,C and E followed by 1 Block F. TATA boxes and the origin of replication (ORI) are labeled. (Adapted from Marshall et al. 2010 (38)).

genes is dependent on the interactions between the RR sequence and these transcription factors. Numerous transcription factors have been shown to activate viral transcription, including NF-1, Oct-6/tst-1/SCIP, DDX1, NFAT4, EGF-1, YB-1, Pur-α, LCP-1, GF-1, Sp1 and Spi-B. Conversely, AP-1, C/EBPb and NF-1A have been shown to repress transcription. Different forms of the regulatory region have different numbers and types of transcription factor binding sites, which is thought to contribute to the neurotropism and neurovirulence of JCV (38).

Although it is not clear which form of JCV RR is present at the time of primary infection, it has been hypothesized that JCV with archetype RR remains confined in the kidneys of most healthy individuals. Rearrangements which confer neurotropism are thought to occur prior to viral migration to the brain where glial cells and neurons are infected. The RR of JCV, with its transcription control factor binding sites, is closely associated with pathogenesis, with rearranged forms correlating with poor clinical outcome in PML patients (40).

miRNAs in JCV replication

The first mirocRNA (miRNA) of a polyomavirus was identified in SV40 by Sullivan et al. based on miRNA precursors predicted by a computer algorithm (41). They identified a precursor miRNA located on the late pre-mRNA in the untranslated region 3' to the polyadenylation cleavage site, which produces 5 miRNAs. The miRNAs are expressed late in infection, and were found to target the early SV40 mRNA, resulting in down regulation of early mRNA expression. While the loss of these miRNAs did not negatively affect virion production, it was found to increase the Cytotoxic T lymphocyte (CTL) response against T Ag, indicating that these miRNAs may play a role in immune evasion (41).

These miRNAs were also predicted to be present in JCV and BKV. A follow up study found that both JCV and BKV expressed a pre-miRNA similar to the previously studied SV40 pre-miRNA (41, 42). These are also processed into miRNAs targeting the same sequence in the early mRNA (41, 42). The JCV miRNAs downregulate T Ag expression, and were shown to be present in the brain tissue of PML patients (42). Further study found that the 3p arm miRNA produced by JCV and BKV downregulates the expression of UL16 binding protein 3 (ULBP3), a ligand for activation of NK cell cytotoxicity (43). This may function as an immune evasion mechanism during JCV and BKV infection (43). Prevention of the expression of these miRNAs in BKV has also been shown to cause an increase in early mRNA and protein levels in archetype BKV, but not rearranged BKV (44). Loss of the miRNA gave archetype BKV the ability to replicate in a cell line which normally only replicates rearranged BKV, indicating that this miRNA can also regulate viral replication (44).

JCV AND HUMAN DISEASE

Progressive Multifocal Leukoencephalopathy

PML was first described in 1958 in patients with hematological malignancies who also had multiple sites of demyelinating disease in the brain (45). In 1965, electron microscopy (EM) demonstrated the presence of papovavirus-like particles in PML lesions, leading to a hypothesis that PML was caused by a viral infection (46). JCV was first isolated in 1971 from the brain of a patient with PML through inoculation of PML brain extract onto primary human fetal glial cells (47). It was given the name JC after the initials of the patient it was isolated from (47). EM revealed the presence of virions in cell nuclei in the pattern of a crystalline array similar to that seen with SV40 and the virus was classified as a papovavirus, which is now the polyomavirus family (47).

PML is a demyelinating disease of the white matter of the central nervous system (CNS) caused by lytic infection of oligodendrocytes and astrocytes by JCV (12). Neurological symptoms vary depending on the area of demyelination in the brain, and include aphasia, cognitive dysfunction, sensory deficits, weakness and coordination difficulties. 18% of PML patients will also develop seizures. PML is usually diagnosed through magnetic resonance imaging (MRI), brain biopsy and/or polymerase chain reaction (PCR) for JCV in the CSF. Brain lesions are detected by MRI as hyperintense regions in the white matter on some MRI sequences, and there are often multiple lesions present in one patient (Figure 1.5A). PML diagnosis is confirmed either through the detection of JCV by in situ hybridization (ISH) for JCV DNA or immunohistochemistry (IHC) staining for JCV proteins on a brain biopsy sample, or through a positive JCV PCR in the CSF. PML is characterized in histological samples

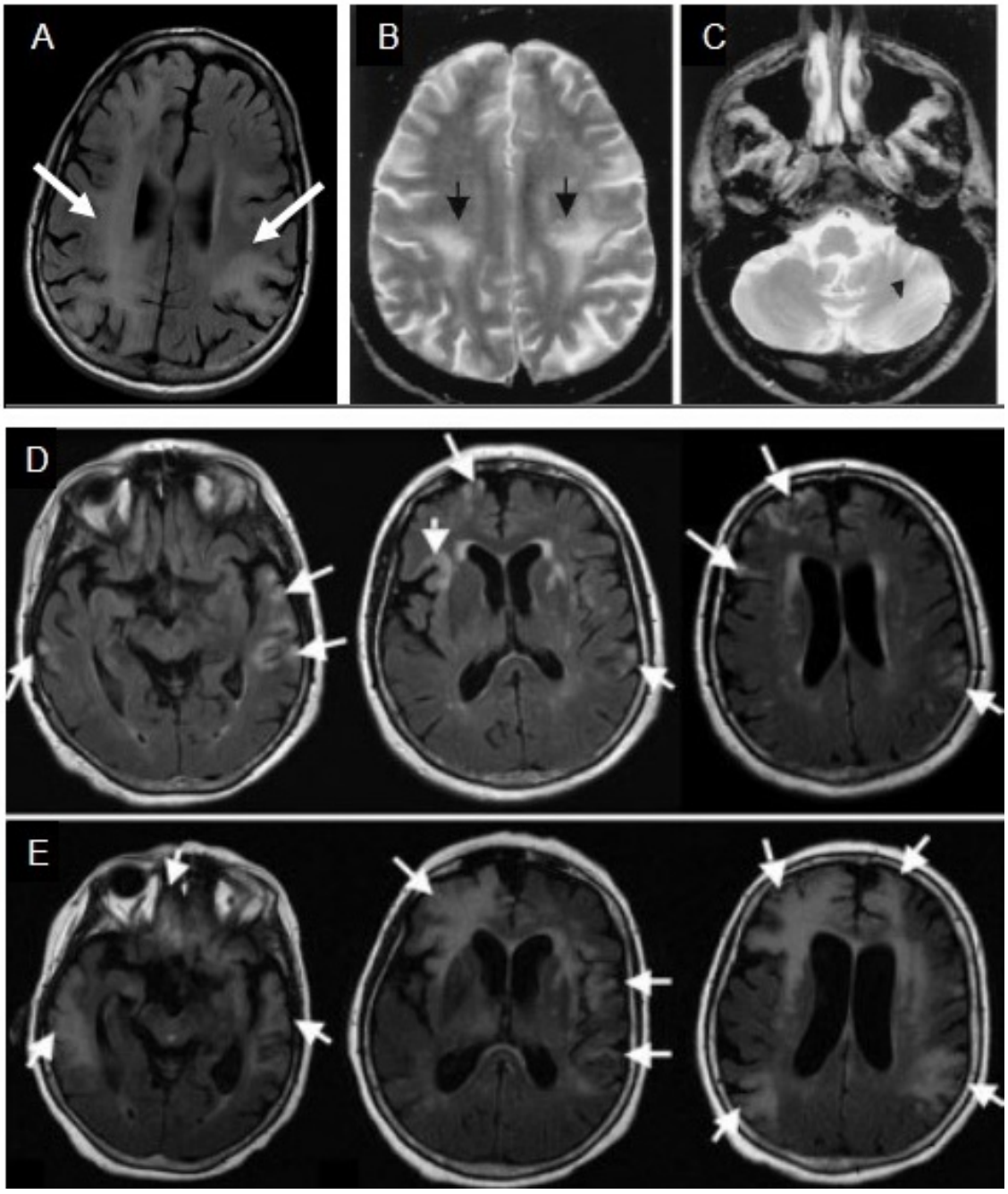

Figure 1.5 MRI of PML, JCV GCN and JCVE brains. (A) Fluid-attenuated inversion recovery (FLAIR) MRI of a typical PML brain. Arrows indicate lesions in the white matter. (B and C) T2-weighted MRI images of JCV GCN brain showing (B) subcortical hyperintensities and (C) mild cortical atrophy in both cerebellar hemispheres. (Adapted from Du Pasquier et al 2003 (67)). (D and E) FLAIR MRI images of JCVE brain at diagnosis (D) and 3 months later (E). (D) Areas of hyperintensity are seen in temporal, parietal and frontal cortex. (E) Additional cortical areas are affected and the hyperintense signal extends into the subcortical white matter (Adapted from Wuthrich et al. 2009 (34)).

by lytic infection of oligodendrocytes and astrocytes in areas of demyelination, and enlarged oligodendrocytes and giant, bizarre multinucleated astrocytes (12, 15).

PML primarily occurs in the setting of severe cellular immune suppression, such as in patients with hematological malignancies, organ transplants and chronic inflammatory conditions. Before the development of highly active antiretroviral therapy (HAART), up to 5% of acquired immunodeficiency syndrome (AIDS) patients developed PML (48). Recently, a new risk group has emerged in patients taking immunomodulatory drugs such as natalizumab (49-51), rituximab (52) and efalizumab (53, 54). Up to 3.50 in 1000 patients taking natalizumab for multiple sclerosis (MS) develop PML and 437 patients have been diagnosed to date (55). PML can also occur in individuals with occult or minimal immune suppression, such as individuals with alcoholic cirrhosis or pregnant women (56).

There are currently no known antiviral drugs specific to JCV. Studies have tested cytarabine (57, 58), cidofovir (59), and mefloquine (12), but did not show significant benefit with treatment. Since the identification of the serotonin receptor, 5HT-2α, as the cellular receptor for JCV, some patients are being treated with the serotonin receptor inhibitor mirtazapine, although there is not solid clinical evidence to indicate this is efficacious (15, 60). PML patients are therefore treated with measures to restore the function of the immune system in the hopes that the immune system will control JCV infection. Combination antiretroviral therapy (cART) is used with Human Immunodeficiency Virus (HIV)-positive PML patients, while HIV-negative patients may be treated with the reduction of immunosuppressive medications if possible (19).

PML is a fatal disease, but with improved treatments, more patients are surviving for extended periods. Risk factors that influence survival have been identified, such as CD4+ T cell count (61), viral load in the CSF (62, 63), Human Leukocyte Antigen (HLA) type (64), and the magnitude of the cellular immune response to JCV (65).

JCV Granule Cell Neuronopathy

Recently, two new syndromes caused by JCV infection in the CNS have been identified. The first of these is JCV Granule Cell Neuronopathy (JCV GCN) (66). With PML, demyelination results from lytic infection of oligodendrocytes, whereas JCV GCN occurs when JCV infects and destroys the granule cell neurons in the cerebellum (67). The first case of JCV GCN was the first time that JCV infection of neurons was observed.

JCV GCN was first identified in an HIV-1 positive patient who presented with cerebellar dysfunction. They had lesions in the white matter of the frontal lobes and cerebellar atrophy identified by MRI (Figure 1.5B and 1.5C). Disease progressed and the patient died after 6 months. Autopsy revealed both lesions in the white matter typical of PML and tissue destruction in the internal granule cell layer (IGCL) of the cerebellum. Granule cell neurons were identified by staining with Map-2 and NeuN, and were found to be positive for JCV VP1. ISH indicated that there were also granule cell neurons that were positive for JCV DNA but did not express VP1 protein. Additionally, EM demonstrated the presence of 40 nm polyomavirus particles in these cells (67). Sequencing of the DNA extracted from frozen brain samples from this patient indicated that both the strains from the white matter (JCV_{HWM}) and the granule cell neurons

(JCV_{GCN1}) had a rearranged RR (68). JCV_{GCN1}, but not JCV_{HWM}, also had a 10 bp deletion in the c-terminal region of the VP1 gene, resulting in a frame shift and change in amino acid sequence (68).

Since the identification of the first case, multiple additional patients, both HIV-positive and HIV-negative, have been diagnosed with JCV GCN, both with and without the presence of classic PML in the patient's brain (66, 67, 69-75). To date, there have been two cases of JCV GCN diagnosed in MS patients treated with natalizumab (55). Patients with JCV GCN present with cerebellar dysfunctions, such as incoordination, gait ataxia and dysarthria, due to the area of the brain affected with JCV GCN (12). A retrospective study of archival PML brain samples found that up to 51% have granule cell neurons infected by JCV (33). Sequencing of DNA samples from additional JCV GCN patients found that they also contained deletions or mutations in the VP1 c-terminal region, suggesting that alteration of the C terminus of the VP1 protein is somehow involved in JCV infection of granule cell neurons and the development of JCV GCN (69).

JCV Encephalopathy

JCV Encephalopathy (JCVE) was first identified in a 74-year-old HIV-negative woman who presented with progressive aphasia and global cognitive decline, and cortical gray matter lesions on MRI (Figure 1.5D) (34). She had a history of non-small cell lung cancer treated with chemotherapy. A biopsy of the right frontal brain stained positive for JCV and PCR of the CSF confirmed the presence of JCV in the CNS. An MRI taken three months later showed new areas with cortical lesions and lesions now

extended into the subcortical white matter (Figure 1.5E). The patient experienced worsening of her neurological symptoms and developed seizures. She passed away 4 1/2 months after the onset of symptoms. Autopsy samples were obtained for further study (34).

Postmortem analysis of the brain found laminar necrosis in both subcortical white matter and deep cortical layers. Giant multinucleated astrocytes and pyramidal neurons with enlarged nuclei were seen throughout the cortex and at the gray-white junction (GWJ) (Figure 1.6A and 1.6B). IHC staining demonstrated JCV infection at areas of tissue necrosis at the GWJ and areas of cell loss in the cortex (Figure 1.6C and 1.6D). JCV infected astrocytes were observed in the cortex and at the GWJ. Few infected oligodendrocytes were seen, and there was limited demyelination present. Many of the JCV positive cells were not oligodendrocytes, and double immunofluorescence (IF) staining with the neuronal marker MAP-2 and either JCV T Ag or VP1 showed that JCV infected many neurons in the brain, specifically cortical pyramidal neurons (Figure 1.6E and 1.6F). Infection of neurons by JCV was confirmed by staining with NeuN (Figure 1.7). JCV proteins were found in the cytoplasm and nucleus, as well as in the axons and dendritic processes of the neurons (Figure 1.7B and 1.7C). This finding was novel in that it is the first time JCV has been found to infect cortical pyramidal neurons. qPCR for JCV in frozen cortical samples containing lesions had a high viral load, with a mean of 4.6×10^8 copies/μg of brain DNA (34).

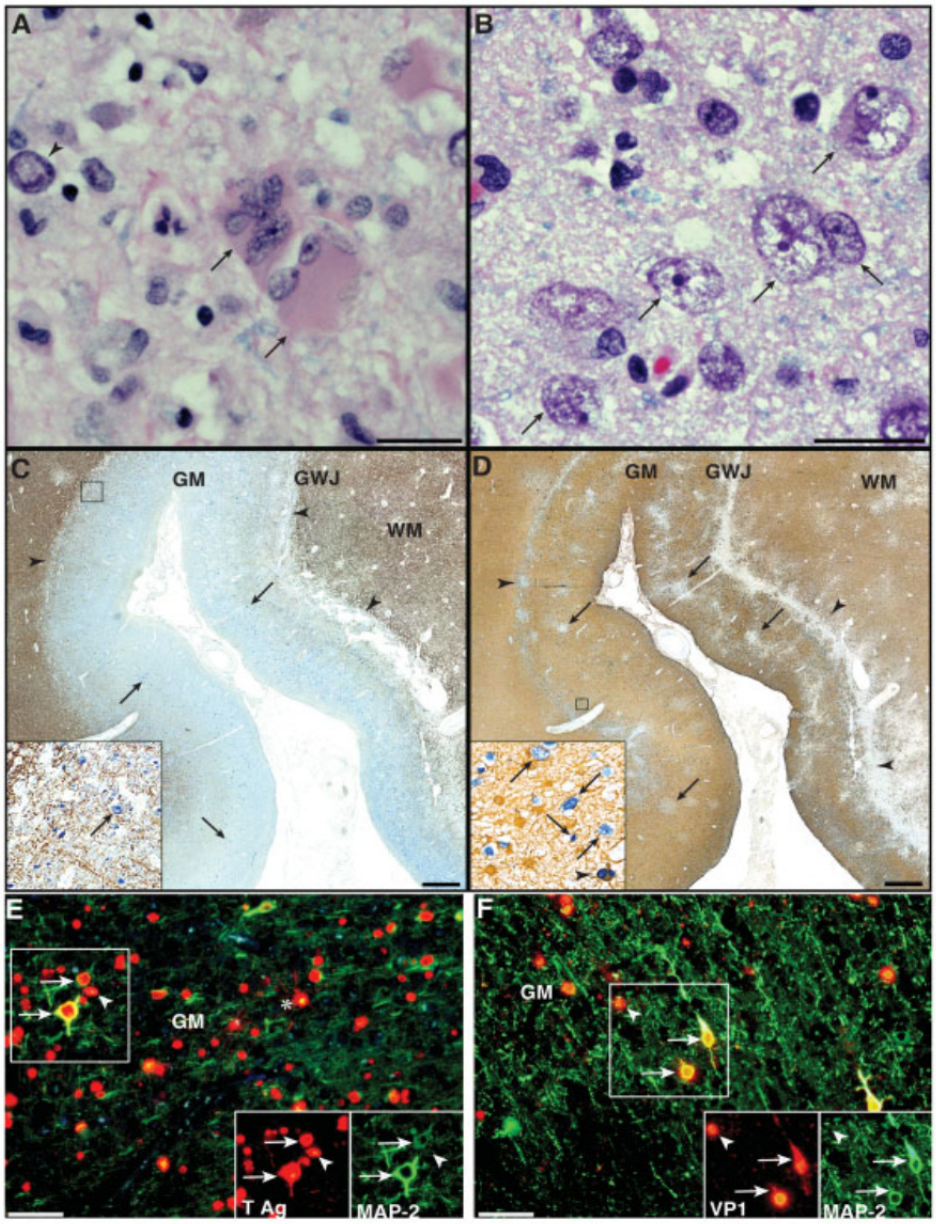

Figure 1.6 JCV infection in astrocytes and neurons in the cortex and GWJ in a JCVE patient. (A and B) Hematoxylin and eosin staining. (A) Giant bizarre astrocytes and a neuron with an enlarged nucleus. (B) Cortical pyramidal neurons with enlarged nuclei. (C and D) Double IHC for JCV T Ag (dark blue) and myelin (C, CNPase, brown) or astrocytes (D, glial fibrillary acidic protein, light brown). (C) Most JCV-infected cells located in the cortex and GWJ are not oligodendrocytes. (D) Numerous JCV infected astrocytes are present. (E and F) Double Immunofluorescence (IF) staining for neuronal marker MAP-2 (green) and either JCV T Ag or VP1 (red). Numerous neurons are infected with JCV and express T Ag and/or VP1. GM is gray matter; WM is white matter. (From Wuthrich et al. 2009 (34)).

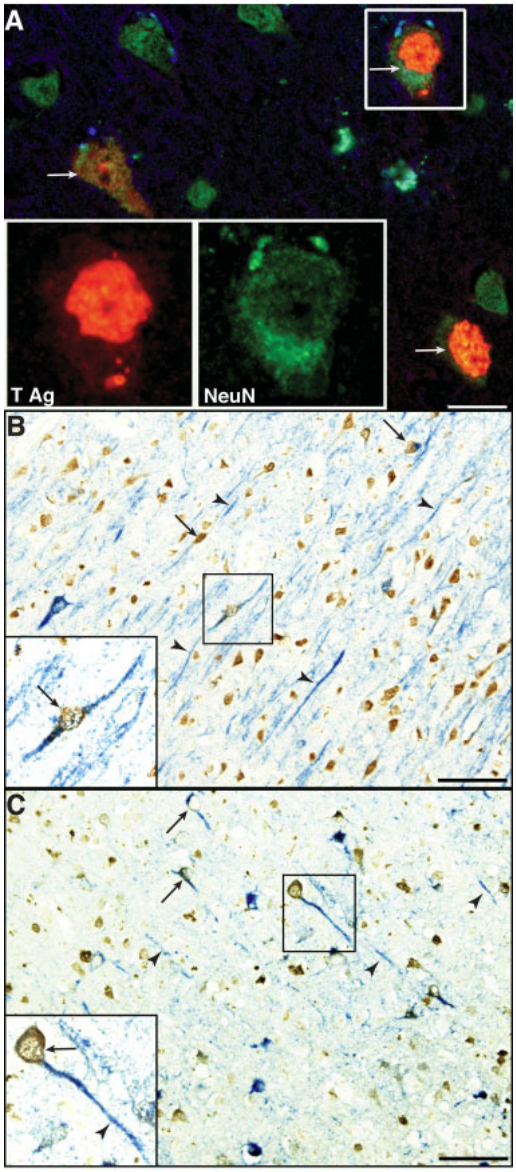

Figure 1.7 Confirmation of JCV infection in neuronal cells. (A) Double IF staining for NeuN (green) and JCV T Ag (red). (B,C) Double IHC staining for NeuN (brown) and JCV T Ag (B, blue) or VP1 (C, blue). JCV T Ag and VP1 can be seen in numerous neurons, in the cell body, axons and dendritic processes. (From Wuthrich et al. 2009 (34)).

JCV CORTICAL PYRAMIDAL NEURON 1 (JCV_{CPN1})

Isolation and sequencing

JCV DNA was isolated from frozen brain samples of the JCVE patient described above, and the full viral genome was amplified, cloned and sequenced (76). This initial strain was named JCV Cortical Pyramidal Neuron 1 (JCV_{CPN1}). Compared to the prototype JCV_{Mad-1}, JCV_{CPN1} has 8 single nucleotide mutations resulting in amino acid changes and 15 silent mutations (Table 1.1). The RR of the virus was found to be archetype-like, containing portions of the 23-bp and 66-bp inserts (Figure 1.8A). The largest mutation present in the virus is a 143-nucleotide deletion in the agnoprotein gene, which results in the encoded agnoprotein being truncated to 10 amino acids compared to the 71 amino acid wild type protein (Figure 1.8B). Further studies found that additional forms of JCV_{CPN1} were present. $JCV_{CPN1.2}$ contains an additional 75-bp duplication between the agnogene and the VP2 gene, encompassing the start of the VP2 gene (Figure 1.9) (76). The mutations and deletions present in JCV_{CPN} do not affect the sequences which produce miRNAs or the target sequence of these miRNAs.

Molecular Biology studies

Further studies of the brain of the JCVE patient found that JCV_{CPN1} coexists with a JCV strain with an intact agnogene. Primers encompassing the agnogene region that can amplify both full length and deleted agnogene were used in PCR screening. It was found that $JCV_{CPN1.2}$ was the predominant strain in the JCVE brain, and the intact agnogene strain was the minority species in the brain. In contrast, PCR screening of the blood and CSF found only JCV with a full length agnogene (76).

Table 1.1 Single nucleotide mutations in JCV_{CPN1}. (Adapted from Dang et al. 2012 (76)).

Amino acid mutations

Position	Location	Nucleotide	Mutation	Amino Acid	Mutation
		Mad-1	CPN1	Mad-1	CPN1
1100	VP2	G	A	S	N192S
1689	VP1	A	G	N	S74N
1692	VP1	G	A	R	K75R
1850	VP1	A	G	T	A128T
1940	VP1	C	G	L	V158L
2502	VP1	A	G	K	R345K
3035	T	C	T	J	V545G
4286	T	T	C	F	S128F

Silent Mutations

Position	Location	Nucleotide	Mutation
1086	VP2	A	G
1843	VP1	G	T
2245	VP1	C	T
2260	VP1	A	T
2311	VP1	G	T
2518	VP1	G	A
2592	Non-coding	G	T
2712	T	A	G
3131	T	T	C
3134	T	T	C
3440	T	T	C
3545	T	T	C
3599	T	G	A
4095	T	C	A
5019	Early mRNA	C	T

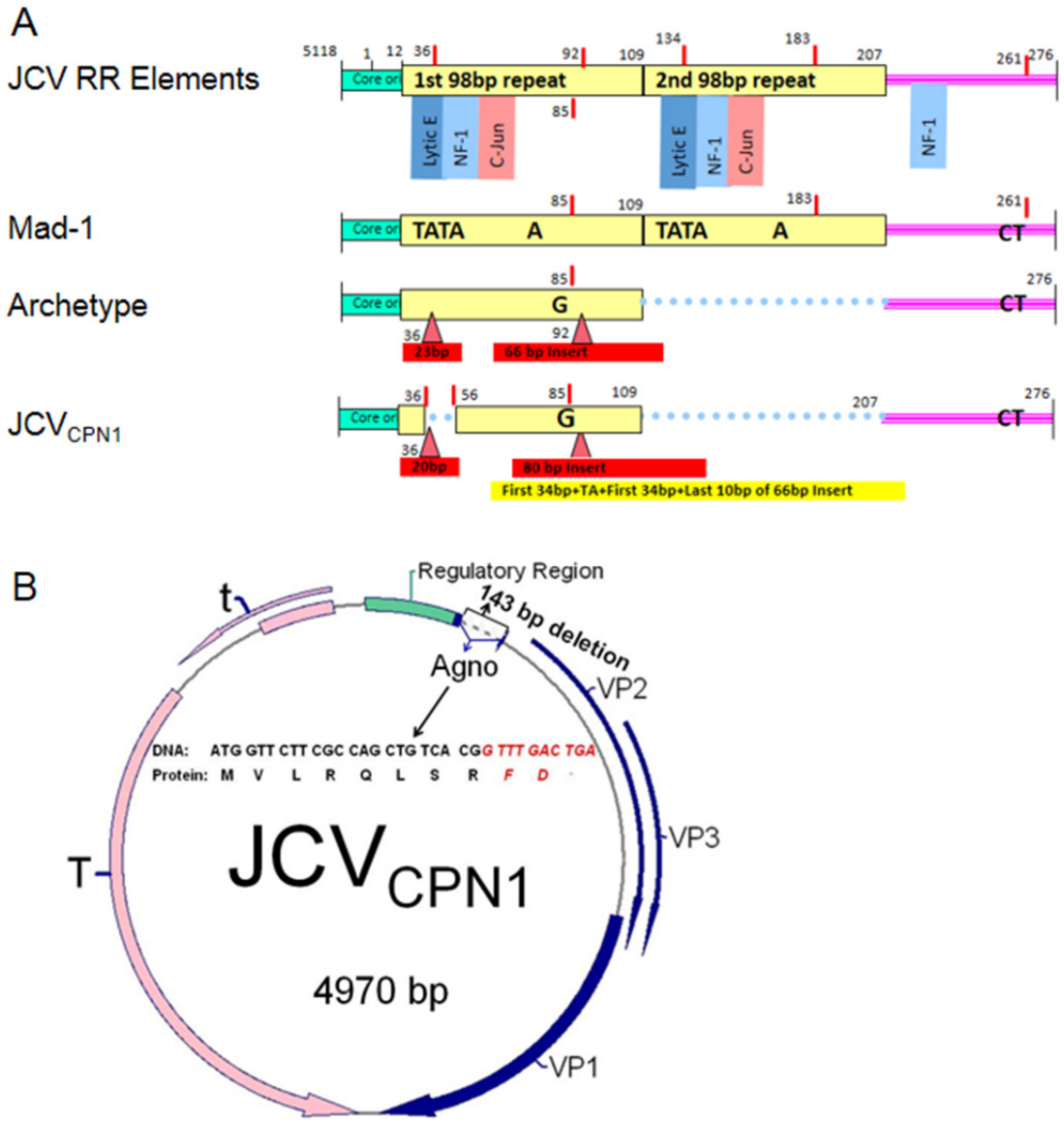

Figure 1.8 JCV_{CPN1} Genome map and RR. (A) JCV_{CPN1} RR compared to JCV_{Mad-1} and Archetype. JCV_{CPN1} has an archetype-like RR with a 19-bp deletion in the 98-bp element, a 3 nt deletion in the 23-bp insert and mutations in the 66-bp insert resulting in an 80-bp insert. (B) JCV_{CPN1} has a 143-bp deletion in the Agno gene (nt 300-442) resulting in a 10 amino acid truncated Agno peptide. (Adapted from Dang et al. 2012 (76)).

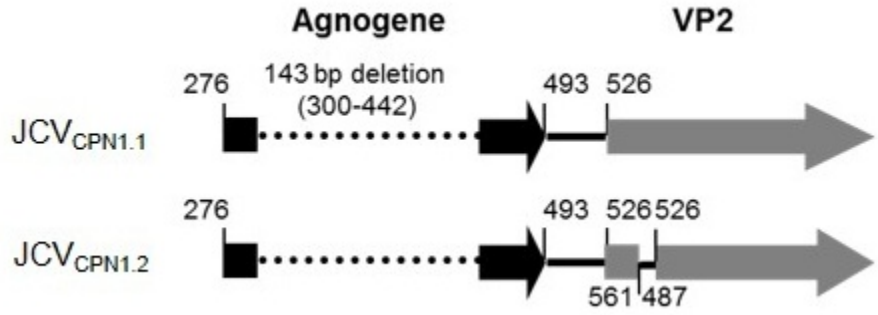

Figure 1.9 Structure of $JCV_{CPN1.1}$ and $JCV_{CPN1.2}$. $JCV_{CPN1.2}$ contains the same RR and agnogene deletion as $JCV_{CPN1.1}$, and has an additional 75-basepair duplication covering the VP2 start codon.

Histological studies of JCVE brain samples

To determine whether JCV_{CPN1} or the JCV with an intact agnogene was responsible for the infection of cortical pyramidal neurons, two different agnoprotein antibodies were used to stain formalin fixed paraffin embedded (FFPE) JCVE brain samples. Anti-$agno_{1-71}$ can recognize the entire agnoprotein including the N terminus of the protein. Anti-$agno_{48-71}$ recognizes only the C terminus of the protein. Both antibodies will stain a full length agnoprotein but only Anti-$agno_{1-71}$ can recognize the truncated agnoprotein of JCV_{CPN1}. Control PML brain samples show agnoprotein staining with both antibodies (Figure 1.10). Double staining of the JCVE brain for VP1 and agnoprotein shows that all the VP1 positive cells stain for agnoprotein when Anti-$agno_{1-71}$ is used, while only 1% of VP1 positive cells are agnoprotein positive when Anti-$agno_{48-71}$ is used (Figure 1.11). Double staining with Anti-$agno_{1-71}$ and MAP-2, a neuron marker, indicate that these infected cells are neuronal (Figure 1.12). No double staining with MAP-2 and Anti-$agno_{48-71}$ was seen (Figure 1.12). These results indicated that the infected cells were primarily infected with JCV_{CPN1} type virus, and that these infected cells were neurons.

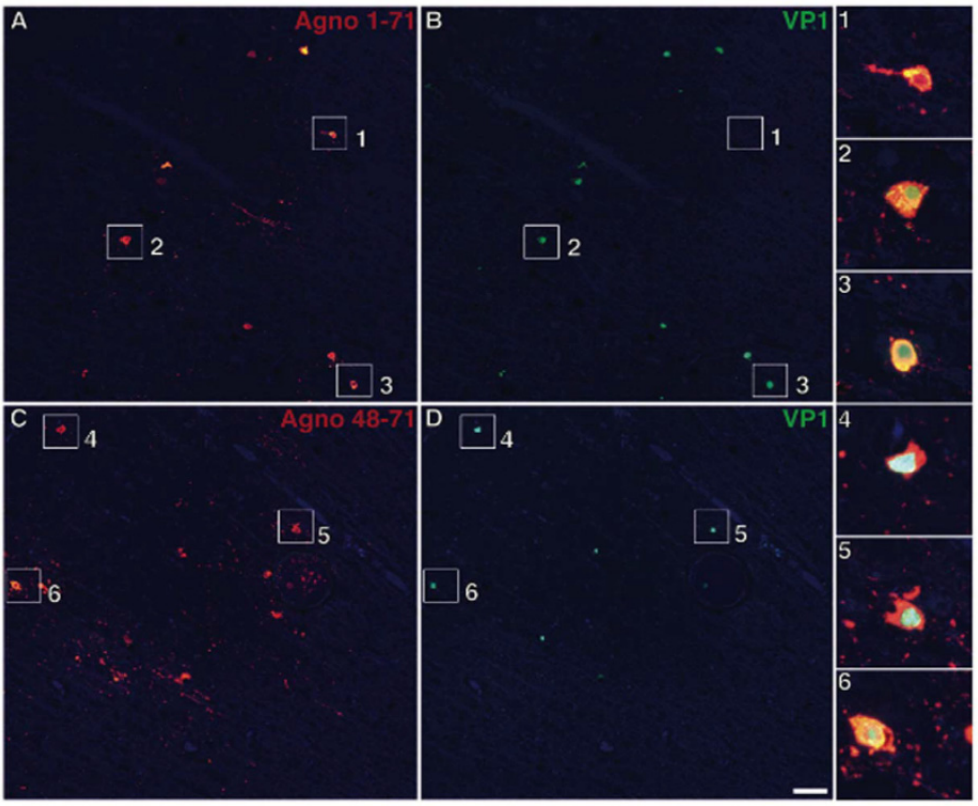

Figure 1.10 Double IF staining of classic PML patient for JCV VP1 and Agnoprotein. Double IF staining for (A) Anti-Agno 1-71 or (C) Anti-Agno 48-71 and (B and D) VP1 in FFPE samples from a patient with classic PML. Staining for both Anti-Agno 1-71 and Anti-Agno 48-71 colocalizes with VP1 staining. (From Dang et al. 2012 (76)).

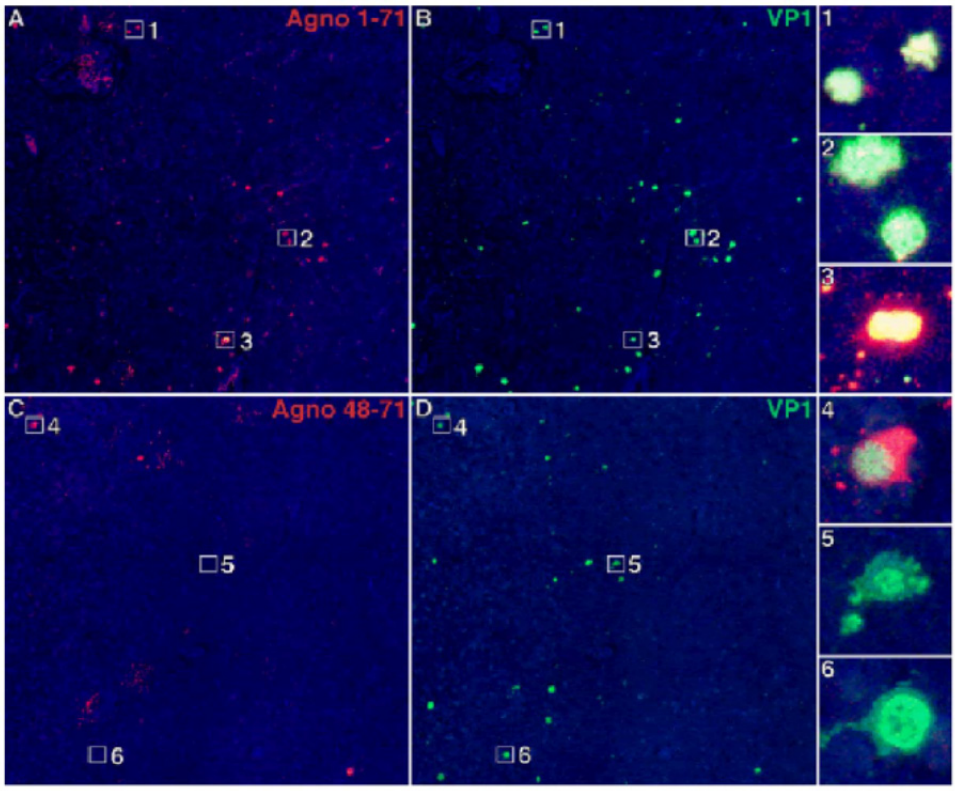

Figure 1.11 Double IF staining of JCVE patient for JCV VP1 and Agnoprotein. Double IF staining for (A) Anti-Agno 1-71 or (C) Anti-Agno 48-71 and (B and D) VP1 in FFPE samples from a patient with JCVE. Staining with Anti-Agno 1-71 colocalizes with VP1 positive cells, while very few Anti-Agno 48-71 positive cells are seen. (From Dang 2012 (76)).

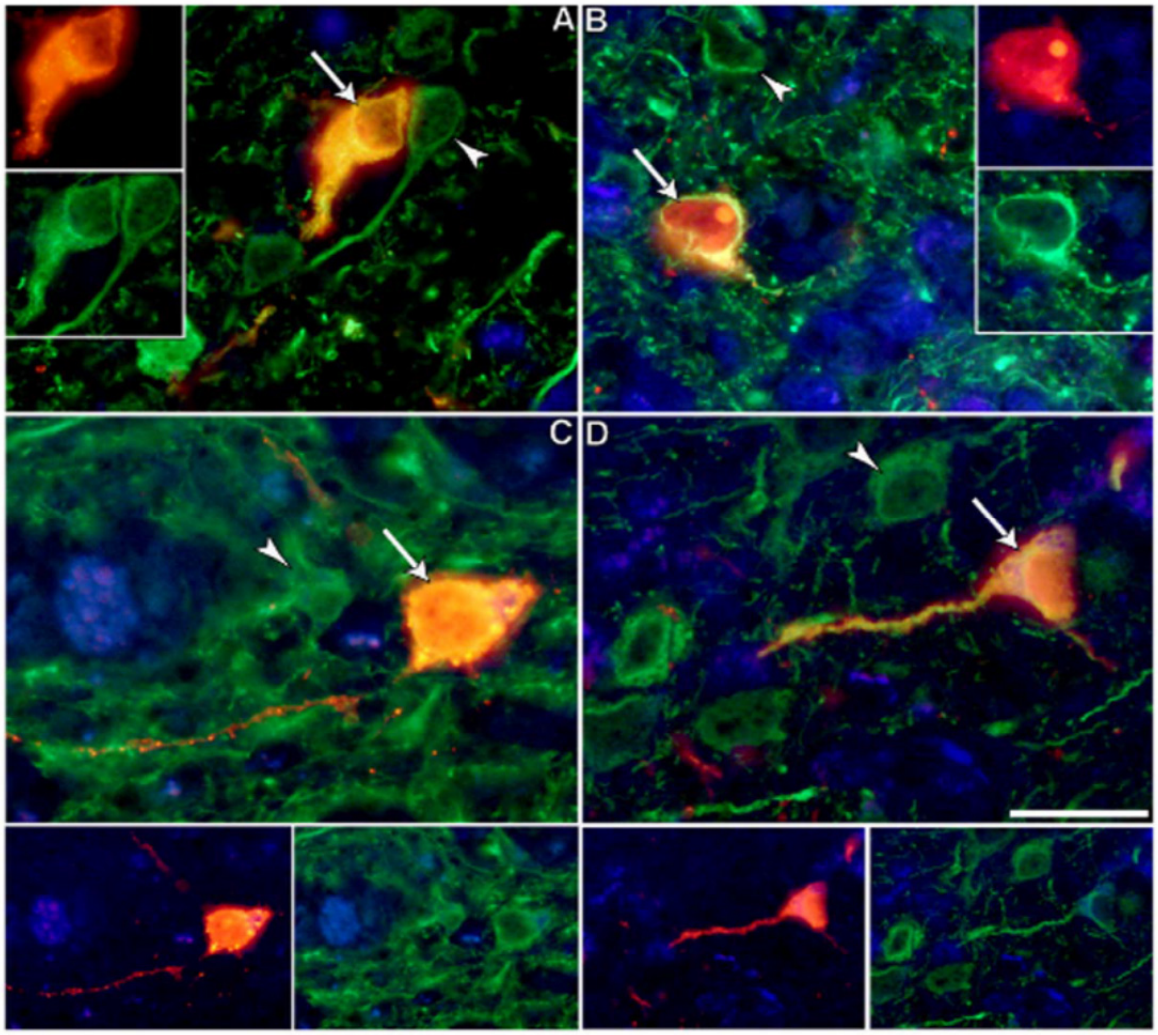

Figure 1.12 Double IF of JCV Agnoprotein and neuronal marker in JCVE patient. Double staining with Anti-Agno1-71 (red) and the neuronal marker MAP-2 (green). Double IF staining for (A) Anti-Agno 1-71 or (C) Anti-Agno 48-71 and (B and D) VP1 in FFPE samples from a patient with JCVE. Staining with Anti-Agno 1-71 colocalizes with VP1 positive cells, while very few Anti-Agno 48-71 positive cells are seen. (From Dang et al. 2012 (76)).

AGNOPROTEIN

Agnoprotein

The JCV agnoprotein is a small 71 amino acid highly basic protein encoded in the leader region of the late transcript (Figure 1.13A). It is not incorporated into virions (27, 77, 78). JCV, BKV and SV40 encode agnoproteins, but none of the more recently identified polyomaviruses including KIV, WUV and MCPyV encode an agnoprotein (2-4). Some polyomaviruses of other mammals also encode agnoproteins (79). Agnoprotein expression has been observed both in the brains of PML patients and JCV infected cells in culture (77, 80). The N- and C-terminal regions of the agnoprotein are hydrophilic and the center region is hydrophobic (81). The N-terminal region is highly conserved between JCV, BKV and SV40, while more variation is present in the C-terminal region (27). The structure of agnoprotein has not been determined, but computer models predict the presence of an alpha helix formed from amino acids 17-42, which contains an Ile/Leu/Phe-rich domain (Figure 1.13B) (82). Agnoprotein can form both homodimers and oligomers, an interaction which is mediated by the Leu/Ile/Phe rich domain of the protein (82, 83). Agnoprotein is found mainly in the cytoplasm, primarily in the perinuclear region, with a small amount detected in the nucleus (77). There are 3 phosphorylation sites on the agnoprotein (Ser7, Ser11 and Thr21), which can be phosphorylated by Protein Kinase C (PKC) (Figure 1.13A) (84). Agnoprotein is dephosphorylated by Protein Phosphatase 2A (PP2A), a process which can be inhibited by small t ag (84, 85). It has been suggested that the phosphorylation state of agnoprotein can influence both the localization and function of agnoprotein during infection (77, 84-86). While agnoprotein is not essential for JCV replication, viruses

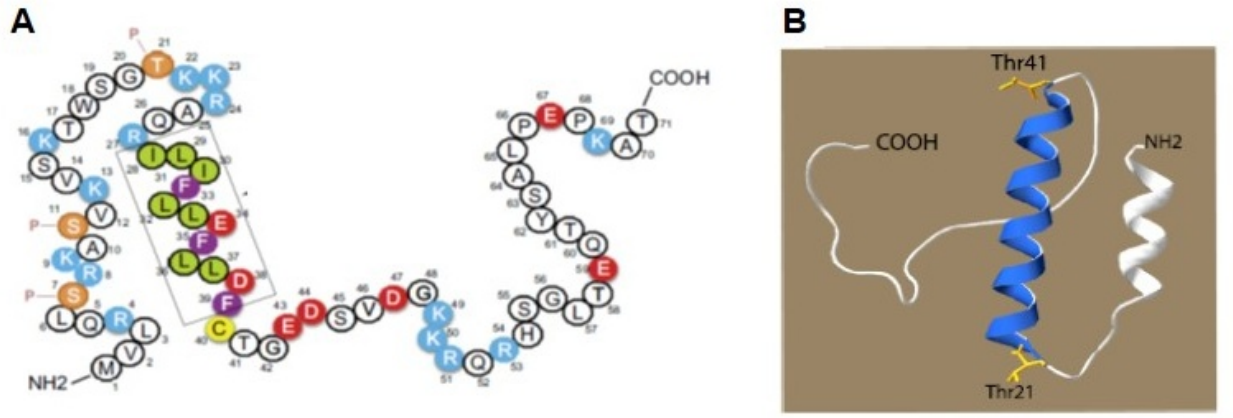

Figure 1.13 Structure of the JCV agnoprotein. (A) The primary structure of the agnoprotein. P stands for phosphorylation and indicates the previously identified sites at Ser7, Ser11 and Ser21. (B) The predicted structure of the agnoprotein. (Adapted from et al. Saribas 2013 (82)).

lacking agnoprotein replicate less efficiently (87, 88). Studies have implicated agnoprotein in a number of viral processes during infection, as well as the alteration of host cell functions.

Roles in Viral Replication

Agnoprotein has been shown to play a role in the regulation of viral genome replication. Using a reporter assay, Safak et al. demonstrated that agnoprotein inhibits Large T Ag activation of DNA replication by interacting with the Large T Ag protein (19). In contrast, another study found that JCV that does not express agnoprotein has decreased viral DNA replication (88). It has also been shown that the presence of agnoprotein increases the binding of T Ag to the origin of replication, which influences the efficiency of DNA replication (83).

Agnoprotein has also been implicated in the regulation of transcription from the early and late promoters (79). However, the results of the studies are not all in

agreement. In one study, cells transfected with a Mad-1 virus in which the agnoprotein start codon was mutated had no mRNA detectable by RT-PCR for Large T Ag, agnoprotein or VP1 (77). Agnoprotein has been show to negatively regulate Large T Ag activation of the late promoter in a CAT reporter assay (19). Agnoprotein can interact with the transcription factor YB-1 and negatively regulate activation of both the early and late promoters in CAT assays (89). A Mad-1 virus lacking the agnoprotein due to deletion of the start codon showed down regulation of both early and late proteins (90). Agnoprotein may also influence the splicing of late transcripts (82).

Agnoprotein has also been implicated in JCV virion assembly, maturation and release. JCV agnoprotein has been shown to facilitate nuclear accumulation of VP1 and production of infectious virions (26, 91, 92). JCV which does not express agnoprotein due to a mutated start codon has been shown to release viral particles which lack viral DNA and which have an irregular morphology (84, 91, 92). *In vitro* assays have indicated that JCV agnoprotein can bind to VP1 and facilitate VP1 pentamer formation (92). In addition, JCV agnoprotein has been shown to interact with the protein HP-1α which destabilizes the nuclear envelope and facilitates release of virions from the nucleus (93). JCV agnoprotein has been demonstrated to have properties of a viroporin, a group of viral proteins which help proteins which help permeabilize cell membranes (92).

Alterations of Host Cell Processes

In addition to its roles in viral processes, agnoprotein has been shown to interact with host cell proteins and alter host cell processes (79). Agnoprotein can dysregulate

cell cycle progression through an interaction with p53, which results in the upregulation of p21 expression and causes cells to accumulate at the G2/M stage (94). Binding of Ku70 by agnoprotein results in the inhibition of DNA repair and the regulation of cell cycle in response to DNA damage (95). Agnoprotein can inhibit the differentiation of oligodendrocytes *in vitro* and induce apoptosis (96). An interaction between YB-1 and JCV agnoprotein has been shown to negatively regulate the transcriptional activation activity of YB-1 on the JCV promoters (89). Agnoprotein also colocalizes with microtubules and dissociates the protein fasciculation and elongation protein zeta 1 (FEZ1) from the microtubules, which may facilitate JCV infection (97). Binding of agnoprotein to heterochromatin protein 1 alpha (HP1α) causes it to dissociate from the lamin B receptor (LBR). This destabilizes the nuclear membrane and assists with virion release from the nucleus (93). Finally, the agnoprotein has been shown to interact with HIV-1 Tat, inhibiting the promoter activity of Tat on HIV-1 (81).

Agnogene Cis-Acting Regulatory Element

In addition to the agnoprotein itself, the agnoprotein coding region has been shown to influence transcription due to the presence of a cis-acting DNA element. Deletion of the agnoprotein coding region results in decreased activity of the early promoter and increased activity of the late promoter in a CAT assay. Using nuclease protection and gel shift assays, it was demonstrated that the agnogene contains 3 cellular factor binding sites, although the identity of the proteins which bind to the agnogene remain unknown (88).

SCOPE OF THE DISSERTATION

JCV is known to cause at least 3 fatal human diseases, PML, JCV GCN and JCVE. A better understanding of JCV replication is crucial for the development of effective treatments for these diseases. Additionally, understanding how the changes present in the JCV strains isolated from patients with the newly discovered JCV GCN and JCVE may add to our knowledge of the pathogenesis of these newly identified diseases. Therefore, we undertook studies of the JCV_{CPN} strain, which was isolated from a patient with JCVE. These studies were done to further our knowledge of the pathogenesis of JCVE, and to better understand the role of the agnoprotein and agnogene in JCV replication. JCV_{CPN} is the first naturally occurring isolate with a large deletion in the agnogene, giving us a unique tool with which to probe the role of the agnoprotein.

In Chapter 2, we sought to better understand the biology of the JCV_{CPN} virus. We studied the replication of the virus compared to the prototype JCV_{Mad-1} in kidney, glial and neuronal cell lines to determine if the virus had a replication advantage over JCV_{Mad-1} in neuronal cells. We found that JCV_{CPN} did not have a replication advantage in neuronal cells, and was unable to establish the persistent high level infection seen with JCV_{Mad-1} in all cell lines tested. JCV_{CPN} failed to express detectable VP1 protein and was impaired for the production of infectious virions. We generated a series of chimeras between JCV_{CPN} and JCV_{Mad-1} to determine whether the archetype-like RR or the 143 nucleotide agnogene deletion was responsible for the observed differences in phenotypes between JCV_{CPN} and JCV_{Mad-1}. We found that the deletion in the agnogene was responsible for the majority of the phenotype of JCV_{CPN}. Interestingly, this was due

to the loss of the agnogene DNA and not the loss of expression of the full length agnoprotein.

In Chapter 3, we sought to further understand the role of the agnogene DNA in JCV replication. Previous studies have indicated that there is a cis-acting DNA regulatory element present in the agnogene and three host cell protein binding sites have been identified. To determine which nucleotides of the agnogene are critical for viral propagation, we generated a series of additional smaller agnogene deletion mutants and tested their replication. We found that the deletion of nucleotides 376-396 prevents the expression of VP1 protein. We also sought to identify the proteins binding to the agnogene. We used biotinylated JCV agnogene DNA probes to immunoprecipitate proteins from JCV permissible cells. We then used mass spectrometry (MS) analysis to identify proteins that were binding specifically to the JCV agnogene DNA. This study identified a number of candidate agnogene binding proteins. We were not able to confirm any of these proteins as binding specifically to the agnogene DNA. Further investigation into these binding factors is warranted.

In summary, we have studied the biology of JCV_{CPN} to better understand the broadened pathogenesis of JCV represented by the newly discovered disease JCVE. We have used this novel, pathogenic isolate to better understand the biology of JCV, in particular the effect of the RR form and agnogene deletion on viral replication. Additionally, we have studied the role of the agnogene DNA, and attempted to identify host cell proteins that bind the agnogene DNA. Further studies to identify the host cell proteins that bind to the agnogene are needed, and our deletion mutants will be useful for identifying specific binding sites for host cell binding proteins.

REFERENCES

1. Frisque RJ, Bream GL, Cannella MT. 1984. Human polyomavirus JC virus genome. *J Virol* 51: 458-69

2. Allander T, Andreasson K, Gupta S, Bjerkner A, Bogdanovic G, Persson MA, Dalianis T, Ramqvist T, Andersson B. 2007. Identification of a third human polyomavirus. *J Virol* 81: 4130-6

3. Gaynor AM, Nissen MD, Whiley DM, Mackay IM, Lambert SB, Wu G, Brennan DC, Storch GA, Sloots TP, Wang D. 2007. Identification of a novel polyomavirus from patients with acute respiratory tract infections. *PLoS Pathog* 3: e64

4. Feng H, Shuda M, Chang Y, Moore PS. 2008. Clonal integration of a polyomavirus in human Merkel cell carcinoma. *Science* 319: 1096-100

5. Schowalter RM, Pastrana DV, Pumphrey KA, Moyer AL, Buck CB. 2010. Merkel cell polyomavirus and two previously unknown polyomaviruses are chronically shed from human skin. *Cell Host Microbe* 7: 509-15

6. van der Meijden E, Janssens RW, Lauber C, Bouwes Bavinck JN, Gorbalenya AE, Feltkamp MC. 2010. Discovery of a new human polyomavirus associated with trichodysplasia spinulosa in an immunocompromized patient. *PLoS Pathog* 6: e1001024

7. Scuda N, Hofmann J, Calvignac-Spencer S, Ruprecht K, Liman P, Kuhn J, Hengel H, Ehlers B. 2011. A novel human polyomavirus closely related to the african green monkey-derived lymphotropic polyomavirus. *J Virol* 85: 4586-90

8. Buck CB, Phan GQ, Raiji MT, Murphy PM, McDermott DH, McBride AA. 2012. Complete genome sequence of a tenth human polyomavirus. *J Virol* 86: 10887

9. Siebrasse EA, Reyes A, Lim ES, Zhao G, Mkakosya RS, Manary MJ, Gordon JI, Wang D. 2012. Identification of MW polyomavirus, a novel polyomavirus in human stool. *J Virol* 86: 10321-6

10. Yu G, Greninger AL, Isa P, Phan TG, Martinez MA, de la Luz Sanchez M, Contreras JF, Santos-Preciado JI, Parsonnet J, Miller S, DeRisi JL, Delwart E, Arias CF, Chiu CY. 2012. Discovery of a novel polyomavirus in acute diarrheal samples from children. *PLoS One* 7: e49449

11. Pastrana DV, Fitzgerald PC, Phan GQ, Raiji MT, Murphy PM, McDermott DH, Velez D, Bliskovsky V, McBride AA, Buck CB. 2013. A divergent variant of the eleventh human polyomavirus species, saint louis polyomavirus. *Genome Announc* 1

12. Tan C, Koralnik I. 2010. Beyond progressive multifocal leukoencephalopathy: expanded pathogenesis of JC virus infection in the central nervous system. *Lancet Neurology* 9: 425-37

13. Trowbridge PW, Frisque RJ. 1995. Identification of three new JC virus proteins generated by alternative splicing of the early viral mRNA. *J Neurovirol* 1: 195-206

14. Ferenczy MW, Marshall LJ, Nelson CD, Atwood WJ, Nath A, Khalili K, Major EO. 2012. Molecular biology, epidemiology, and pathogenesis of progressive multifocal leukoencephalopathy, the JC virus-induced demyelinating disease of the human brain. *Clin Microbiol Rev* 25: 471-506

15. Gheuens S, Wuthrich C, Koralnik IJ. 2013. Progressive multifocal leukoencephalopathy: why gray and white matter. *Annu Rev Pathol* 8: 189-215

16. Gallia GL, Safak M, Khalili K. 1998. Interaction of the single-stranded DNA-binding protein Puralpha with the human polyomavirus JC virus early protein T-antigen. *J Biol Chem* 273: 32662-9

17. Safak M, Gallia GL, Ansari SA, Khalili K. 1999. Physical and functional interaction between the Y-box binding protein YB-1 and human polyomavirus JC virus large T antigen. *J Virol* 73: 10146-57

18. Safak M, Gallia GL, Khalili K. 1999. Reciprocal interaction between two cellular proteins, Puralpha and YB-1, modulates transcriptional activity of JCVCY in glial cells. *Mol Cell Biol* 19: 2712-23

19. Safak M, Barrucco R, Darbinyan A, Okada Y, Nagashima K, Khalili K. 2001. Interaction of JC virus agno protein with T antigen modulates transcription and replication of the viral genome in glial cells. *J Virol* 75: 1476-86

20. Topalis D, Andrei G, Snoeck R. 2013. The large tumor antigen: a "Swiss Army knife" protein possessing the functions required for the polyomavirus life cycle. *Antiviral Res* 97: 122-36

21. White MK, Safak M, Khalili K. 2009. Regulation of gene expression in primate polyomaviruses. *J Virol* 83: 10846-56

22. White MK, Khalili K. 2006. Interaction of retinoblastoma protein family members with large T-antigen of primate polyomaviruses. *Oncogene* 25: 5286-93

23. Khalili K, Sariyer IK, Safak M. 2008. Small tumor antigen of polyomaviruses: role in viral life cycle and cell transformation. *J Cell Physiol* 215: 309-19

24. Hirsch HH, Kardas P, Kranz D, Leboeuf C. 2013. The human JC polyomavirus (JCPyV): virological background and clinical implications. *APMIS* 121: 685-727

25. Gasparovic ML, Gee GV, Atwood WJ. 2006. JC virus minor capsid proteins Vp2 and Vp3 are essential for virus propagation. *J Virol* 80: 10858-61

26. Shishido-Hara Y, Ichinose S, Higuchi K, Hara Y, Yasui K. 2004. Major and minor capsid proteins of human polyomavirus JC cooperatively accumulate to nuclear domain 10 for assembly into virions. *J Virol* 78: 9890-903

27. Khalili K, White MK, Sawa H, Nagashima K, Safak M. 2005. The agnoprotein of polyomaviruses: a multifunctional auxiliary protein. *J Cell Physiol* 204: 1-7

28. Neu U, Maginnis MS, Palma AS, Stroh LJ, Nelson CD, Feizi T, Atwood WJ, Stehle T. 2010. Structure-function analysis of the human JC polyomavirus establishes the LSTc pentasaccharide as a functional receptor motif. *Cell Host Microbe* 8: 309-19

29. Elphick GF, Querbes W, Jordan JA, Gee GV, Eash S, Manley K, Dugan A, Stanifer M, Bhatnagar A, Kroeze WK, Roth BL, Atwood WJ. 2004. The human polyomavirus, JCV, uses serotonin receptors to infect cells. *Science* 306: 1380-3

30. Assetta B, Maginnis MS, Gracia Ahufinger I, Haley SA, Gee GV, Nelson CD, O'Hara BA, Allen Ramdial SA, Atwood WJ. 2013. 5-HT2 receptors facilitate JC polyomavirus entry. *J Virol* 87: 13490-8

31. Flint SJ. 2004. *Principles of virology : molecular biology, pathogenesis, and control of animal viruses*. Washington, D.C.: ASM Press. xxvi, 918 p. pp.

32. Major EO, Amemiya K, Tornatore CS, Houff SA, Berger JR. 1992. Pathogenesis and molecular biology of progressive multifocal leukoencephalopathy, the JC virus-induced demyelinating disease of the human brain. *Clin Microbiol Rev* 5: 49-73

33. Wuthrich C, Cheng YM, Joseph JT, Kesari S, Beckwith C, Stopa E, Bell JE, Koralnik IJ. 2009. Frequent infection of cerebellar granule cell neurons by polyomavirus JC in progressive multifocal leukoencephalopathy. *J Neuropathol Exp Neurol* 68: 15-25

34. Wuthrich C, Dang X, Westmoreland S, McKay J, Maheshwari A, Anderson MP, Ropper AH, Viscidi RP, Koralnik IJ. 2009. Fulminant JC virus encephalopathy with productive infection of cortical pyramidal neurons. *Ann Neurol* 65: 742-8

35. Tan CS, Ellis LC, Wuthrich C, Ngo L, Broge TA, Jr., Saint-Aubyn J, Miller JS, Koralnik IJ. 2010. JC virus latency in the brain and extraneural organs of patients with and without progressive multifocal leukoencephalopathy. *J Virol* 84: 9200-9

36. Ault GS, Stoner GL. 1993. Human polyomavirus JC promoter/enhancer rearrangement patterns from progressive multifocal leukoencephalopathy brain are unique derivatives of a single archetypal structure. *J Gen Virol* 74 (Pt 8): 1499-507

37. Jensen PN, Major EO. 2001. A classification scheme for human polyomavirus JCV variants based on the nucleotide sequence of the noncoding regulatory region. *J Neurovirol* 7: 280-7

38. Marshall LJ, Major EO. 2010. Molecular regulation of JC virus tropism: insights into potential therapeutic targets for progressive multifocal leukoencephalopathy. *J Neuroimmune Pharmacol* 5: 404-17

39. Yogo Y, Iida T, Taguchi F, Kitamura T, Aso Y. 1991. Typing of human polyomavirus JC virus on the basis of restriction fragment length polymorphisms. *J Clin Microbiol* 29: 2130-8

40. Pfister LA, Letvin NL, Koralnik IJ. 2001. JC virus regulatory region tandem repeats in plasma and central nervous system isolates correlate with poor clinical outcome in patients with progressive multifocal leukoencephalopathy. *J Virol* 75: 5672-6

41. Sullivan CS, Grundhoff AT, Tevethia S, Pipas JM, Ganem D. 2005. SV40-encoded microRNAs regulate viral gene expression and reduce susceptibility to cytotoxic T cells. *Nature* 435: 682-6

42. Seo GJ, Fink LH, O'Hara B, Atwood WJ, Sullivan CS. 2008. Evolutionarily conserved function of a viral microRNA. *J Virol* 82: 9823-8

43. Bauman Y, Nachmani D, Vitenshtein A, Tsukerman P, Drayman N, Stern-Ginossar N, Lankry D, Gruda R, Mandelboim O. 2011. An identical miRNA of the human JC and BK polyoma viruses targets the stress-induced ligand ULBP3 to escape immune elimination. *Cell Host Microbe* 9: 93-102

44. Broekema NM, Imperiale MJ. 2013. miRNA regulation of BK polyomavirus replication during early infection. *Proc Natl Acad Sci U S A* 110: 8200-5

45. Astrom KE, Mancall EL, Richardson EP, Jr. 1958. Progressive multifocal leuko-encephalopathy; a hitherto unrecognized complication of chronic lymphatic leukaemia and Hodgkin's disease. *Brain* 81: 93-111

46. Zurhein G, Chou SM. 1965. Particles Resembling Papova Viruses in Human Cerebral Demyelinating Disease. *Science* 148: 1477-9

47. Padgett BL, Walker DL, ZuRhein GM, Eckroade RJ, Dessel BH. 1971. Cultivation of papova-like virus from human brain with progressive multifocal leucoencephalopathy. *Lancet* 1: 1257-60

48. Berger JR, Kaszovitz B, Post MJ, Dickinson G. 1987. Progressive multifocal leukoencephalopathy associated with human immunodeficiency virus infection. A review of the literature with a report of sixteen cases. *Ann Intern Med* 107: 78-87

49. Kleinschmidt-DeMasters BK, Tyler KL. 2005. Progressive multifocal leukoencephalopathy complicating treatment with natalizumab and interferon beta-1a for multiple sclerosis. *N Engl J Med* 353: 369-74

50. Langer-Gould A, Atlas SW, Green AJ, Bollen AW, Pelletier D. 2005. Progressive multifocal leukoencephalopathy in a patient treated with natalizumab. *N Engl J Med* 353: 375-81

51. Van Assche G, Van Ranst M, Sciot R, Dubois B, Vermeire S, Noman M, Verbeeck J, Geboes K, Robberecht W, Rutgeerts P. 2005. Progressive multifocal leukoencephalopathy after natalizumab therapy for Crohn's disease. *N Engl J Med* 353: 362-8

52. Carson KR, Evens AM, Richey EA, Habermann TM, Focosi D, Seymour JF, Laubach J, Bawn SD, Gordon LI, Winter JN, Furman RR, Vose JM, Zelenetz AD, Mamtani R, Raisch DW, Dorshimer GW, Rosen ST, Muro K, Gottardi-Littell NR, Talley RL, Sartor O, Green D, Major EO, Bennett CL. 2009. Progressive multifocal leukoencephalopathy after rituximab therapy in HIV-negative patients: a report of 57 cases from the Research on Adverse Drug Events and Reports project. *Blood* 113: 4834-40

53. Korman BD, Tyler KL, Korman NJ. 2009. Progressive multifocal leukoencephalopathy, efalizumab, and immunosuppression: a cautionary tale for dermatologists. *Arch Dermatol* 145: 937-42

54. Molloy ES, Calabrese LH. 2009. Therapy: Targeted but not trouble-free: efalizumab and PML. *Nat Rev Rheumatol* 5: 418-9

55. Idec B. 2014. TYSABRI (natalizumab): PML Incidence in Patients Receiving TYSABRI. medinfo.biogenidec.com

56. Gheuens S, Pierone G, Peeters P, Koralnik IJ. 2010. Progressive multifocal leukoencephalopathy in individuals with minimal or occult immunosuppression. *J Neurol Neurosurg Psychiatry* 81: 247-54

57. Hall CD, Dafni U, Simpson D, Clifford D, Wetherill PE, Cohen B, McArthur J, Hollander H, Yainnoutsos C, Major E, Millar L, Timpone J. 1998. Failure of cytarabine in progressive multifocal leukoencephalopathy associated with human immunodeficiency virus infection. AIDS Clinical Trials Group 243 Team. *N Engl J Med* 338: 1345-51

58. De Luca A, Fantoni M, Tartaglione T, Antinori A. 1999. Response to cidofovir after failure of antiretroviral therapy alone in AIDS-associated progressive multifocal leukoencephalopathy. *Neurology* 52: 891-2

59. De Luca A, Ammassari A, Pezzotti P, Cinque P, Gasnault J, Berenguer J, Di Giambenedetto S, Cingolani A, Taoufik Y, Miralles P, Marra CM, Antinori A. 2008. Cidofovir in addition to antiretroviral treatment is not effective for AIDS-

associated progressive multifocal leukoencephalopathy: a multicohort analysis. *AIDS* 22: 1759-67

60. Lanzafame M, Ferrari S, Lattuada E, Corsini F, Deganello R, Vento S, Concia E. 2009. Mirtazapine in an HIV-1 infected patient with progressive multifocal leukoencephalopathy. *Infez Med* 17: 35-7

61. Marzocchetti A, Tompkins T, Clifford DB, Gandhi RT, Kesari S, Berger JR, Simpson DM, Prosperi M, De Luca A, Koralnik IJ. 2009. Determinants of survival in progressive multifocal leukoencephalopathy. *Neurology* 73: 1551-8

62. Taoufik Y, Gasnault J, Karaterki A, Pierre Ferey M, Marchadier E, Goujard C, Lannuzel A, Delfraissy JF, Dussaix E. 1998. Prognostic value of JC virus load in cerebrospinal fluid of patients with progressive multifocal leukoencephalopathy. *J Infect Dis* 178: 1816-20

63. Yiannoutsos CT, Major EO, Curfman B, Jensen PN, Gravell M, Hou J, Clifford DB, Hall CD. 1999. Relation of JC virus DNA in the cerebrospinal fluid to survival in acquired immunodeficiency syndrome patients with biopsy-proven progressive multifocal leukoencephalopathy. *Ann Neurol* 45: 816-21

64. Gheuens S, Fellay J, Goldstein DB, Koralnik IJ. 2010. Role of human leukocyte antigen class I alleles in progressive multifocal leukoencephalopathy. *J Neurovirol* 16: 41-7

65. Lima MA, Bernal-Cano F, Clifford DB, Gandhi RT, Koralnik IJ. 2010. Clinical outcome of long-term survivors of progressive multifocal leukoencephalopathy. *J Neurol Neurosurg Psychiatry* 81: 1288-91

66. Koralnik IJ, Wuthrich C, Dang X, Rottnek M, Gurtman A, Simpson D, Morgello S. 2005. JC virus granule cell neuronopathy: A novel clinical syndrome distinct from progressive multifocal leukoencephalopathy. *Ann Neurol* 57: 576-80

67. Du Pasquier RA, Corey S, Margolin DH, Williams K, Pfister LA, De Girolami U, Mac Key JJ, Wuthrich C, Joseph JT, Koralnik IJ. 2003. Productive infection of cerebellar granule cell neurons by JC virus in an HIV+ individual. *Neurology* 61: 775-82

68. Dang X, Koralnik IJ. 2006. A granule cell neuron-associated JC virus variant has a unique deletion in the VP1 gene. *J Gen Virol* 87: 2533-7

69. Dang X, Vidal JE, Oliveira AC, Simpson DM, Morgello S, Hecht JH, Ngo LH, Koralnik IJ. 2012. JC virus granule cell neuronopathy is associated with VP1 C terminus mutants. *J Gen Virol* 93: 175-83

70. Granot R, Lawrence R, Barnett M, Masters L, Rodriguez M, Theocharous C, Pamphlett R, Hersch M. 2009. What lies beneath the tent? JC-virus cerebellar granule cell neuronopathy complicating sarcoidosis. *J Clin Neurosci* 16: 1091-2

71. Hecht JH, Glenn OA, Wara DW, Wu YW. 2007. JC virus granule cell neuronopathy in a child with CD40 ligand deficiency. *Pediatr Neurol* 36: 186-9

72. Otis CN, Moral LA. 2005. Images in pathology: granule cell loss in AIDS-associated progressive multifocal leukoencephalopathy. *Int J Surg Pathol* 13: 360

73. Schippling S, Kempf C, Buchele F, Jelcic I, Bozinov O, Bont A, Linnebank M, Sospedra M, Weller M, Budka H, Martin R. 2013. JC virus granule cell neuronopathy and GCN-IRIS under natalizumab treatment. *Ann Neurol* 74: 622-6

74. Tan IL, Brew BJ. 2009. Possible JCV granular cell neuronopathy in a patient with HIV infection. *Neurology* 73: 1598-9

75. Shin HW, Kang SY, Sohn YH. 2008. JC viral infection-related cerebellar degeneration as the first manifestation of AIDS. *Eur Neurol* 59: 205-7

76. Dang X, Wuthrich C, Gordon J, Sawa H, Koralnik IJ. 2012. JC virus encephalopathy is associated with a novel agnoprotein-deletion JCV variant. *PLoS One* 7: e35793

77. Okada Y, Endo S, Takahashi H, Sawa H, Umemura T, Nagashima K. 2001. Distribution and function of JCV agnoprotein. *J Neurovirol* 7: 302-6

78. Jackson V, Chalkley R. 1981. Use of whole-cell fixation to visualize replicating and maturing simian virus 40: identification of new viral gene product. *Proc Natl Acad Sci U S A* 78: 6081-5

79. Gerits N, Moens U. 2012. Agnoprotein of mammalian polyomaviruses. *Virology* 432: 316-26

80. Okada Y, Sawa H, Endo S, Orba Y, Umemura T, Nishihara H, Stan AC, Tanaka S, Takahashi H, Nagashima K. 2002. Expression of JC virus agnoprotein in progressive multifocal leukoencephalopathy brain. *Acta Neuropathol* 104: 130-6

81. Kaniowska D, Kaminski R, Amini S, Radhakrishnan S, Rappaport J, Johnson E, Khalili K, Del Valle L, Darbinyan A. 2006. Cross-interaction between JC virus agnoprotein and human immunodeficiency virus type 1 (HIV-1) Tat modulates transcription of the HIV-1 long terminal repeat in glial cells. *J Virol* 80: 9288-99

82. Saribas A, Abou-Gharbia M, Childers W, Sariyer IK, White MK, Safak M. 2013. Essential roles of Leu/Ile/Phe-rich domain of JC virus agnoprotein in dimer/oligomer formation, protein stability and splicing of viral transcripts. *Virology* 443: 161-76

83. Saribas AS, White MK, Safak M. 2012. JC virus agnoprotein enhances large T antigen binding to the origin of viral DNA replication: evidence for its involvement in viral DNA replication. *Virology* 433: 12-26

84. Sariyer IK, Akan I, Palermo V, Gordon J, Khalili K, Safak M. 2006. Phosphorylation mutants of JC virus agnoprotein are unable to sustain the viral infection cycle. *J Virol* 80: 3893-903

85. Sariyer IK, Khalili K, Safak M. 2008. Dephosphorylation of JC virus agnoprotein by protein phosphatase 2A: inhibition by small t antigen. *Virology* 375: 464-79

86. Johannessen M, Myhre MR, Dragset M, Tummler C, Moens U. 2008. Phosphorylation of human polyomavirus BK agnoprotein at Ser-11 is mediated by PKC and has an important regulative function. *Virology* 379: 97-109

87. Margolskee RF, Nathans D. 1983. Suppression of a VP1 mutant of simian virus 40 by missense mutations in serine codons of the viral agnogene. *J Virol* 48: 405-9

88. Akan I, Sariyer IK, Biffi R, Palermo V, Woolridge S, White MK, Amini S, Khalili K, Safak M. 2006. Human polyomavirus JCV late leader peptide region contains important regulatory elements. *Virology* 349: 66-78

89. Safak M, Sadowska B, Barrucco R, Khalili K. 2002. Functional interaction between JC virus late regulatory agnoprotein and cellular Y-box binding transcription factor, YB-1. *J Virol* 76: 3828-38

90. Lanitis E, Dangaj D, Hagemann IS, Song DG, Best A, Sandaltzopoulos R, Coukos G, Powell DJ, Jr. 2012. Primary Human Ovarian Epithelial Cancer Cells Broadly Express HER2 at Immunologically-Detectable Levels. *PLoS One* 7: e49829

91. Suzuki T, Orba Y, Okada Y, Sunden Y, Kimura T, Tanaka S, Nagashima K, Hall WW, Sawa H. 2010. The human polyoma JC virus agnoprotein acts as a viroporin. *PLoS Pathog* 6: e1000801

92. Suzuki T, Semba S, Sunden Y, Orba Y, Kobayashi S, Nagashima K, Kimura T, Hasegawa H, Sawa H. 2012. Role of JC virus agnoprotein in virion formation. *Microbiol Immunol* 56: 639-46

93. Okada Y, Suzuki T, Sunden Y, Orba Y, Kose S, Imamoto N, Takahashi H, Tanaka S, Hall WW, Nagashima K, Sawa H. 2005. Dissociation of heterochromatin protein 1 from lamin B receptor induced by human polyomavirus agnoprotein: role in nuclear egress of viral particles. *EMBO Rep* 6: 452-7

94. Darbinyan A, Darbinian N, Safak M, Radhakrishnan S, Giordano A, Khalili K. 2002. Evidence for dysregulation of cell cycle by human polyomavirus, JCV, late auxiliary protein. *Oncogene* 21: 5574-81

95. Darbinyan A, Siddiqui KM, Slonina D, Darbinian N, Amini S, White MK, Khalili K. 2004. Role of JC virus agnoprotein in DNA repair. *J Virol* 78: 8593-600

96. Merabova N, Kaniowska D, Kaminski R, Deshmane SL, White MK, Amini S, Darbinyan A, Khalili K. 2008. JC virus agnoprotein inhibits in vitro differentiation of oligodendrocytes and promotes apoptosis. *J Virol* 82: 1558-69

97. Suzuki T, Okada Y, Semba S, Orba Y, Yamanouchi S, Endo S, Tanaka S, Fujita T, Kuroda S, Nagashima K, Sawa H. 2005. Identification of FEZ1 as a protein that interacts with JC virus agnoprotein and microtubules: role of agnoprotein-induced dissociation of FEZ1 from microtubules in viral propagation. *J Biol Chem* 280: 24948-56

CHAPTER 2: Agnogene deletion in a novel pathogenic JC Virus isolate impairs VP1 expression and virion production

Laura C. Ellis[1,2,3], Elizabeth Norton[1,2], Xin Dang[1,2], Igor J. Koralnik[1,2#]

[1]Division of Neurovirology, Department of Neurology, Beth Israel Deaconess Medical Center, Harvard Medical School, Boston, MA, USA

[2]Center for Virology and Vaccine Research, Department of Medicine, Beth Israel Deaconess Medical Center, Harvard Medical School, Boston, MA, USA

[3]Harvard Program in Virology, Harvard Medical School, Boston, Massachusetts, USA

This chapter is adapted from the published article (see Appendix A):

Ellis LC, Norton E, Dang X, Koralnik IJ. 2013. Agnogene deletion in a novel pathogenic JC virus isolate impairs VP1 expression and virion production. *PLoS One* 8: e80840

Contributions: I designed and carried out the experiments and wrote the manuscript. Elizabeth Norton assisted with DNA extractions and Flow Cytometry experiments. Xin Dang provided protocols and reagents. Igor Koralnik provided guidance on experiments and writing the manuscript.

ABSTRACT

Infection of glial cells by the human polyomavirus JCV causes PML. JCVE is a newly identified disease characterized by JCV infection of cortical pyramidal neurons. The virus JCV_{CPN} associated with JCVE contains a unique 143 nucleotide deletion in the agnogene. Contrary to most JCV brain isolates, JCV_{CPN} has an archetype-like RR usually found in kidney strains. This provided us with the unique opportunity to determine for the first time how each of these regions contributed to the phenotype of $JCV_{CPN.}$ We characterized the replication of JCV_{CPN} compared to the prototype virus JCV_{Mad-1} in kidney, glial and neuronal cell lines. We found that JCV_{CPN} is capable of replicating viral DNA in all cell lines tested, but is unable to establish the persistent infection seen with JCV_{Mad-1}. JCV_{CPN} does not have an increased ability to replicate in the neuronal cell line tested. To determine whether this phenotype results from the archetype-like RR or the agnogene deletion, we generated chimeric viruses between JCV_{CPN} and JCV_{Mad-1}. We found that the deletion in the agnogene is the predominant cause of the inability of the virus to maintain a persistent infection, with the introduction of a full length agnogene, either with or without agnoprotein expression, rescues the replication of JCV_{CPN}. Studying this naturally occurring pathogenic variant of JCV provides a valuable tool for understanding the functions of the agnogene and RR form in JCV replication.

INTRODUCTION

The human polyomavirus JCV has a circular double stranded DNA genome which can be divided into 3 regions. The early coding region encodes the regulatory proteins small t ag and large T Ag. The late coding region encodes the VP1, VP2 and VP3 structural proteins, and the agnoprotein (1). The RR contains the origin of replication, as well as the early and late promoters (2, 3). While the coding regions are well conserved, the RR is hypervariable, with different sequences being isolated from individuals (1). Archetype RR, which has one 98-bp element and contains a 23-bp and a 66-bp insert, is generally found in the kidneys or urine of healthy and immunosuppressed individuals (4). RRs from the brain or CSF of PML patients are generally of the rearranged type, containing two 98-bp tandem repeats with additional mutations, insertions and deletions (1, 2).

JCV is the etiological agent of PML, an often fatal demyelinating disease caused by lytic infection of oligodendrocytes by the virus (5). Infection with JCV is widespread in the population, but remains asymptomatic in healthy people (6, 7). Development of PML is associated with immune suppression, such as in patients with AIDS (8), organ transplants (9) or hematological malignancies (10). We have identified two additional syndromes caused by JCV infection in the brain, JCV GCN (11-13) and JCVE (14). The viruses isolated from patients with these syndromes contain previously unreported unique mutations. JCV GCN is associated with deletions in the C-terminus of the VP1 protein (15, 16) and JCVE with a deletion in the agnogene (17). These naturally occurring pathogenic variants provide a unique tool for studying the basic biology of JCV replication and pathogenesis.

JCVE was described in an HIV-negative patient with a history of lung cancer treated with chemotherapy, who presented with cortical lesions, aphasia and progressive cognitive decline. Post-mortem analysis of the brain showed cortical lesions with productive infection of cortical pyramidal neurons (14). Isolation and sequencing of the JCV DNA present in the brain of this patient identified a virus with an archetype-like RR and a 143 nucleotide deletion in the agnogene (17). This virus was named JCV Cortical Pyramidal Neuron 1 (JCV_{CPN1}). The deleted agnogene encodes a 10 amino acid truncated peptide. Further analysis found that multiple forms of JCV_{CPN} were present, and that these strains co-existed with a virus containing a full length agnogene. Immunostaining analysis indicated that the majority of the cortical cells infected with JCV contained the truncated form of the agnoprotein (17).

JCV agnoprotein is a highly basic, 71 amino acid, non-essential protein that is expressed late in infection, but not incorporated into virions (18). It is primarily expressed in the cytoplasm, particularly in the perinuclear region, with a small amount found in the nucleus (19). Agnoprotein has been shown to form homodimers and oligimers (20). Agnoprotein contains 3 phosphorylation sites, which can be phosphorylated by protein kinase C (21) and dephosphorylated by protein phosphatase 2A (22). The phosphorylation state may impact agnoprotein localization (19). Agnoprotein has been shown to bind to T Ag, down regulating DNA replication (23) and enhancing T Ag origin binding (24). Agnoprotein may also influence viral gene expression and splicing of viral transcripts (25). Loss of agnoprotein expression has been associated with loss of early and late mRNA expression (19). Agnoprotein has also been shown to suppress activity of the late promoter (23), and to interact with the

transcription factor YB-1, inhibiting its ability to activate the early and late promoters (26). Prevention of agnoprotein expression also has been shown to result in decreased levels of T Ag and VP1 protein expression (27). Viruses lacking agnoprotein are less efficient at packaging DNA and virion formation, with infected cells releasing empty particles (27, 28). The agnoprotein may also function as a viroporin, aiding in the release of virions from infected cells (29). These studies have added to our knowledge of agnoprotein function in recent years, but the exact mechanisms by which this protein influences the viral life cycle remain unclear.

In addition to agnoprotein function, the DNA of the agnogene has been shown to contain 3 host cell factor binding sites. Deletion of the agnogene DNA has a greater effect on replication than prevention of agnoprotein expression by mutation of the start codon (30). In the agnogene deletion present in JCV_{CPN}, 1 of the 3 sites is completely deleted, and a second is shortened by 1 nucleotide.

We hypothesized that the agnogene deletion of JCV_{CPN} allowed the virus to infect cortical pyramidal neurons. We used cell culture models to study the replication of JCV_{CPN} compared to the prototype strain JCV_{Mad-1} (31) in different cell types. We generated chimeric viruses of JCV_{CPN} and JCV_{Mad-1}, swapping both the agnogene and RR, to determine the specific effects of the agnogene deletion and the archetype-like RR on viral replication in cell culture. In these experiments we characterized the replication of JCV_{CPN} in different cell types, and determined the relative contributions of the agnogene deletion and archetype-like RR to the JCV_{CPN} replication phenotype. Studying these novel naturally occurring changes in JCV_{CPN} provided unique insights into our understanding of the function of the agnogene and RR form in JCV replication.

MATERIALS AND METHODS

Cell Culture Cos-7 (32), SVG (33) and IMR-32 (34) cells were purchased from the ATCC. Cos-7 cells were maintained in Dulbecco's Modified Eagle Medium (DMEM) supplemented with 10% fetal bovine serum (FBS), Penicillin (500 units/mL) and Streptomycin (500 µg/mL). SVG cells were maintained in Minimum Essential Medium (MEM) supplemented with Sodium Bicarbonate (1.5 g/L), 10% FBS, Penicillin (500 units/mL) and Streptomycin (500 µg/mL). IMR-32 cells were maintained in MEM supplemented with Sodium Bicarbonate (1.5 g/L), Sodium Pyruvate (1 mM), Non-Essential Amino Acids (NEAA) (Invitrogen), 10% FBS, Penicillin (500 units/mL) and Streptomycin (500 µg/mL).

Plasmids Construction of the JCV_{CPN} and $JCV_{Mad\text{-}1}$ plasmids was previously described by Dang et al. (17). To generate the agnogene chimeric viruses Mad-1 C-Agno and CPN M-Agno, the agnogene region was excised using the restriction enzymes ApaI and PciI (New England Biolabs), and the digested DNA was run on an agarose gel. The agnogene DNA and the virus minus the agnogene DNA bands were excised and purified using the QIAquick Gel Extraction Kit (QIAGEN). Agnogene DNA segments were ligated into the viral backbone using T4 ligase (New England Biolabs). The resulting plasmids were transformed into TOP10 (Invitrogen) or XL1-Blue cells (Agilent). Plasmid DNA was maxi prepped (QIAGEN), and plasmids were fully sequenced. The RR chimeras were generated with the same protocol, using the restriction enzymes BamHI and PciI (NEB) to excise the RR. Mad-1 Pt and Mad-1 Del plasmids were previously described (30), and obtained as a generous gift from Dr. Safak. The

agnogene from these viruses was introduced into our JCV_{Mad-1} or JCV_{CPN} plasmid using the ApaI and PciI restriction sites as previously described.

Transfection Full-length JCV genomes were digested out of the plasmid backbone using EcoRI (NEB) and run on a 0.8% agarose gel. The 5kb virus band was purified using the QIAquick Gel Extraction Kit (QIAGEN). Cells were transfected with 1 µg (for IMR-32 and SVG cells) or 2 µg (for Cos-7 cells) of purified JCV DNA using FuGENE6 transfection reagent (Roche or Promega) in 6 well plates. 3 days post-transfection, cells were passaged 1:3 to T25 flasks, and subsequently every 3-4 days 1:4 in T25 flasks. At each passage, supernatant was collected and cells were collected, pelleted and stored at -80°C until further analysis.

DNA Extraction and Quantitative PCR (QPCR) DNA was extracted from cell pellets and supernatant samples using the QIAamp DNA Blood Mini Kit (QIAGEN). QPCR was performed as previously described (15). An RNAase P primer/probe set (Applied Biosystems) was used in a multiplex assay with the JCV primer/probe set on cell lysate samples. Copies RNAse P per reaction was determine and divided by 2 to determine the number of input cells for each reaction. Copies JCV/cell was calculated by dividing the copies JCV per reaction by the number of cells per reaction. All samples were run in triplicate.

RNA Extraction and qRT-PCR RNA was extracted using the RNEasy Mini Kit (QIAGEN). RNA samples were digested with rDNAse I (Ambion) to remove any

contaminating DNA. Reverse transcription was done using the High Capacity RNA-to-cDNA Kit (Applied Biosystems). QPCR was performed on a 7300 Real-time PCR System using Gene Expression Master Mix (Applied Biosystems). For amplification of the early transcript mRNA, a primer probe set spanning the Large T Ag splice site was used. The primers were JCT208F (5'-CATCAGCCTGATTTTGGTACATG-3', reverse complement of position 4784-4806) and JCT 279R (5'-CCAGGATTCCCATTCATCTGTT-3', position 4392-4412). The probe used was JCT-232p (6FAM-5'-AAT AGT TCA GAG GTG CCA AC-3'-MGB, reverse complement of position 4419-4426 and 4771-4482). For detection of late transcript mRNA we used the primers JCVP1-745F (5'-GGTGACAACTTATACTTGTCAGCTGTT-3', position 2213-2239) and JCVP1-812R (5'-TGCTGGGAACCAGACCTGTT-3', reverse complement of position 2261-2280) and the probe JCVP1-773p (6FAM-5'-ATG TCT GTG GCA TGT TTA-3'-MGB, position 2241-2248). A TATA-box binding protein (TBP) primer/probe set (Invitrogen) was used as the endogenous control for determination of relative quantity by the comparative C_T method (also known as the $\Delta\Delta$Ct method) (35). All samples were run in triplicate wells.

Western Blotting Cells were lysed in TNN lysis buffer (50 mM Tris-HCl pH 7.5, 150 mM NaCl, 0.1% NP40) with 0.2 mM Na-Orthovanadate and 1% protease inhibitor cocktail for 30 minutes on ice. Samples were centrifuged at 8000 rpm for 4 min to remove cell debris. Laemmli Buffer (Bio-Rad) was added to whole cell lysate. Samples were boiled for 10 min and run on a 10% SDS-PAGE gel in Tris/Glycine/SDS running buffer (Bio-Rad). Samples were transferred for 2 hours at 150 mAmps to a nitrocellose

membrane in Transfer Buffer (Tris/Glycine with 20% methanol) or to a nitrocellulose membrane using the iBlot system (Invitrogen). Membranes were blocked using 5% milk in PBST and incubated overnight at 4ºC with VP1 antibody pAB597 (1 mg/mL) diluted 1:1000 or loading control anti-alpha tubulin [DM1A] (abcam) in 2% milk in PBST. An HRP conjugated goat-anti mouse IgG secondary antibody (Bio-Rad) was used and detection was done with ECL Plus reagent (Thermo Scientific). Signal was detected on film.

Flow Cytometry Analysis of JCV-Positive Cells Cells were trypsinized, collected and washed with 2% FBS in PBS. Cells were passed through a 30 µm filter (Miltenyi Biotec) and incubated for 20 minutes at 4ºC with Aqua Amine to stain dead cells, and then washed with PBS. Cells were fixed with Cytofix/Cytoperm (BD Biosciences) for 20 minutes at 4ºC then washed with PBS. Staining with the primary antibody PAB597 (mouse monoclonal anti-VP1) in Perm/Wash Buffer (BD Biosciences) was done for 2 hours at 4ºC. Cells were washed with Perm/Wash Buffer, then PBS and then stained with Alexa 488 conjugated Anti-Mouse IgG (Invitrogen) secondary antibody in Perm/Wash Buffer for 1 hour at 4ºC. Cells were washed, and then analyzed using a BD LSR II Flow Cytometer (BD Biosciences).

JCV Infectivity Test Cos-7 cells were plated in 6 well plates at low density and allowed to adhere overnight. Cell free supernatant collected from transfected cells was put on the Cos-7 cells, and incubated 2 hours at room temperature with rocking. The infection

was allowed to proceed for 7 days. Cells were then collected and analyzed for either VP1 expression by flow cytometry or JCV DNA by QPCR as previously described.

DNAse Digestion 170 uL of supernatant was digested with 20 units of DNAse I (Ambion) in DNAse I Buffer for 1 hour at 37ºC. Undigested samples were incubated in DNAse I buffer and subject to the sample digestion conditions. Digestion control samples were generated by adding concentrated JCV_{Mad-1} plasmid to supernatant collected from JCV negative cells. After digestion, DNA was extracted using the DNA Blood Mini Kit as describe above, or supernatant was used to infect Cos-7 cells in 6 well plates as described above.

Statistical Analyses Analyses were done using SAS Software version 9.3. Data was tested for normality before statistical analysis. P-values for DNA levels were determined using the non-parametric Wilcoxon Rank Test. P-values for mRNA levels were done using univariate analysis, and taking the student's t p value. Flow cytometry p-values were determined using Student's t test.

RESULTS

JCV_{CPN} has a 143 nucleotide deletion in the agnogene and an archetype-like RR. The JCV_{CPN1} RR is archetype-like, lacking a duplication of the TATA-box and containing 20-bp and 80-bp inserts, which contain portions of the 23-bp and 66-bp inserts present in archetype RR (Figure 2.1A) (17). A 143 nucleotide deletion in the agnogene is also present in JCV_{CPN1} (Figure 2.1B) (17). This deletion creates a premature stop codon, and is predicted to code for a truncated 10 amino acid agnoprotein. Multiple forms of JCV_{CPN} were identified, including $JCV_{CPN1.1}$ and $JCV_{CPN1.2}$ which both contain the same regulatory region and agnogene deletion. In addition, $JCV_{CPN1.2}$ contains a 75-bp duplication between the agnogene and the VP2 gene, encompassing the start of the VP2 gene (Figure 2.1B). This form is predicted to encode for both a truncated and a full length VP2. Our studies determined that $JCV_{CPN1.1}$ and $JCV_{CPN1.2}$ are phenotypically equivalent in our cell cultures model (data not shown). Therefore, we chose to conduct the experiments in this study using the $JCV_{CPN1.2}$ strain, because it was the predominant strain in the JCVE patient's brain. $JCV_{CPN1.2}$ is referred to as JCV_{CPN} for the remainder of this work.

JCV_{CPN} can replicate DNA in cell culture, but at a lower level than JCV_{Mad-1}. To determine the cellular tropism of JCV_{CPN}, we studied its replication in cell culture. We used multiple cell lines to model the replication of the virus in three different types of cells, kidney cells, glial cells and neurons. Cos-7 cells are African Green Monkey kidney cells which express SV40 T Ag, and are known to replicate JCV well (32). SVG cells are human fetal glial cells, also transformed with SV40 T Ag (33). IMR-32 cells are

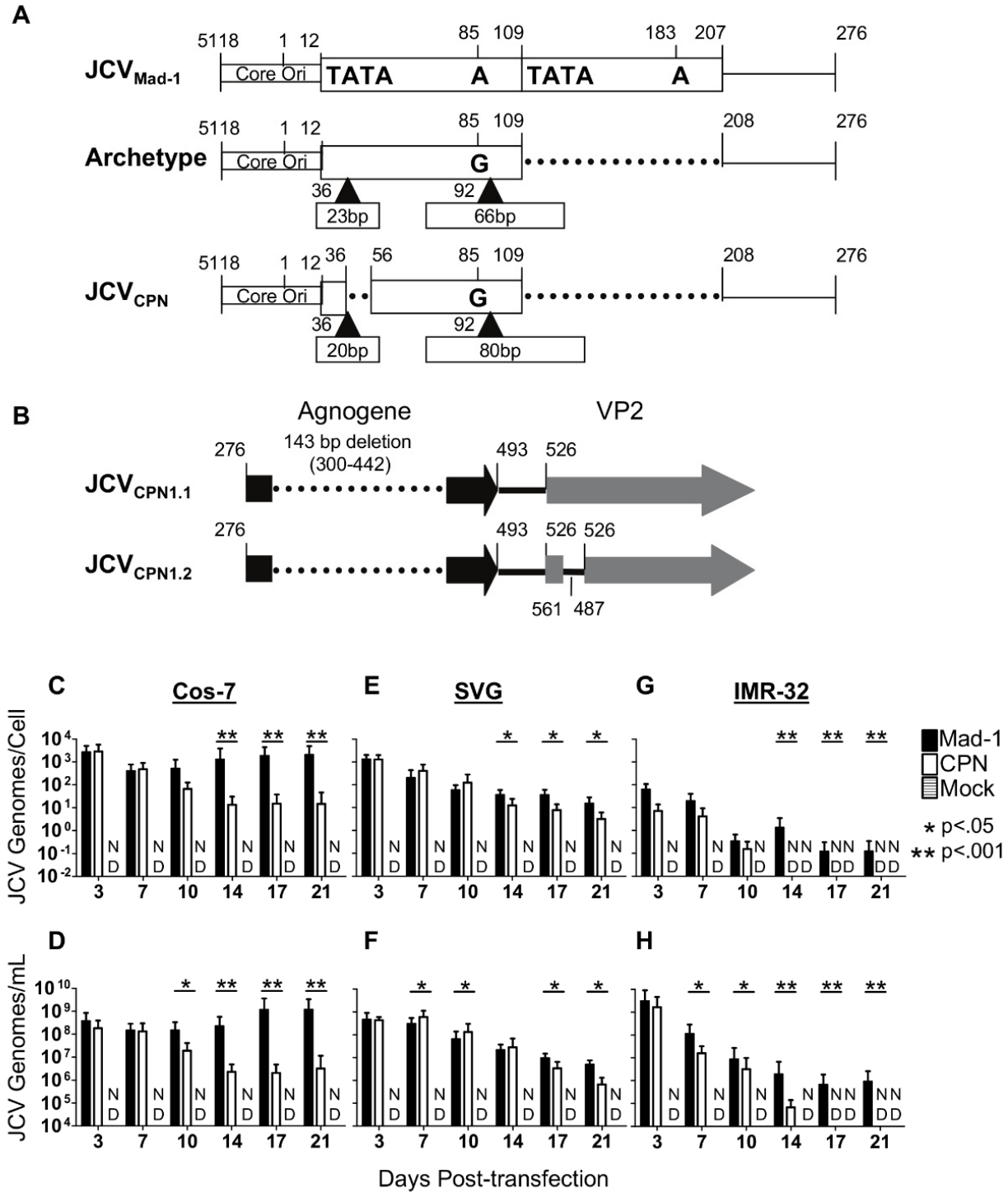

Figure 2.1 JCV_{CPN} replicates viral DNA, but at lower levels than JCV_{Mad-1}. (A) JCV_{CPN} RR is archetype-like (adapted from (17)). (B) $JCV_{CPN1.2}$ (hereafter referred to as simply JCV_{CPN}) agnogene contains a 143-bp deletion followed by a 75-bp

Figure 2.1 (Continued). duplication at the beginning of the VP2 gene. (C-H) Cos-7, SVG and IMR-32 cells were transfected with linearized JCV genomes, or mock transfected. Cells were subcultured every 3-4 days and cell and supernatant samples were collected. DNA was extracted from the samples, digested with DpnI to remove input plasmid DNA, and analyzed by QPCR. Data represents the average of 4-10 independent experiments. In Cos-7 cell lysate (C) and supernatant (D) JCV_{Mad-1} but not JCV_{CPN} establishes a persistent infection. In SVG cell lysate (E) and supernatant (F) JCV_{Mad-1} and JCV_{CPN} both establish persistent infections. In IMR-32 cells, JCV_{Mad-1} infection persists for 21 days, while JCV_{CPN} becomes undetectable in cell lysate (G) and in supernatant (H). Error bars represent standard deviation. P-values were calculated using the Wilcoxon Rank Test. ND is not detected.

a human neuroblastoma cell line, derived from a tumor isolated from the abdominal cavity of a child, which do not express any polyomavirus T Ag (34). We first wanted to determine if JCV_{CPN} is capable of genome replication. To do so, linearized genomes of JCV_{CPN} and JCV_{Mad-1} were transfected into Cos-7, SVG and IMR-32 cells. DNA from cell lysate, representing JCV DNA replicated in the transfected cells, and supernatant, representing DNA released from the transfected cells, was extracted and digested with DpnI to remove any remaining input plasmid DNA. JCV genome copy number was determined by QPCR. We found that JCV_{CPN} replicated DNA after transfection in all 3 cell lines tested (Figure 2.1C-H). However, the levels of DNA were not equivalent to those seen with the prototype strain JCV_{Mad-1}.

In Cos-7 kidney cells, JCV_{Mad-1} establishes a high level infection that persists over 3 weeks, as measured by copies JCV DNA in the cell lysate and supernatant (Figure 2.1C and 2.1D). JCV_{CPN} has equivalently high levels of JCV genomes present in the cell lysate and supernatant during the first week post-transfection, but does not maintain such a high viral load, with the copy number decreasing with time. In SVG glial cells, both JCV_{Mad-1} and JCV_{CPN} establish persistent infections (Figure 2.1E and 2.1F). Levels

of JCV_{CPN} genome copies in cell lysate and supernatant at later time points post-transfection are significantly lower than those of JCV_{Mad-1}, but with a smaller magnitude of difference than observed in Cos-7 cells. In IMR-32 neuronal cells, JCV_{Mad-1} DNA decreased over the first 2 weeks after transfection, and then leveled off, remaining detectable over 3 weeks (Figure 2.1G and 2.1H). In contrast, JCV_{CPN} decreased and dropped below the limit of detection at 14 days post-transfection in cell lysate and 17 days post-transfection in the supernatant. These results indicate that JCV_{CPN} is able to replicate its genome after transfection into Cos-7, SVG and IMR-32 cells, but may have a decreased capacity to persist and spread within the culture compared to prototype JCV_{Mad-1}. Additionally, JCV_{CPN} does not display a replication advantage in the neuronal cell culture line tested.

JCV_{CPN} expresses both early and late transcripts, but at decreased levels compared to JCV_{Mad-1}. Knowing that JCV_{CPN} is able to replicate viral DNA, but not establish a persistent high level infection, we wanted to determine if JCV_{CPN} is able to initiate transcription of mRNAs from the early and late promoters. To do so, we used qRT-PCR on RNA from transfected cells using primer and probe sets located in T Ag to detect early transcripts, and in VP1 to detect late transcripts. In Cos-7, SVG and IMR-32 cells, JCV_{CPN} expresses detectable levels of both the early and late transcripts (Figure 2.2). In Cos-7 cells, the level of early transcripts is significantly lower than those seen with JCV_{Mad-1} 3 and 10 days post-transfection (Figure 2.2A). In SVG cells, the level of early transcripts is similar between JCV_{CPN} and JCV_{Mad-1} 3 and 7 days post-transfection, and significantly lower 10 days post-transfection (Figure 2.2B). In IMR-32 cells, the

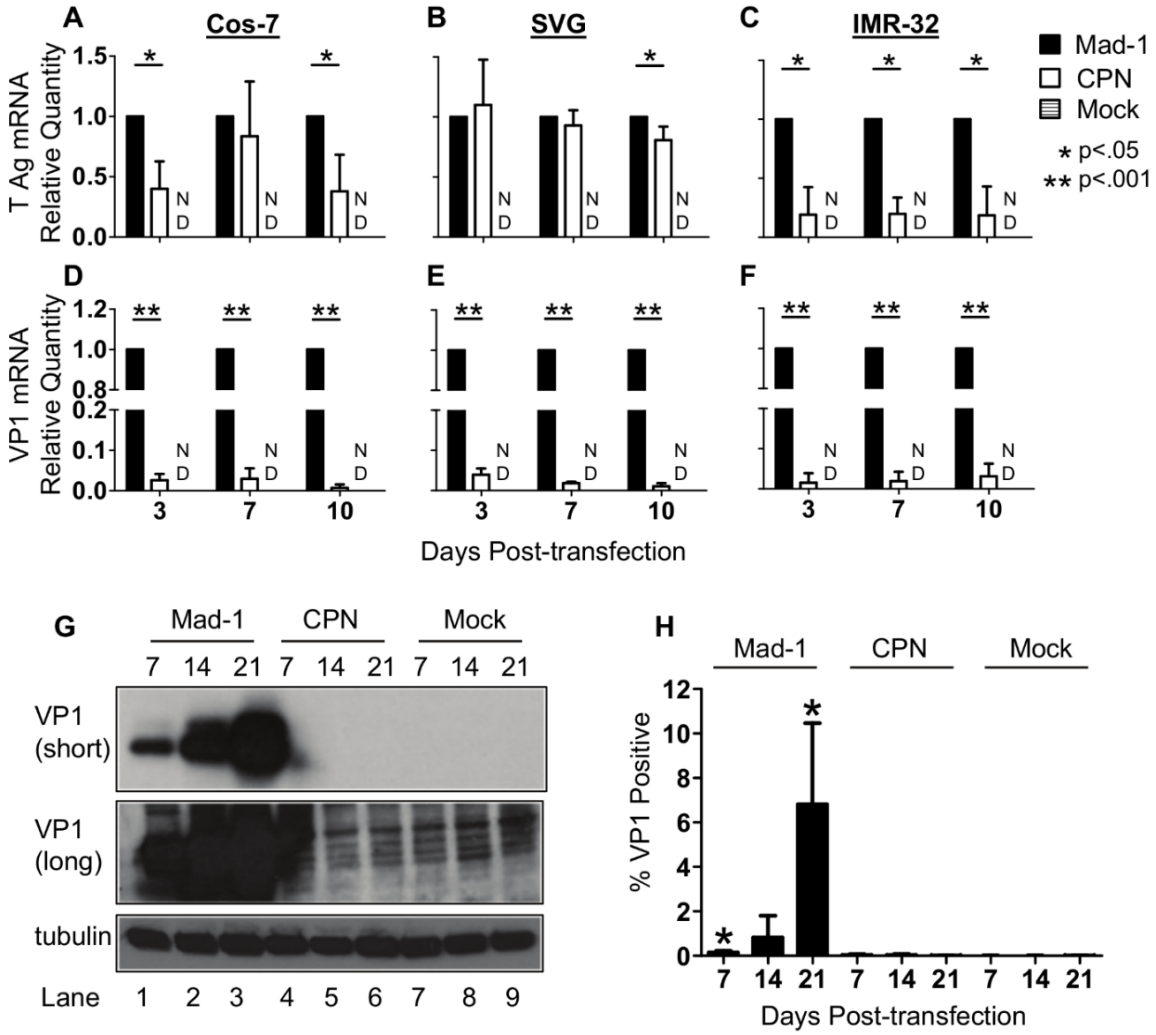

Figure 2.2. JCV_{CPN} expresses less early and late mRNA and VP1 protein than JCV_{Mad-1}. (A-F) Cos-7, SVG and IMR-32 cells were transfected with JCV_{Mad-1}, JCV_{CPN} or mock transfected and samples were collected as described in Figure 2.1. qRT-PCR was used to determine the levels of early (T Ag) and late (VP1) transcripts. Relative Quantity (RQ) was calculated using the $\Delta\Delta$Ct method, using TATA-Box Binding Protein (TBP) as the endogenous control and JCV_{Mad-1} as the calibrator sample. Data represents the average of 5-6 independent experiments. (A and D) In Cos-7 cells, JCV_{CPN} expresses significantly lower levels of T Ag (A) and VP1 (D) mRNA. (B and E) In SVG cells, levels of T Ag (B) mRNA expressed by JCV_{CPN} are similar to JCV_{Mad-1}, while VP1 (E) mRNA is significantly lower. (C and F) JCV_{CPN} expresses significantly less T Ag (C) and VP1 (F) mRNA in IMR-32 cells. Error Bars represent standard deviation. P values were calculated for Student's t test using univariate analysis. ND is not detected. (G) Western blots

Figure 2.2 (continued) were done with PAB597 (anti-VP1) using cell lysate from Cos-7 cells transfected with either JCV_{Mad-1} (Lanes 1-3), JCV_{CPN} (Lanes 7-9) or mock transfected cells (Lanes 4-6) collected 7 (Lanes1,4,7), 14 (Lanes 2,5,8) or 21 (Lanes 3,6,9) days post-transfection. VP1 can be detected in JCV_{Mad-1} transfected cells at all time points, but not at any time with JCV_{CPN}, with either a short (upper panel) or long (middle panel) exposure. Anti-tubulin antibody was used for loading control (lower panel). Blots are representative of 3 independent experiments (H) JCV_{Mad-1}, JCV_{CPN} or mock transfected Cos-7 cells were analyzed for VP1 expression by flow cytometry. JCV_{Mad-1} but not JCV_{CPN} transfected cells have significantly higher levels of VP1 positive cells than Mock transfected samples. Results are the average of 4 independent experiments. Error bars represent standard deviation. P values were calculated using students t test, comparing JCV_{Mad-1} and JCV_{CPN} to mock.

level of early transcripts produced by JCV_{CPN} is significantly lower than those of JCV_{Mad-1} at 3, 7 and 10 days post-transfection (Figure 2.2C). In all three cell lines, the level of late transcripts is markedly lower in JCV_{CPN} transfected cells compared to JCV_{Mad-1} transfected cells (Figure 2.2D-F). These results indicate that, although both the early and late promoter of JCV_{CPN} are transcriptionally active, they function at a level lower than JCV_{Mad-1}. The decrease in transcript levels is larger for the late than the early promoter.

JCV_{CPN} fails to produce detectable levels of VP1 protein in Cos-7 cells. We then wanted to determine if JCV_{CPN} produces VP1 protein from the late mRNA. JCV_{Mad-1} transfected cells produce VP1 protein, with the amount of VP1 present increasing with later times post-transfection (Figure 2.2G). JCV_{CPN} does not produce detectable levels of VP1 protein, even with long exposure times (Figure 2.2G).

To determine if there is VP1 present in a small number of JCV_{CPN} transfected cells, which cannot be detected by Western Blot, we developed a protocol to analyze transfected Cos-7 cells for VP1 expression using flow cytometry. JCV_{Mad-1} transfected

cells were positive for VP1 expression, with an increase in the percentage of cells positive for VP1 over time, with the highest percentage of VP1 positive cells seen 21 days post-transfection (Figure 2.2H). The percentage of JCV_{Mad-1} VP1 positive cells is significantly higher than the background observed in Mock transfected cells. JCV_{CPN} transfected cells are not positive for VP1 by flow cytometry at a level significantly higher than Mock transfected cells (Figure 2.2H). This supports the results seen using Western blotting, that JCV_{CPN} does not express detectable levels of VP1 protein.

JCV_{CPN} produces low levels of infectious virions. Although we could not detect VP1 expression by Western Blot or flow cytometry in transfected cells, there may be a very low level of expression below our limit of detection. We therefore wanted to determine if JCV_{CPN} transfected cells are producing virions capable of infecting a new round of cells. To do so, supernatant was collected from transfected Cos-7, SVG and IMR-32 cells 7, 14 and 21 days post-transfection and was used to infect Cos-7 cells. Infection was allowed to proceed for 7 days. Cells were collected, and analyzed for JCV DNA by QPCR or stained for VP1 and analyzed by flow cytometry. Supernatant was not digested with DNAse to remove free JCV DNA, as previous experiments have shown that digesting with DNAse does not affect the levels of JCV DNA detected in the supernatant by qPCR, or the percentage of cells subsequently infected from the supernatant (Figure 2.3).

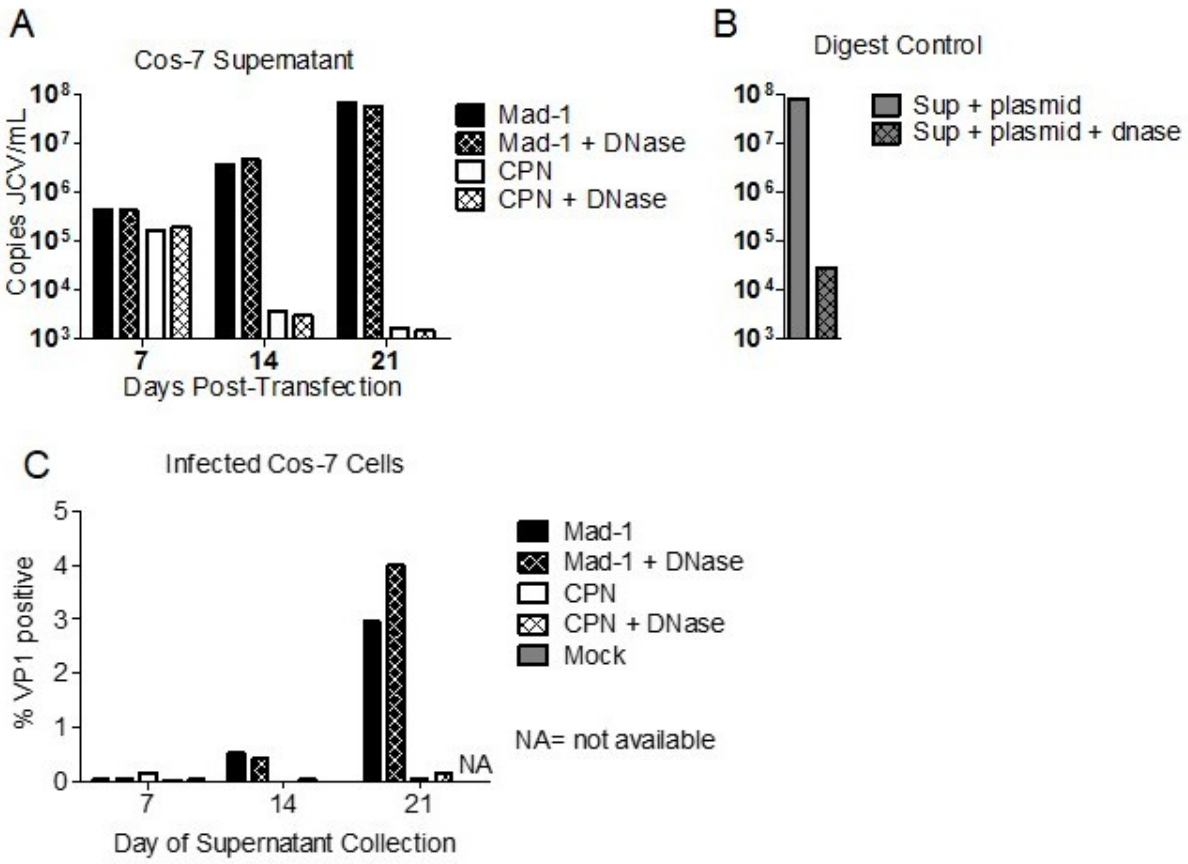

Figure 2.3 DNAse digestion of Supernatant from infected Cos-7 cells. (A-C) Supernatant collected from either JCV_{Mad-1} or JCV_{CPN} transfected Cos-7 cells was digested with DNAse, or mock digested by incubating only with Buffer. (A) qPCR was used to quantify the number of JCV genomes/mL Supernatant. Digestion with DNAse does not decrease the amount of DNA detected in either JCV_{Mad-1} or JCV_{CPN} containing supernatant. (B) To determine if the DNAse digestion conditions would digest JCV DNA, JCV_{Mad-1} plasmid was added to supernatant from JCV negative cells and digested with DNAse. This digestion caused an almost 4 log drop in copies JCV/mL supernatant. (C) Digested or mock digested Cos-7 supernatant was used to infect Cos-7 cells. The percentage of VP1 positive cells was determined by Flow Cytometry. Digestion did not decreased the amount of observed infection.

JCV_{Mad-1} containing supernatant from Cos-7 cells was able to establish an infection in the new cells, with the viral load and the percentage of cells infected increasing with supernatant collected at later time points post-transfection (Figure 2.4A and 2.4B). The percentage of VP1 positive cells was significantly higher than in the samples treated with supernatant from mock transfected cells (Figure 2.4B). In contrast, cells infected with JCV_{CPN} containing supernatant had significantly lower levels of viral DNA detected, which decreased over time, becoming undetectable in samples infected with supernatant collected 21 days post transfection (Figure 2.4A). The percentage of JCV_{CPN} VP1 positive cells was not significantly higher than observed with Mock supernatant (Figure 2.4B), which is most likely due to the lack of detectable expression of VP1 protein in JCV_{CPN} transfected cells.

Similar results were seen using supernatant from transfected SVG and IMR-32 cells, with low levels JCV DNA detected in cells infected with JCV_{CPN} containing supernatant collected 7 days post-transfection, and then decreasing (Figure 2.4C and 2.4D). Using supernatant from SVG cells, JCV_{CPN} DNA remains detectable with supernatant collected 14, but not 21, days post-transfection and JCV_{Mad-1} infected cells had DNA levels that were significantly higher than those observed with JCV_{CPN} at all time points (Figure 2.4C). In contrast to the results observed using Cos-7 supernatant, the viral loads in JCV_{Mad-1} infected cells decreased with later collection points using SVG supernatant (Figure 2.4C). Cells infected with supernatant collected 14 and 21 days post-transfection from IMR-32 cells had undetectable JCV_{CPN} DNA levels (Figure 2.4D). JCV_{Mad-1} DNA was detected in cells infected with supernatant collected from

IMR-32 cells at 7 and 21 days, but not 14 days, post-transfection (Figure 2.4D). This is most likely due to the levels of JCV DNA being below the limit of detection of our assay.

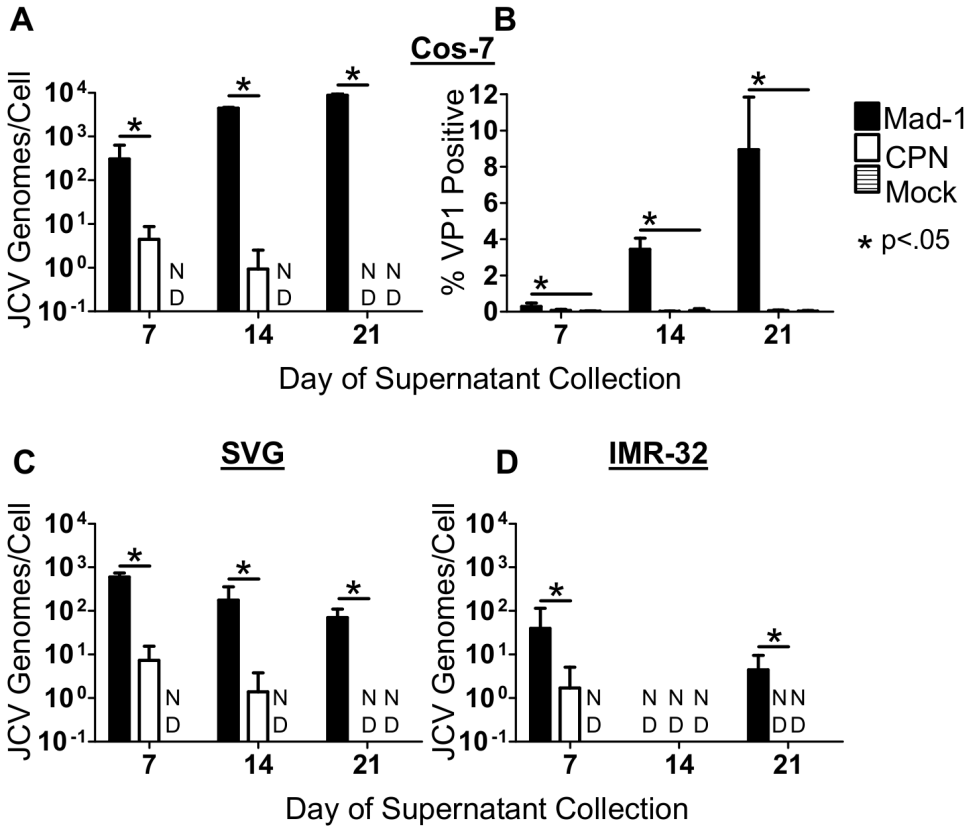

Figure 2.4 JCV_{CPN} transfected IMR-32, SVG and Cos-7 cells produce low levels of infectious virions. Supernatant from transfected Cos-7, SVG and IMR-32 cells was collected 7, 14 and 21 days post-transfection, and used to infect naive Cos-7 cells. At 7 days post-infection, cells were collected and either analyzed for JCV DNA using QPCR (A, C and D) or stained for VP1 and analyzed using flow cytometry (B). Supernatant collected 7 days post-transfection from JCV_{CPN} transfected Cos-7 (A), SVG (C) or IMR-32 (D) cells can establish an infection in naïve Cos-7 cells, as measured by the presence of JCV DNA 7 days post-infection. Levels of DNA detected with JCV_{CPN} infection are significantly lower than with JCV_{Mad-1} infection (A, C and D). (B) VP1 positive cells are detected after infection with JCV_{Mad-1}, but not JCV_{CPN} containing supernatant. Data is the average of 3-4 independent experiments. Error bars represent standard deviation. P vales were calculated using Wilcoxon rank test for QPCR data, comparing JCV_{CPN} to JCV_{Mad-1}. P-values for flow cytometry data were calculated using students t test, comparing JCV_{Mad-1} and JCV_{CPN} to mock at each time point. ND is not detected.

Generation of chimeras and agnogene mutants. The results of the above experiments comparing JCV_{CPN} and JCV_{Mad-1} suggest that JCV_{CPN} has a block preventing late gene expression and protein production, as well as in the production and release of infectious virions. The two major regions of difference between JCV_{CPN} and JCV_{Mad-1} are the RR and the agnogene. To determine which area of the virus is the major contributor to the phenotype of JCV_{CPN}, we generated chimeric viruses of JCV_{CPN} and JCV_{Mad-1} (Figure 2.5). We swapped the agnogene genes of the two viruses to generate Mad-1 C-Agno and CPN M-Agno. Mad-1 C-RR and CPN M-RR were generated by exchanging the RRs of the two viruses. We obtained two agno deletion mutations, Mad-1 Pt, which has a start codon point mutation which prevents the expression of agnoprotein, and Mad-1 Del, which has the entire agnogene deleted. CPN M-Pt contains the full length agnogene with the start codon point mutation from Mad-1 Pt. We studied these additional mutants in Cos-7 cells, because these cells displayed the greatest difference in phenotype between JCV_{Mad-1} and JCV_{CPN}.

The agnogene deletion is the major contributor to the phenotype of JCV_{CPN}. To begin characterizing the phenotypes of the viruses shown in Figure 2.5, linearized DNA was transfected into Cos-7 cells, and JCV DNA levels in cell lysate and supernatant were monitored for 3 weeks using QPCR (Figure 2.6). Mad-1 C-Agno has significantly lower levels of DNA from 10-21 days post-transfection compared to JCV_{Mad-1}, while Mad-1 C-RR has DNA levels similar to JCV_{Mad-1} (Figure 2.6A and 2.6C). This indicates that introducing the agnogene deletion of JCV_{CPN} into JCV_{Mad-1} results in a decrease in DNA replication. In contrast, the introduction of the JCV_{CPN} RR does not.

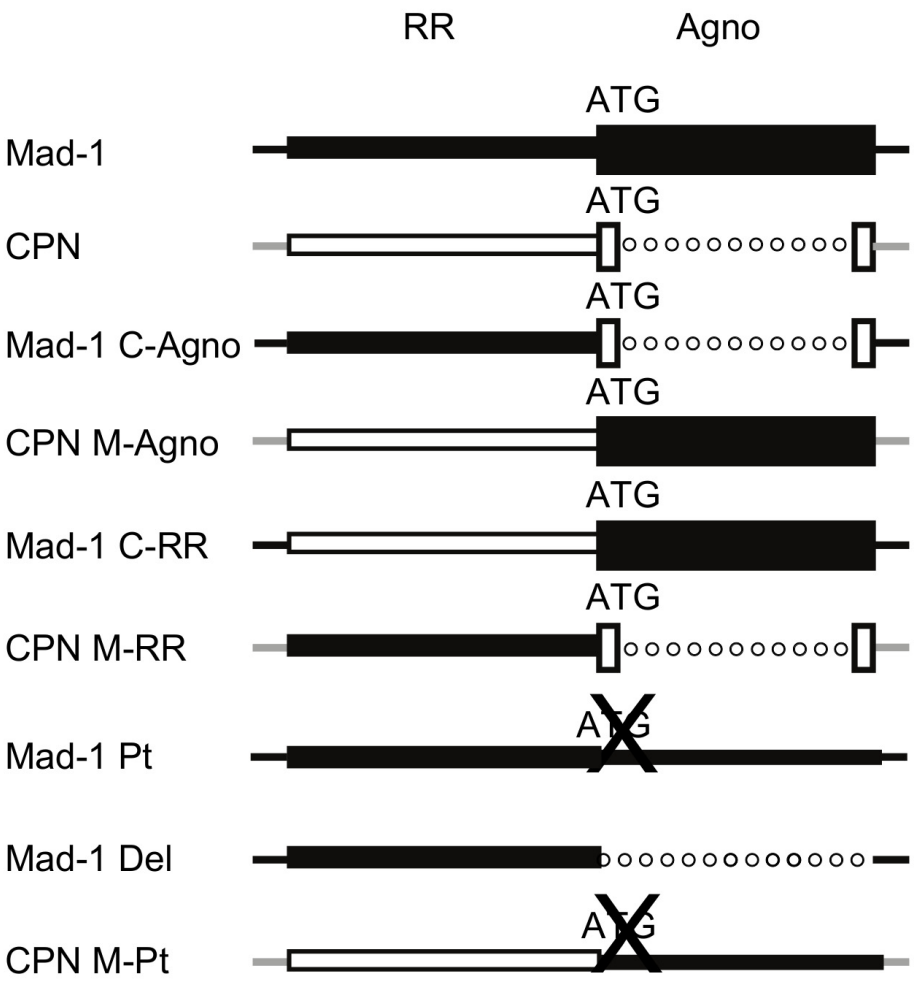

Figure 2.5 $JCV_{Mad\text{-}1}$ and JCV_{CPN} chimeras and agno deletion mutants. This diagram shows the various chimeric viruses and deletion mutants generated. Black represents sequences from $JCV_{Mad\text{-}1}$ and white represents sequences from JCV_{CPN}. Lines represent DNA sequences. Dotted Lines represent deletions. Boxes represent genes. An X through ATG represents mutation of the start codon to eliminate protein expression. Mad-1 C-Agno is $JCV_{Mad\text{-}1}$ with the JCV_{CPN} agnogene introduced. CPN M-Agno is JCV_{CPN} with a full length agnogene from $JCV_{Mad\text{-}1}$ introduced. Mad-1 C-RR is $JCV_{Mad\text{-}1}$ with the JCV_{CPN} RR and CPN M-RR is JCV_{CPN} with the $JCV_{Mad\text{-}1}$ RR. Mad-1 Pt is $JCV_{Mad\text{-}1}$ with a mutated start codon which prevents the expression of the agnoprotein and Mad-1 Del is $JCV_{Mad\text{-}1}$ with the entire agnogene deleted. CPN M-Pt is JCV_{CPN} with the agnogene of Mad-1 Pt.

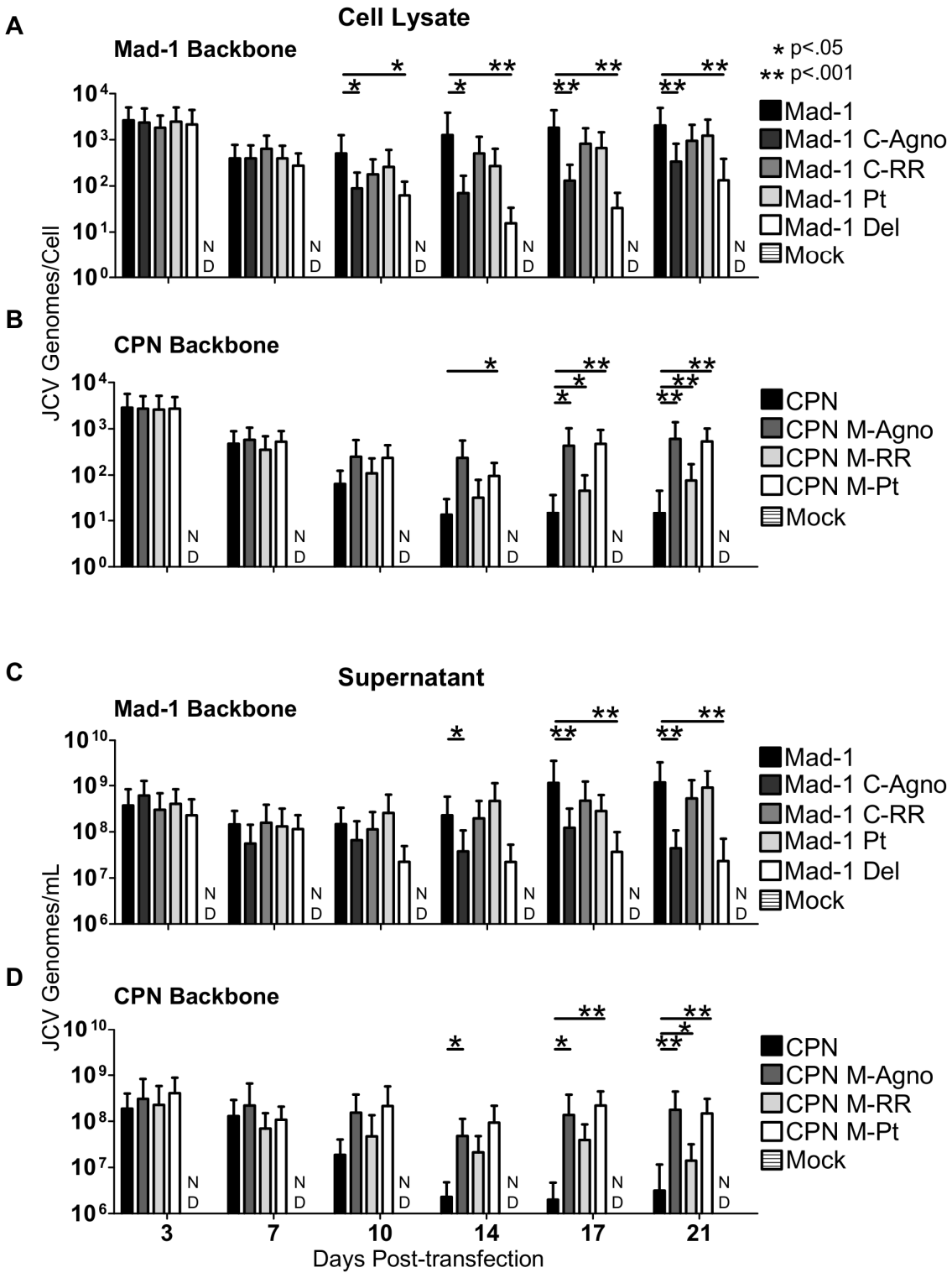

Figure 2.6 The agnogene deletion of JCV_{CPN} is the primary cause of its replication defect. Linearized JCV DNA of JCV_{Mad-1}, Mad-1 C-Agno, Mad-1 C-RR, Mad-1 Pt, Mad-1 Del, JCV_{CPN}, CPN M-Agno, CPN M-RR, and CPN M-Pt were

Figure 2.6 (Continued). transfected into Cos-7 cells and DNA levels were quantified over 3 weeks, as described in Figure 2.1. (A and C) Levels of DNA with JCV_{Mad-1} and the chimeras and agno deletion viruses on the JCV_{Mad-1} backbone were measured in the cell lysate (A) and supernatant (C). Mad-1 C-Agno and Mad-1 Del show significantly lower levels of DNA late in infection. (B and D) Levels of DNA with JCV_{CPN} and the chimeras and agno deletion viruses on the JCV_{CPN} backbone were measured in the cell lysate (B) and supernatant (D). Introduction of a full length agnogene causes the greatest increase in DNA levels. Data represents the average of 4-10 independent experiments. Error bars represent standard deviation. P-values were calculated with the Wilcoxon Rank Test. ND is not detected.

This suggests that the major cause of the replication kinetics seen with JCV_{CPN} is the agnogene deletion, and the not the archetype-like RR. When comparing the agno deletion viruses to JCV_{Mad-1}, Mad-1 Pt has similar DNA levels, while Mad-1 Del had decreased levels late in infection similar to JCV_{CPN} (Figure 2.6A and 2.6C). This provides evidence that the gene deletion is more important than the loss of the agnoprotein for the observed phenotype. Furthermore, the results seen with the viruses on the JCV_{CPN} backbone support these conclusions. CPN M-Agno, with the full length agnogene and agnoprotein, and CPN M-Pt, with just a full length agnogene, have the greatest increase of JCV DNA levels compare to JCV_{CPN}, and in both cases the level of DNA increase is similar (Figure 2.6B and 2.6D). This supports the conclusion that the deletion in the agnogene causes the decreased replication ability of JCV_{CPN}. CPN M-RR, with the JCV_{Mad-1} RR, also show some increase in DNA levels, but to a lesser extent than CPN M-Agno (Figure 2.6B and 2.6D).

Deletion in the agnogene prevents expression of VP1 protein. We then sought to determine if the levels of VP1 protein expression would correspond with levels of viral DNA in cells transfected with the chimeras and agno deletion mutants. Western

blots were done for VP1 expression in JCV transfected Cos-7 cells. At 14 days post-transfection, only JCV_{Mad-1}, Mad-1 Pt, Mad-1 C-RR and CPN M-Agno have detectable levels of VP1 (Figure 2.7A). At 21 days post-transfection, all of these viruses and CPN M-Pt have detectable VP1 protein expression (Figure 2.7B). All of these viruses have full length agnogenes, but Mad-1 Pt does not have agnoprotein expression. Compared to JCV_{Mad-1}, Mad-1 Pt shows some decrease in VP1 expression, while Mad-1 Del has a complete lack of VP1 expression. All of the viruses with the JCV_{CPN} agnogene deletion, JCV_{CPN}, Mad-1 C-Agno and CPN M-RR lack VP1 expression (Figure 2.7A and 2.7B). Taken together, these results indicate that the deletion in the agnogene results in decreased or undetectable levels of VP1 protein expression, and that the levels of DNA replication correspond with the presence of VP1 protein expression.

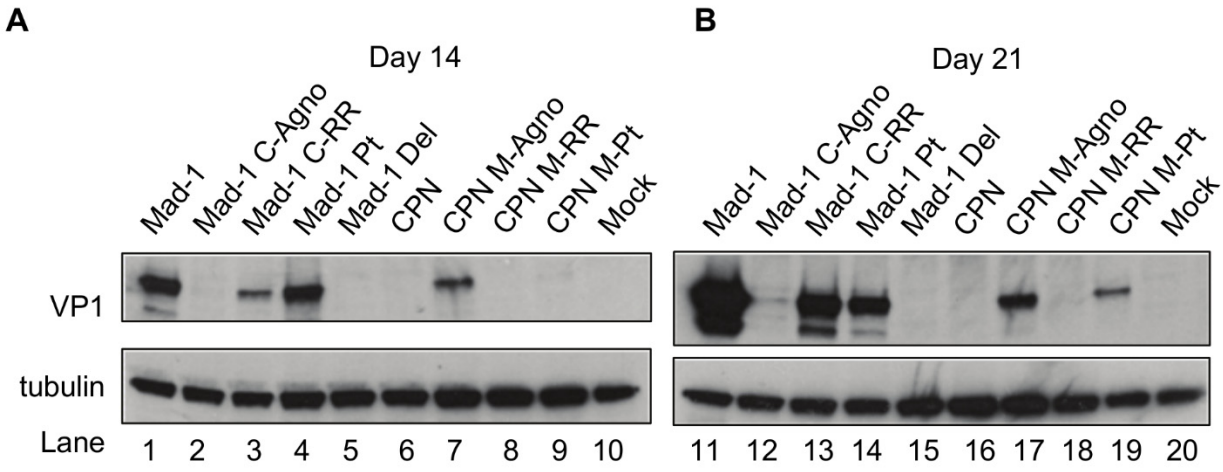

Figure 2.7 Deletion in the agnogene prevents VP1 expression. Western blots for VP1 were done as described in Figure 2.2. (A) VP1 levels in Cos-7 cell lysate 14 days post-transfection. (B) VP1 levels in Cos-7 cells 21 days post-transfection. Levels of VP1 expression are drastically reduced in Mad-1 C-Agno, and expression is rescued by the full length agnogene in CPN M-Agno. Deletion of the agnogene in Mad-1 Del results in a greater decrease in VP1 expression than just the prevention of the protein expression in Mad-1 Pt. Blots are representative of 3 or 4 independent experiments.

Deletions in the agnogene reduce the production of infectious virions.

Finally, we sought to determine if the ability to produce infectious virions of the chimeric and agno deletion viruses also corresponds with DNA levels and VP1 protein production in these cells. Supernatant collected from Cos-7 cells 21 days post-transfection was used to infect naïve Cos-7 cells, and the DNA levels (Figure 2.8A) and percentage of cells expressing VP1 (Figure 2.8B) were determined by QPCR and flow cytometry, respectively, at day 7. Compared to $JCV_{Mad\text{-}1}$-infected cells, both Mad-1 C-agno and Mad-1 Del infected cells have significantly lower viral loads, showing a 1.5-2 log decrease (Figure 2.8A). Mad-1 Pt and Mad-1 C-RR infected cells also have significantly lower viral loads than $JCV_{Mad\text{-}1}$ infected cells, but tended to have a smaller magnitude of decrease (Figure 2.8A). Mad-1 C-agno and Mad-1 Del infected cells have significantly lower percentages of cells expressing VP1, while Mad-1 Pt and Mad-1 C-RR infected cells do not (Figure 2.8B). CPN M-Agno, CPN M-RR and CPN M-Pt-infected cells all have detectable DNA levels, with significantly higher viral loads compared to JCV_{CPN} (Figure 2.8A). Compared with JCV_{CPN} infected cells, CPN M-Agno infected cells have a significantly higher percentage cells expressing VP1, and CPN M-Pt infected cells tended to have more cells expressing VP1. Interestingly, introduction of only the full length gene without protein expression in CPN M-Pt is enough to rescue the DNA levels, and show some increase in percent of cells expressing VP1.

The results of these infection experiments suggest that the deletion in the agnogene is the primary cause of the phenotype observed with JCV_{CPN}. However, CPN M-RR, with the $JCV_{Mad\text{-}1}$ RR does show some increase in DNA replication and

production of infectious virions compare to JCV_{CPN}, which may indicate that the RR composition is also affecting replication of the virus, but to a lesser degree than the agnogene deletion. It is likely that the combination of the agnogene deletion together with archetype-like RR is the cause of the overall phenotype of JCV_{CPN}. Overall, these experiments have used the unique naturally occurring JCV_{CPN} agnogene deletion and archetype-like RR to clarify the role of the agnogene and RR forms in JCV replication in cell culture.

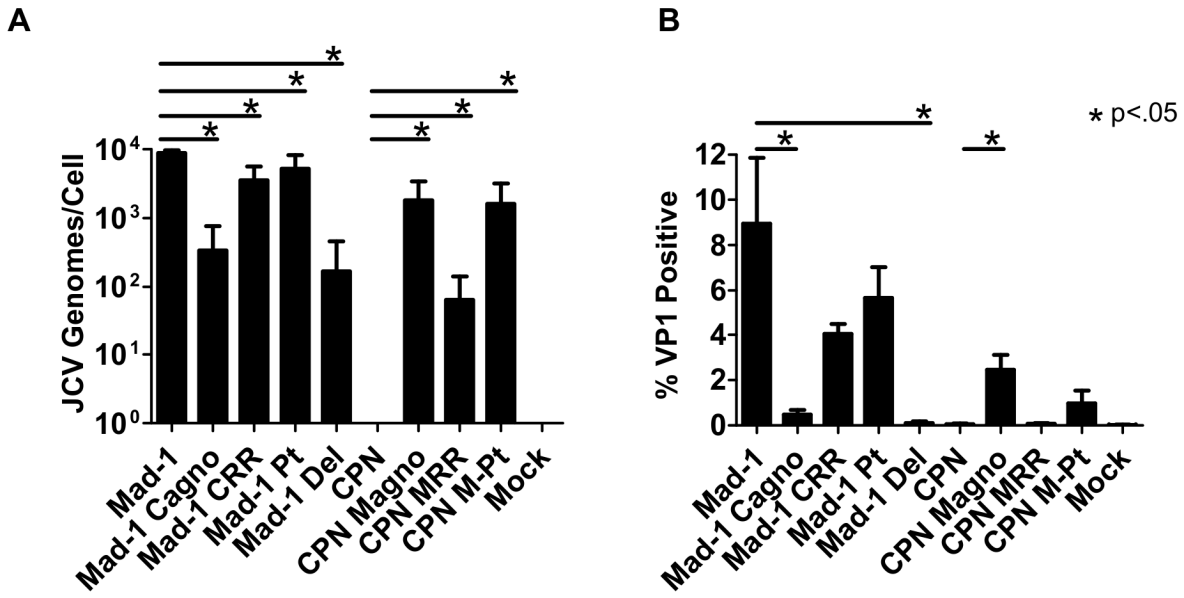

Figure 2.8 Loss of the agnogene results in decreased production of infectious virions. Supernatant was collected from Cos-7 cells 21 days post-transfection and used to infect naive Cos-7 cells. After 7 days, the cells were analyzed for (A) JCV DNA by QPCR or (B) VP1 expression by flow cytometry. Deletions in the agnogene in JCV_{Mad-1}-infected cells resulted in a significant decrease in JCV genomes/cell and percentage of cells expressing VP1, while introduction of a full length agnogene into JCV_{CPN} results in a significant increase in the viral load and percentage of cells expressing VP1. Data is the average of 3 independent experiments. Error bars represent standard deviation. P values were calculated using Wilcoxon rank test for QPCR data, comparing each virus to its parent virus, either JCV_{Mad-1} or JCV_{CPN}. P-vales for flow cytometry data were calculated using students t test using the same sets of comparisons. ND is not detected.

DISCUSSION

JCV_{CPN} was isolated from the brain of the first patient to be diagnosed with JCVE, a novel syndrome characterized by infection of cortical pyramidal neurons. JCV_{CPN} is the first naturally occurring isolate with a large deletion in the agnogene, which was originally called agno due to the unknown nature of its function. While studies have begun to shed light on the function of the agnoprotein and agnogene, there is still much to be learned. JCV_{CPN} presents the opportunity to study the function of the agnogene and agnoprotein in a naturally occurring pathogenic variant of JCV, isolated in association with infection of a new cell type.

In this study, we compared the replication of JCV_{CPN} to that of the prototype virus JCV_{Mad-1}. We used Cos-7 cells to model infection in kidney cells and SVG cells as a glial cell model. Both of these cell lines are widely used to study the replication of JCV in kidney and glial cells, and it is commonly thought that the results obtained in them are applicable to what would occur in these cell types during JCV infection in humans. Studying the replication of JCV in cortical pyramidal neurons is challenging, as there are no cortical pyramidal neuron cell lines available. We therefore used IMR-32 neuroblastoma cells to model neuronal infection. Using these cell lines allowed us to study the replication of JCV_{CPN} in different cell types in cell culture. We found that JCV_{CPN} was capable of replicating its genome in cell culture. However, it could not establish an infection at the same level observed with JCV_{Mad-1} over time and did not display any replication advantage over JCV_{Mad-1} in any cell line. Levels of JCV_{CPN} DNA replication in Cos-7 and IMR-32 cells were similar to JCV_{Mad-1} at early time points, and then decreased at later time points, indicating that the virus is able to replicate viral DNA

after transfection but the infection could not spread and persist in the cell culture at the same level as JCV_{Mad-1}. In addition, mRNA and VP1 protein analyses showed some decrease in early transcription and a marked decrease in late transcription, with no detectable VP1 protein production. In all three cell lines, low levels of infection were observed using supernatant from JCV_{CPN} transfected cells, but only using supernatant collected at early times post-transfection, and at levels significantly lower than seen with JCV_{Mad-1}. These data indicate that the virus has a block in late gene expression and protein production, which results in low levels of infectious virions being released, and an inability to sustain a persistent high level infection in cell culture. Furthermore, since agnoprotein has been implicated in the late stages of viral maturation, there may be an additional block at the level of virion formation and/or release independent of the lack of VP1 production.

JCV_{CPN} and JCV_{Mad-1} are different in two regions, the RR and the agnogene. This provided us with the unique opportunity to determine for the first time how each of these regions contributed to the phenotype of JCV_{CPN}. We therefore studied a series of chimeric viruses of the RR and agnogene. Interestingly, the agnogene deletion in JCV_{CPN} was the predominant cause of its phenotype, not the archetype-like RR. Moreover, the loss of the agnogene DNA had a larger effect on the replication of the virus than the loss of agnoprotein expression. Finally, the archetype-like RR also showed a detrimental effect on JCV_{CPN} replication, but of a smaller magnitude than that of the agnogene deletion. For these experiments we used Cos-7 cells, because they displayed the largest difference in phenotype between JCV_{CPN} and JCV_{Mad-1} and allowed us to use the greatest number of techniques to study these viruses. We believe

that the results obtained in these experiments are representative of what would be observed with the other cell lines used in this study.

Previous studies have implied that agnoprotein plays a role in viral DNA replication (23, 24). However, JCV_{CPN} is able to produce levels of DNA similar to JCV_{Mad-1} early after transfection, with DNA levels decreasing with time. These results suggest that an agnogene-deletion mutant can indeed replicate DNA, but levels drop off due to blocks at later steps in infection, thereby preventing spread within the cell culture. Conflicting studies have associated agnoprotein with gene expression, with both the loss of agnoprotein (19, 30) or its presence (23, 26) suppressing activity of the late promoter of JCV in different experimental systems. Additionally, deletion of the full agnogene causes a greater decrease in VP1 expression than prevention of agnoprotein expression without deletion of the agnogene DNA (30). Our data shows that the deletion in the agnogene of JCV_{CPN} results in a block in late gene expression, impairing the release of virions capable of infecting new cells and propagating the infection in cell culture. This is consistent with the results of Akan et al (30) and highlights the importance of the agnogene DNA in addition to the protein it codes for. Further studies are needed to determine the mechanism of the block in VP1 expression. One possibility is that a host cell factor which binds to one of the sites in the agnogene, identified by Akan et al (30), is involved in expression of the late transcript. Further investigations to identify these cellular proteins are warranted to determine the mechanism by which they act during JCV replication. Another potential mechanism is that deletions in the agnogene somehow alter the splicing or translation of VP1 from the late mRNA.

Previous studies of JCV deletion mutants lacking agnoprotein expression have implicated the agnoprotein in genome packaging and/or virion formation and release, with empty capsids being produced by viruses lacking the agnoprotein (27, 28). In our study however, the agnoprotein start codon point mutant was able to replicate its DNA and produce infectious virions at a level similar to JCV_{Mad-1} in Cos-7 cells, which suggests that at least in these cells, the agnoprotein is not necessary for formation and release of virions containing viral genomes.

Archetype RR is typically found in the urine, but the JCV_{CPN} RR isolated from the brain of the JCVE patient is archetype-like. Studies of the replication of different forms of RR have shown that archetype RR form has less active early and late promoters (36). Surprisingly, our study did not find the archetype-like RR of JCV_{CPN} to be the primary cause of the decreased levels of late transcription and VP1 protein expression. Introducing the archetype-like RR of JCV_{CPN} into JCV_{Mad-1} had little effect on the ability of the virus to replicate. JCV_{Mad-1} RR introduced into JCV_{CPN} partially rescues replication, but had a lesser impact than introduction of a full length agnogene. In fact the archetype-like RR only has a significant impact on the virus once it has already been impaired by a deletion in the agnogene, indicating that not all archetype-like RR forms found in nature lead to lower levels of viral replication.

While JCV_{CPN} was unable to establish a persistent infection in our cell culture model, it was found at high levels in the brain of the JCVE patient. JCV_{CPN} does produce some infectious virions in cell culture, but at much lower levels than JCV_{Mad-1}. This does not, however, mean that the virus was unable to establish an infection in the brain of the JCVE patient. There are limitations to the cell culture model we utilized in

this study. First, the infection in a person can take place on the timescale of years to decades, while our experiments were done over weeks. Second, this individual was also infected with a strain of JCV with a full length agnogene and agnoprotein, which may have influenced the replication of JCV_{CPN}. Third, it may be that having low levels of replication in the brain was actually advantageous to the virus while faced with a healthy immune system, allowing it to accumulate until the immune system became compromised and JCVE developed.

After observing the infection of granule cell neurons in JCV GCN and cortical pyramidal neurons in JCVE, we conducted studies to determine if infection of neurons by JCV was limited to these syndromes, or if it is more widespread. Based on staining of PML brain samples, it is predicted that up to 51% of patients have granule cell neurons infected by JCV (37). Additionally, infection of cortical neurons by JCV in classic PML cases has been observed with infection present in the gray white junction and gray matter (38). These studies demonstrate that infection of neurons occurs in a large number of PML patients, and is not limited to patients with JCV GCN or JCVE. Further studies of the molecular composition of JCV in neurons of patients with classic PML are needed to determine whether these cells are also infected by JCV-deletion mutants.

The study of unique pathogenic isolates of JCV, such as JCV_{CPN} or JCV_{GCN} allows us to decipher the basic biology of JCV replication using mutations that have arisen naturally during infection in humans. Our studies of JCV_{CPN} have provided valuable insights into both the function of the agnogene and agnoprotein, as well as a naturally occurring variation of the regulatory region, on JCV replication. Our results

have helped clarify the role of the agnogene and agnoprotein in DNA replication, transcription and protein expression, demonstrating that a deletion in the agnogene has a dramatic effect on the expression of VP1 protein and the production of infectious virions. Further studies of naturally occurring variants of JCV will continue to add clarity to our understanding of the biology of JCV replication and pathogenesis.

Acknowledgements:

We would like to thank Dr. Long Ngo for advice in statistical analysis. We would like to thank Dr. Mahmut Safak for the generous gift of Mad-1 Pt and Mad-1 Del plasmids.

REFERENCES

1. Gheuens S, Wuthrich C, Koralnik IJ. 2013. Progressive multifocal leukoencephalopathy: why gray and white matter. *Annu Rev Pathol* 8: 189-215

2. Jensen PN, Major EO. 2001. A classification scheme for human polyomavirus JCV variants based on the nucleotide sequence of the noncoding regulatory region. *J Neurovirol* 7: 280-7

3. Tan CS, Ellis LC, Wuthrich C, Ngo L, Broge TA, Jr., Saint-Aubyn J, Miller JS, Koralnik IJ. 2010. JC virus latency in the brain and extraneural organs of patients with and without progressive multifocal leukoencephalopathy. *J Virol* 84: 9200-9

4. Ferenczy MW, Marshall LJ, Nelson CD, Atwood WJ, Nath A, Khalili K, Major EO. 2012. Molecular biology, epidemiology, and pathogenesis of progressive multifocal leukoencephalopathy, the JC virus-induced demyelinating disease of the human brain. *Clin Microbiol Rev* 25: 471-506

5. Tan CS, Koralnik IJ. 2010. Beyond progressive multifocal leukoencephalopathy: expanded pathogenesis of JC virus infection in the central nervous system. *Lancet Neurol* 9: 425-37

6. Knowles WA, Pipkin P, Andrews N, Vyse A, Minor P, Brown DW, Miller E. 2003. Population-based study of antibody to the human polyomaviruses BKV and JCV and the simian polyomavirus SV40. *J Med Virol* 71: 115-23

7. Weber T, Trebst C, Frye S, Cinque P, Vago L, Sindic CJ, Schulz-Schaeffer WJ, Kretzschmar HA, Enzensberger W, Hunsmann G, Luke W. 1997. Analysis of the systemic and intrathecal humoral immune response in progressive multifocal leukoencephalopathy. *J Infect Dis* 176: 250-4

8. Berger JR, Kaszovitz B, Post MJ, Dickinson G. 1987. Progressive multifocal leukoencephalopathy associated with human immunodeficiency virus infection. A review of the literature with a report of sixteen cases. *Ann Intern Med* 107: 78-87

9. Molloy ES, Calabrese LH. 2009. Progressive multifocal leukoencephalopathy: a national estimate of frequency in systemic lupus erythematosus and other rheumatic diseases. *Arthritis Rheum* 60: 3761-5

10. Shimizu N, Imamura A, Daimaru O, Mihara H, Kato Y, Kato R, Oguri T, Fukada M, Yokochi T, Yoshikawa K, Komatsu H, Ueda R, Nitta M. 1999. Distribution of JC virus DNA in peripheral blood lymphocytes of hematological disease cases. *Intern Med* 38: 932-7

11. Koralnik IJ, Wuthrich C, Dang X, Rottnek M, Gurtman A, Simpson D, Morgello S. 2005. JC virus granule cell neuronopathy: A novel clinical syndrome distinct from progressive multifocal leukoencephalopathy. *Ann Neurol* 57: 576-80

12. Du Pasquier RA, Corey S, Margolin DH, Williams K, Pfister LA, De Girolami U, Mac Key JJ, Wuthrich C, Joseph JT, Koralnik IJ. 2003. Productive infection of cerebellar granule cell neurons by JC virus in an HIV+ individual. *Neurology* 61: 775-82

13. Hecht JH, Glenn OA, Wara DW, Wu YW. 2007. JC virus granule cell neuronopathy in a child with CD40 ligand deficiency. *Pediatr Neurol* 36: 186-9

14. Wuthrich C, Dang X, Westmoreland S, McKay J, Maheshwari A, Anderson MP, Ropper AH, Viscidi RP, Koralnik IJ. 2009. Fulminant JC virus encephalopathy with productive infection of cortical pyramidal neurons. *Ann Neurol* 65: 742-8

15. Dang X, Vidal JE, Oliveira AC, Simpson DM, Morgello S, Hecht JH, Ngo LH, Koralnik IJ. 2012. JC virus granule cell neuronopathy is associated with VP1 C terminus mutants. *J Gen Virol* 93: 175-83

16. Dang X, Koralnik IJ. 2006. A granule cell neuron-associated JC virus variant has a unique deletion in the VP1 gene. *J Gen Virol* 87: 2533-7

17. Dang X, Wuthrich C, Gordon J, Sawa H, Koralnik IJ. 2012. JC virus encephalopathy is associated with a novel agnoprotein-deletion JCV variant. *PLoS One* 7: e35793

18. Khalili K, White MK, Sawa H, Nagashima K, Safak M. 2005. The agnoprotein of polyomaviruses: a multifunctional auxiliary protein. *J Cell Physiol* 204: 1-7

19. Okada Y, Endo S, Takahashi H, Sawa H, Umemura T, Nagashima K. 2001. Distribution and function of JCV agnoprotein. *J Neurovirol* 7: 302-6

20. Saribas AS, Arachea BT, White MK, Viola RE, Safak M. 2011. Human polyomavirus JC small regulatory agnoprotein forms highly stable dimers and oligomers: implications for their roles in agnoprotein function. *Virology* 420: 51-65

21. Sariyer IK, Akan I, Palermo V, Gordon J, Khalili K, Safak M. 2006. Phosphorylation mutants of JC virus agnoprotein are unable to sustain the viral infection cycle. *J Virol* 80: 3893-903

22. Sariyer IK, Khalili K, Safak M. 2008. Dephosphorylation of JC virus agnoprotein by protein phosphatase 2A: inhibition by small t antigen. *Virology* 375: 464-79

23. Safak M, Barrucco R, Darbinyan A, Okada Y, Nagashima K, Khalili K. 2001. Interaction of JC virus agno protein with T antigen modulates transcription and replication of the viral genome in glial cells. *J Virol* 75: 1476-86

24. Saribas AS, White MK, Safak M. 2012. JC virus agnoprotein enhances large T antigen binding to the origin of viral DNA replication: evidence for its involvement in viral DNA replication. *Virology* 433: 12-26

25. Sami Saribas A, Abou-Gharbia M, Childers W, Sariyer IK, White MK, Safak M. 2013. Essential roles of Leu/Ile/Phe-rich domain of JC virus agnoprotein in dimer/oligomer formation, protein stability and splicing of viral transcripts. *Virology* 443: 161-76

26. Safak M, Sadowska B, Barrucco R, Khalili K. 2002. Functional interaction between JC virus late regulatory agnoprotein and cellular Y-box binding transcription factor, YB-1. *J Virol* 76: 3828-38

27. Sariyer IK, Saribas AS, White MK, Safak M. 2011. Infection by agnoprotein-negative mutants of polyomavirus JC and SV40 results in the release of virions that are mostly deficient in DNA content. *Virol J* 8: 255

28. Suzuki T, Semba S, Sunden Y, Orba Y, Kobayashi S, Nagashima K, Kimura T, Hasegawa H, Sawa H. 2012. Role of JC virus agnoprotein in virion formation. *Microbiol Immunol* 56: 639-46

29. Suzuki T, Orba Y, Okada Y, Sunden Y, Kimura T, Tanaka S, Nagashima K, Hall WW, Sawa H. 2010. The human polyoma JC virus agnoprotein acts as a viroporin. *PLoS Pathog* 6: e1000801

30. Akan I, Sariyer IK, Biffi R, Palermo V, Woolridge S, White MK, Amini S, Khalili K, Safak M. 2006. Human polyomavirus JCV late leader peptide region contains important regulatory elements. *Virology* 349: 66-78

31. Frisque RJ, Bream GL, Cannella MT. 1984. Human polyomavirus JC virus genome. *J Virol* 51: 458-69

32. Gluzman Y. 1981. SV40-transformed simian cells support the replication of early SV40 mutants. *Cell* 23: 175-82

33. Major EO, Miller AE, Mourrain P, Traub RG, de Widt E, Sever J. 1985. Establishment of a line of human fetal glial cells that supports JC virus multiplication. *Proc Natl Acad Sci U S A* 82: 1257-61

34. Tumilowicz JJ, Nichols WW, Cholon JJ, Greene AE. 1970. Definition of a continuous human cell line derived from neuroblastoma. *Cancer Res* 30: 2110-8

35. Schmittgen TD, Livak KJ. 2008. Analyzing real-time PCR data by the comparative C(T) method. *Nat Protoc* 3: 1101-8

36. Ault GS. 1997. Activity of JC virus archetype and PML-type regulatory regions in glial cells. *J Gen Virol* 78 (Pt 1): 163-9

37. Wuthrich C, Cheng YM, Joseph JT, Kesari S, Beckwith C, Stopa E, Bell JE, Koralnik IJ. 2009. Frequent infection of cerebellar granule cell neurons by polyomavirus JC in progressive multifocal leukoencephalopathy. *J Neuropathol Exp Neurol* 68: 15-25

38. Wuthrich C, Koralnik IJ. 2012. Frequent infection of cortical neurons by JC virus in patients with progressive multifocal leukoencephalopathy. *J Neuropathol Exp Neurol* 71: 54-65

CHAPTER 3: Nucleotides 376-396 are critical for VP1 capsid protein expression

Laura C. Ellis[1,2,3] and Igor J. Koralnik[1,2]

[1]Division of Neurovirology, Department of Neurology, Beth Israel Deaconess Medical Center, Harvard Medical School, Boston, MA, USA

[2]Center for Virology and Vaccine Research, Department of Medicine, Beth Israel Deaconess Medical Center, Harvard Medical School, Boston, MA, USA

[3]Harvard Program in Virology, Harvard Medical School, Boston, Massachusetts, USA

Parts of this chapter are included in a manuscript submitted to *Virology*

Contributions: I designed and carried out the experiments and wrote the chapter. Igor Koralnik provided guidance on the experiments and writing.

ABSTRACT

JCV infection of the brain can cause PML, JCV GCN and JCVE. JCV_{CPN}, isolated from the brain of a patient with JCVE, is a naturally occurring strain of JCV with a 143 nucleotide deletion in the agnogene. Cell culture studies of JCV_{CPN} have shown that the loss of these nucleotides in the agnogene results in impaired expression of VP1 and infectious virion production. To better understand the role of this DNA sequence in JCV replication, we generated a series of deletions in the agnogene on the backbone of a virus which has a start codon mutation to prevent agnoprotein expression. We found that deletion of nucleotides 376-396 in the agnogene results in decreased levels of viral DNA replication and a lack of VP1 expression. These results indicate that these nucleotides play a role in JCV VP1 expression and replication. Previous studies have provided evidence of host cell factor binding sites in the agnogene. DNA-Immunoprecipitations were done using agnogene DNA to identify candidate host cell binding proteins. These proteins were visualized by SDS-PAGE and individual bands and entire samples were submitted for Mass Spectrometry analysis. Several candidate proteins, including poly (ADP-ribose) polymerase 1 (PARP-1), Ku70, Replication protein A 70 kDa DNA-binding subunit (RPA1) and General transcription factor II-I (GTF2I), were identified, but none of these proved to bind specifically to the JCV agnogene DNA.

INTRODUCTION

JCV is the etiological agent of the fatal demyelinating disease PML, as well as the more recently described JCV GCN and JCVE (1-3). JCV infection is widespread and asymptomatic in healthy individuals (4, 5). Individuals with immune suppression, such as those with AIDS (6), organ transplants (7) and hematological malignancies (8), are at risk for developing PML.

JCV is a polyomavirus with a circlular double stranded DNA genome. The genome has 3 regions, the highly conserved early and late coding regions and the hypervariable RR (9). The regulatory proteins small t ag and large T Ag are encoded by the early coding region while the structural proteins VP1, VP2 and VP3 and the agnoprotein are encoded by the late coding region (9). The origin of replication and the early and late promoters are contained by the RR (10).

The agnoprotein of JCV is a 71 amino acid, highly basic protein that is non-essential for viral infection (11). It is expressed late in infection, primarily in the cytoplasm, and is not incorporated into virions (11, 12). Recent studies of agnoprotein function have begun to shed light on its roles in JCV replication, but there is still much to be learned. The agnoprotein can be phosphorylated (13, 14) and form both homodimers and oligomers, an interaction which is mediated by the Leu/Ile/Phe rich domain of the protein (15, 16). The agnoprotein has been implicated in a number of different viral processes, including DNA replication (16, 17), gene expression and splicing of viral transcripts (12, 15, 17, 18), early and late protein expression (19) and virion formation and release (19, 20). It has also been reported that agnoprotein may act as a viroporin (21). While these studies have given insights into agnoprotein function, the exact mechanisms of action are still unclear.

Studies have shown that deleting the agnogene DNA is more detrimental to JCV replication than loss of agnoprotein expression without deletion of the DNA sequence, indicating that the agnogene may contain a cis-acting regulatory element (22, 23). Additionally, 3 potential host-factor binding sites have been identified in the agnogene through nuclease protection and gel shift assays (22). These binding sites are nucleotides 350-411 (binding site III), 442-458 (binding site II) and 458-475 (binding site I) (22).

JCV_{CPN} was isolated from the brain of a patient with JCVE, and has an archetype-like RR and a 143-bp deletion from nucleotide 300-442 in the agnogene (24). It was named JCV_{CPN} because it causes productive infection in cortical pyramidal neurons. This was the first time a large deletion in the agnogene was isolated in a naturally occurring viral isolated. We have recently studied the replication of JCV_{CPN} in cell culture to better understand both the pathogenesis of JCVE and the role of the RR and agnogene in JCV replication (23). Our results indicated that, in cell culture, JCV_{CPN} was incapable of establishing a high level persistent infection compared to the prototype strain JCV_{Mad-1} and that this was due to a lack of VP1 expression and infectious virion release (23, 25). Further experiments identified the deletion in the agnogene, specifically the loss of the agnogene DNA more so than the loss of a full length agnoprotein, as the primary cause of this phenotype (23).

To further characterize the role of the agnogene in JCV replication, we generated a series of small deletions in the agnogene. All of the deletions were introduced into JCV_{Mad-1} with a mutated agnoprotein start codon (Mad-1 Pt), which prevents agnoprotein expression. This allowed us to study the function of the deleted regions in isolation from the functions of the agnoprotein. We compared the

replication of these deletion mutants to JCV_{Mad-1} in cell culture by measuring DNA replication, early and late mRNA expression and VP1 protein production to identify smaller regions of the agnogene which are crucial for viral replication. We attempted to identify the host cell proteins which bind to the agnogene DNA through Mass Spectrometry (MS) of proteins from DNA-Immunoprecipitations (DNA-IP) done using JCV agnogene DNA. Candidate proteins were identified, but none have been found to bind specifically to the agnogene DNA.

MATERIALS AND METHODS

Cell Lines Cos-7 (26), SVG (27), IMR-32 (28) and 293T cells were purchased from the ATCC. Cos-7 and 293T cells were maintained in DMEM supplemented with 10% FBS, 500 units/mL Penicillin and 500 µg/mL Streptomycin. SVG cells were maintained in MEM supplemented with 10% FBS, 500 units/mL Penicillin, 500 µg/mL Streptomycin, and 1.5g/L Sodium Bicarbonate. IMR-32 cells were maintained in MEM with 10% FBS, 500 units/mL Penicillin, 500 µg/mL Streptomycin, 1.5g/L Sodium Bicarbonate, 1 mM Sodium Pyruvate and Non-Essential Amino Acids (Invitrogen).

Plasmids Construction of JCV_{Mad-1} and JCV_{CPN} plasmids was previously described by Dang et al. (24). Construction of Mad-1 Pt, Mad-1 Del and Mad-1 C-Agno was previously described by Ellis et al (23). Additional agnogene deletion mutants were introduced using the QuikChange Lightening Site-Directed Mutagenesis Kit (Stratagene) according to the manufacturer's protocol. All deletions were made on the Mad-1 Pt backbone. The primer sequences used were: Mad-1 PtDel300-349 (del300-349F 5'-GGTTCTTCGCCAGCTGTCACGCTCAAAGGATTTTAATTTTTTT-3' and del300-349R 5'-AAAAAAATTAAAATCCTTTGAGCGTGACAGCTGGCGAAGAACC-3'), Mad-1 PtDel350-411 (del350-411F 5'-CTGGAGTGGAACTAAAAAAAGAGGTAGACGGGAAAAAAAGAC-3' and del350-411R 5'- GTCTTTTTTTCCCGTCTACCTCTTTTTTTAGTTCCACTCCAG-3'), Mad-1 PtDel442-458 (del442-458F 5'-AAAAAAAGACAGAGACACAGTATACAGTGCTTTGCCTGAACC-3' and del442-458R 5'-GGTTCAGGCAAAGCACTGTATACTGTGTCTCTGTCTTTTTTT-3'), Mad-1

PtDel356-376 (del356-376F 5'-GTGGAACTAAAAAAAGAGCTCAAAAATTTTTGCTGGACTTTTGCACAG-3' and del356-376R 5'-CTGTGCAAAAGTCCAGCAAAAATTTTTGAGCTCTTTTTTTAGTTCCAC-3'), Mad-1 PtDel376-396 (del376-396F 5'-TAAAAAAAGAGCTCAAAGGATTTTAATTTTTTTGTTAACAGGTGAAGACAGTGTAG-3' and del376-396R 5'-CTACACTGTCTTCACCTGTTAACAAAAAAATTAAAATCCTTTGAGCTCTTTTTTTA-3'), Mad-1 PtDel300-432 (del300-432F 5'-TTCGCCAGCTGTCACGTAGACACAGTGGTTTG-3' and del300-432R 5'-CAAACCACTGTGTCTACGTGACAGCTGGCGAA-3'), Mad-1 PtDel310-442 (del310-442F 5'-GTCACGTAAGGCTTCTGGTTTGACTGAGCAGACA-3' and del310-442R 5'-TGTCTGCTCAGTCAAACCAGAAGCCTTACGTGAC-3') and Mad-1 PtDel411-442 (del411-442F 5'-GCACAGGTGAAGACAGGTTTGACTGAGCAGAC-3' and del411-442R 5'-GTCTGCTCAGTCAAACCTGTCTTCACCTGTGC-3'). Plasmids were transformed into TOP10 (Invitrogen) or XL1-Blue cells (Agilent) and plasmid DNA was maxi prepped (QIAGEN). All plasmids were fully sequenced to confirm the presence of the desired deletions.

Transfection Full-length JCV genomes were digested out of the plasmid backbone using EcoRI (NEB). Digested DNA was run on a 0.8% agarose gel and the virus band (about 5kb) was purified using the QIAquick Gel Extraction Kit (QIAGEN). Cells were transfected with 2 µg of purified JCV DNA using FuGENE6 transfection reagent (Promega) in 6 well plates. 3 days post-transfection, cells were passaged 1:3 into T25 flasks, and subsequently every 3-4 days 1:4 in T25 flasks. Supernatant

and cell pellets were collected at each passage and stored at -80°C until further analysis.

DNA Extraction and QPCR DNA was extracted from cell pellets and supernatant samples using the QIAamp DNA Blood Mini Kit (QIAGEN) according to the manufacturer's protocol. QPCR was performed as previously described (23). An RNAse P primer/probe set (Applied Biosystems) was used to determine the number of input cells for each reaction and the copies JCV/cell as previously described (23). All samples were run in triplicate.

RNA Extraction and qRT-PCR RNA was extracted and reverse transcribed as previously described (23). QPCR was performed on a 7300 Real-time PCR System using Gene Expression Master Mix (Applied Biosystems). Primer probe sets spanning the Large T Ag splice site and located in the VP1 gene were used as previously described (23). TBP (Invitrogen) was used as the endogenous control to determine the relative quantity by the comparative C_T method (also known as the $\Delta\Delta$Ct method) (29). All samples were run in triplicate.

Western Blotting Cells were lysed for 30 minutes in TNN lysis buffer (50 mM TrisHCl pH 7.5, 150 mM NaCl, 0.1% NP40) with 0.2 mM Na-Orthovanadate and 1% protease inhibitor cocktail on ice. Cell lysate was centrifuged at 8000 rpm for 4 min to remove cell debris. Laemmli Buffer (Bio-Rad) was added and cell lysates were boiled for 10 min. Samples were run on a 10% SDS-PAGE gel in Tris/Glycine/SDS running buffer (Bio-Rad) and transferred to a nitrocellulose membrane using the iBlot system (Invitrogen) or run on 4-20% Tris-HCl SDS-PAGE gel and transferred to

PVDF membrane using the iBlot system. Membranes were blocked with 5% milk in PBST. Antibodies against VP1 (pAB597 1 mg/mL) diluted 1:1000, PARP-1 (Santa Cruz) diluted 1:200, Ku70 (Santa Cruz) diluted 1:200, RPA1 (Santa Cruz) 1:100, GTF2I (Santa Cruz) diluted 1:1000 or loading control anti-alpha tubulin [DM1A] (Abcam) in 2% milk in PBST was added and incubated overnight at 4^0C. Membranes were washed and incubated with HRP conjugated goat-anti mouse IgG secondary antibody (Bio-Rad) for 1 hour at room temperature, followed by detection with ECL Plus reagent (Thermo Scientific). Signal was detected on film.

Generation of Biotinylated JCV agnogene DNA probes. Biotinylated JCV agnogene DNA was generated by PCR amplification of the agnogene from JCV_{Mad-1} or JCV_{CPN} plasmid using the Phusion High-Fidelity polymerase (NEB) with one primer being 5'-biotinylated. The primers used were agnoPvuIR+biotin (5'-biotin-TACATTCGATCGCTATGTAGCTTTTGG-3') and agnoPstI (5'-AATAACTGCAGATGGTTCTTCGCCAG-3'). After PCR amplification the MinElute PCR purification kit (QIAgen) was used to remove any remaining biotinylated primer. Probes were checked by agarose gel electrophoresis to confirm that a fragment of the correct size had been generated. Control DNA fragments were amplified from the AmpR gene of the puc18 plasmid backbone. 220-bp and 75-bp regions were amplified to generate probes the same size as either the JCV_{Mad-1} or JCV_{CPN} agnogene. The primer sets used were AmpR1+biotin (5'-biotin-AGTCACAGAAAAGCATCTTACGGAT-3') and AmpR-F1 (5'-TATCACTCATGGTTATGGCAGCAC-3') and AmpR-R2+btion (5'-biotin-GGCGAACTACTTACTCTAGCTTCCC-3') and AmpR-F2 (5'-TGACTCCCCGTCGTGTACATAACTA-3').

Isolation of nuclear proteins. Nuclear proteins were isolated from 293T, IMR-32, SVG or Cos-7 cells that were either JCV negative or transfected with JCV_{Mad-1}. Cells were grown for 3-4 days. Nuclear proteins were extracted using the NE-PER Nuclear and Cytoplasmic Extraction Reagents Kit (Thermo Scientific) as directed by the manufacturer's protocol.

DNA-Immunoprecipitation Biotinylated DNA was bound to streptavidin conjugated magnetic beads (Dynabeads M-280, Invitrogen) by incubating at room temperature (RT) for 15 minutes with rocking. Beads were washed three times with 1X Bind and Wash Buffer (BW Buffer) (5 mM Tris-HCl, 0.5 mM EDTA and 0.5 M NaCl). Nuclear proteins were added to the beads with an equal volume of 2X BW Buffer (10 mM Tris-HCl, .5 mM EDTA and .5 M NaCl) and incubated overnight at 4^0C with rocking. Beads were washed three times with 1X PBS. To elute bound proteins, the beads were boiled for 5 minutes in .1% SDS and the supernatant containing the proteins was removed from the beads. A magnetic rack was used to separate beads from the supernatant.

Gel Analysis 10 µL eluted protein in 10 µL Laemmli Buffer (Bio-Rad) was run on a 4-20% Tris-HCl gel in Tris/Glycine/SDS buffer. Alternatively, larger volumes of eluted protein were concentrated by Trichloroacetic acid (TCA) precipitation, resuspended in 20 µL Laemmli buffer and run on 4-20% or 4-15% Tris-HCl gels. Gels were run at 100V for 1-1.5 hours. Protein was detected either with Coomassie Brilliant Blue Stain (Bio-Rad) or Silver Stain (Pierce Silver Stain Kit for Mass Spectrometry, Thermo Scientific), as directed by the manufacturer's protocol.

Mass Spectrometry To identify specific protein bands, individual bands stained with either Coomassie or Silver Stain were excised from a gel and placed in an eppendorf tube containing Milli-Q water. To identify all the proteins in a sample, the sample was run into a gel for 10 minutes, stained with Coomassie Brilliant Blue, and the band containing all proteins was excised from the gel and placed in an eppendorf tube containing Milli-Q water. Gel fragments were submitted to the Taplin Mass Spectrometry Facility for analysis (https://taplin.med.harvard.edu/).

Statistical analysis P values were calculated using SAS9.3 software. Before analysis, data was tested for normality. The non-parametric Wilcoxon Rank Test was used to determine p values for DNA levels. Univariate analysis to determine student's t p values was used for mRNA levels.

RESULTS

Generation of agnogene deletion mutants. Our previous studies have indicated that the deletion of nucleotides 300-442 in the agnogene in JCV_{CPN} leads to decrease viral replication and a lack of detectable VP1 expression (23). This phenotype is due primarily to the loss of nucleotides in the agnogene and not the loss of wild type agnoprotein expression. To further narrow down the regions of the agnogene which are critical for viral replication and VP1 expression, we generated a series of additional small agnogene deletion mutants. All additional deletions were introduced onto the Mad-1 Pt backbone, which has a mutated start codon to prevent expression of the agnoprotein, in order to investigate only the effects of deletions in the agnogene.

Figure 3.1 shows the locations of the additional mutants that were generated, as well as the locations of the predicted host cell protein binding sites (22). Mad-1 PtΔ300-349 encompasses the region from the beginning of the JCV_{CPN} deletion to the start of binding site III. Mad-1 PtΔ350-411 and Mad-1 PtΔ442-458 delete binding sites III and II, respectively. Both Mad-1 PtΔ356-376 and Mad-1 PtΔ376-396 are located within binding site III. Mad-1 PtΔ356-376 deletes a region predicted to be a possible transcription factor binding site by AliBaba 2 software (http://www.gene-regulation.com/pub/programs.html#alibaba2) (Figure 3.2) and Mad-1 PtΔ376-396 deletes a region of high homology between JCV, BKV and SV40. Mad-1 PtΔ300-432 and Mad-1 PtΔ310-442 encompass the region deleted in JCV_{CPN} (300-432) with the last 10 or first 10 nucleotides of the deletion added back, respectively. Finally, Mad-1 PtΔ411-442 is the region between binding sites III and II. As controls, we used the previously characterized viruses Mad-1 Pt, a start codon deletion mutant,

Mad-1 Del, a full agnogene deletion mutant (22), and Mad-1 C-Agno JCV_{Mad-1} with the JCV_{CPN} agnogene, which has a deletion of nucleotides 300-442 (23).

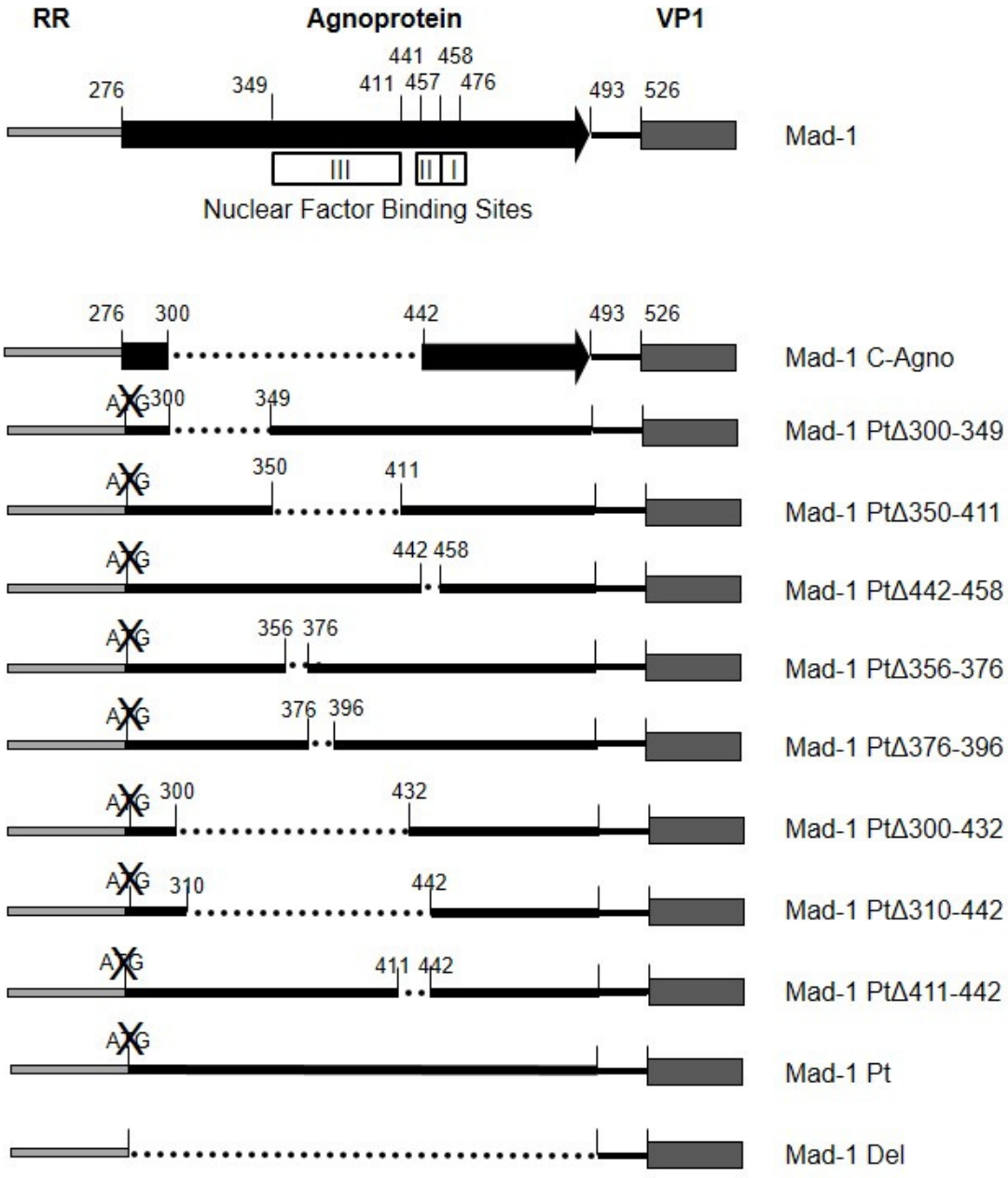

Figure 3.1 Agnogene deletion mutants. This diagram shows all of the viruses used in this study. Boxes represent open reading frames. Lines represent DNA sequences. Dotted lines represent deletions. ATG with an X through it indicates a mutated start codon preventing agnoprotein expression. Nuclear factor binding sites indicate the regions identified by Akan et al. 2006 (22).

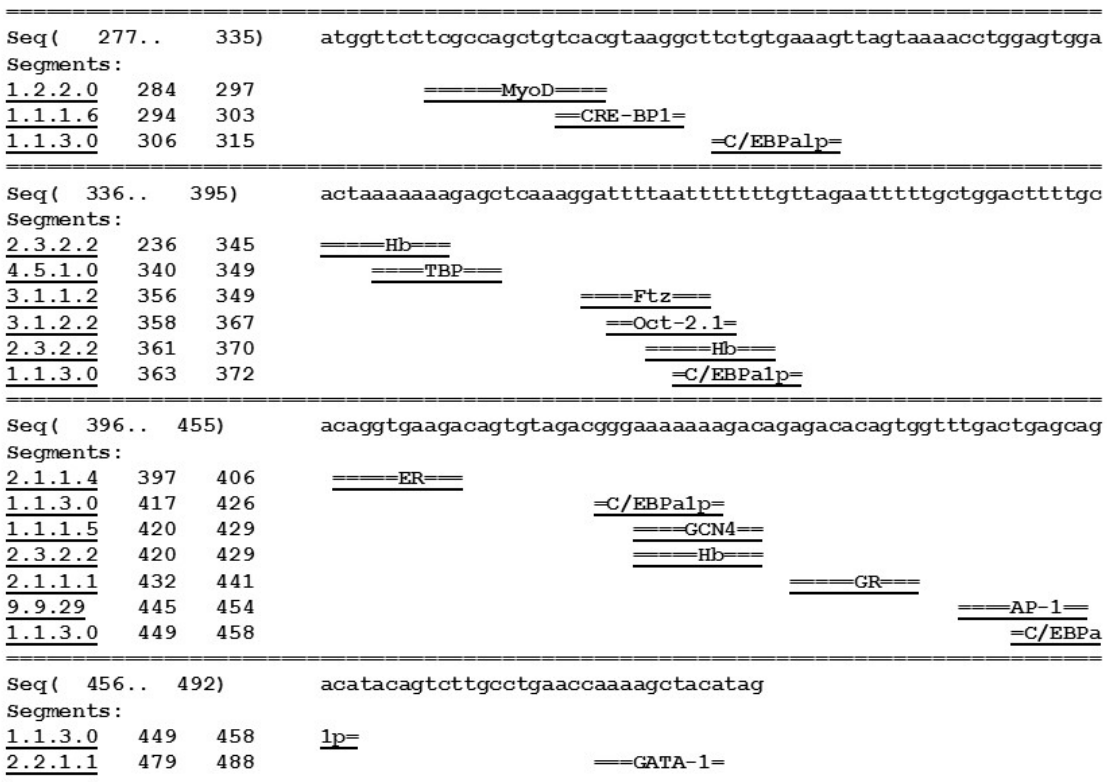

Figure 3.2 Predicted transcription factor binding sites in the agnogene DNA. The JCV_{Mad-1} agnogene sequence was analyzed using the AliBaba2.1 transcription factor binding site prediction software.

Figure 3.3 Alignment of the agnogene sequences of JCV, BKV and SV40. Nucleotides 376-396 of JCV and the corresponding residues in BKV and SV40 are highlighted in red.

Deletion of nucleotides 376-396 decreases levels of viral DNA replication at late time points post-transfection. Linearized JCV genomes were transfected into Cos-7 cells and viral DNA was quantified in the supernatant (Figure 3.4A) and cell lysate (Figure 3.4B) by qPCR 3, 7, 10, 14, 17 and 21 days post-transfection. As previously reported, Mad-1 C-Agno and Mad-1 Del show lower levels of viral DNA in the supernatant and cell lysate from 14-21 days post-transfection compared to JCV_{Mad-1} (23). Most of the new agnogene deletion mutants have replication levels similar to JCV_{Mad-1} and Mad-1 Pt. Interestingly, Mad-1 PtΔ376-396 has drastically decreased levels of JCV DNA in the supernatant and cell lysates at later times post-transfection, similar to Mad-1 C-Agno and Mad-1 Del. Levels of Mad-1 PtΔ376-396 DNA are significantly lower than JCV_{Mad-1} starting 10 days post-transfection in cell lysate and 17 days post-transfection in supernatant. This indicates that nucleotides 376-396 are important for JCV replication.

Deletion of nucleotides 376-396 results in decreased levels of late mRNA expression. RNA was extracted from JCV transfected Cos-7 cells 3, 7 and 10 days post-transfection. RNA was reverse transcribed to cDNA and levels of early (T Ag) and late (VP1) mRNA were determined using qPCR. While there was some decrease in T Ag mRNA expression 10 days post-transfection with most of the deletion mutants, there were no significant decreases observed (Figure 3.5A). Greater differences in expression levels were observed for VP1 mRNA, although none were statistically significantly lower (Figure 3.5B). The greatest decrease in late mRNA expression was seen with Mad-1 PtΔ376-396, which has levels equivalent to Mad-1 Del 7 and 10 days post-transfection. Additionally, Mad-1 PtΔ300-432 and Mad-1 PtΔ310-442 also have decreased levels of VP1 mRNA

expression 7 and 10 days post-transfection. These results indicate that nucleotides 376-396 are involved in the expression of late mRNAs.

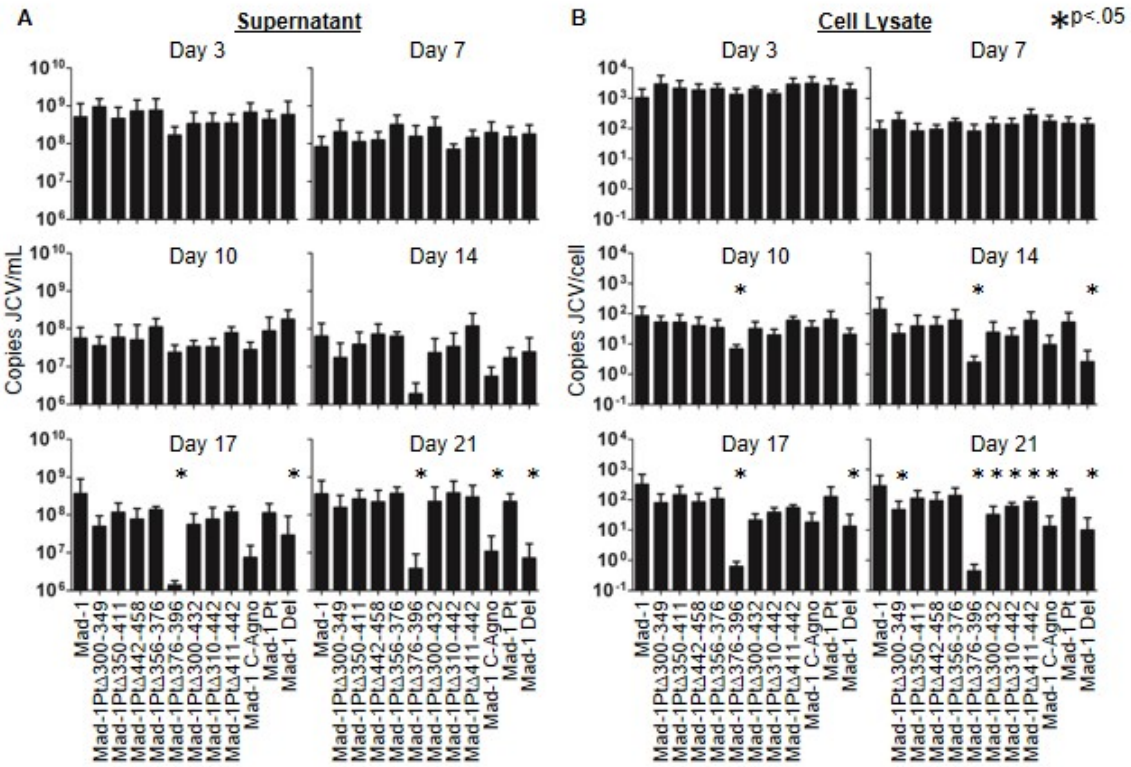

Figure 3.4. Deletion of nucleotides 376-396 reduces viral DNA replication. Cos-7 cells were transfected with linearized JCV genomes and cells were subcultured every 3-4 days. DNA was extracted from the supernatant and cell samples, digested with DpnI to remove input plasmid DNA, and analyzed by QPCR. Data represents the average of 3-5 independent experiments. In supernatant (A) and cell lysate (B) samples, Mad-1 PtΔ376-396 has decreased levels of viral DNA compared to JCV_{Mad-1} at 17-21 days post-transfection in supernatant and 10-21 in cell lysate. Mock transfected cells remained JCV negative. Error bars represent standard deviation. P-values were calculated for all viruses compared to JCV_{Mad-1} using the Wilcoxon Rank Test. * indicates $p<.05$

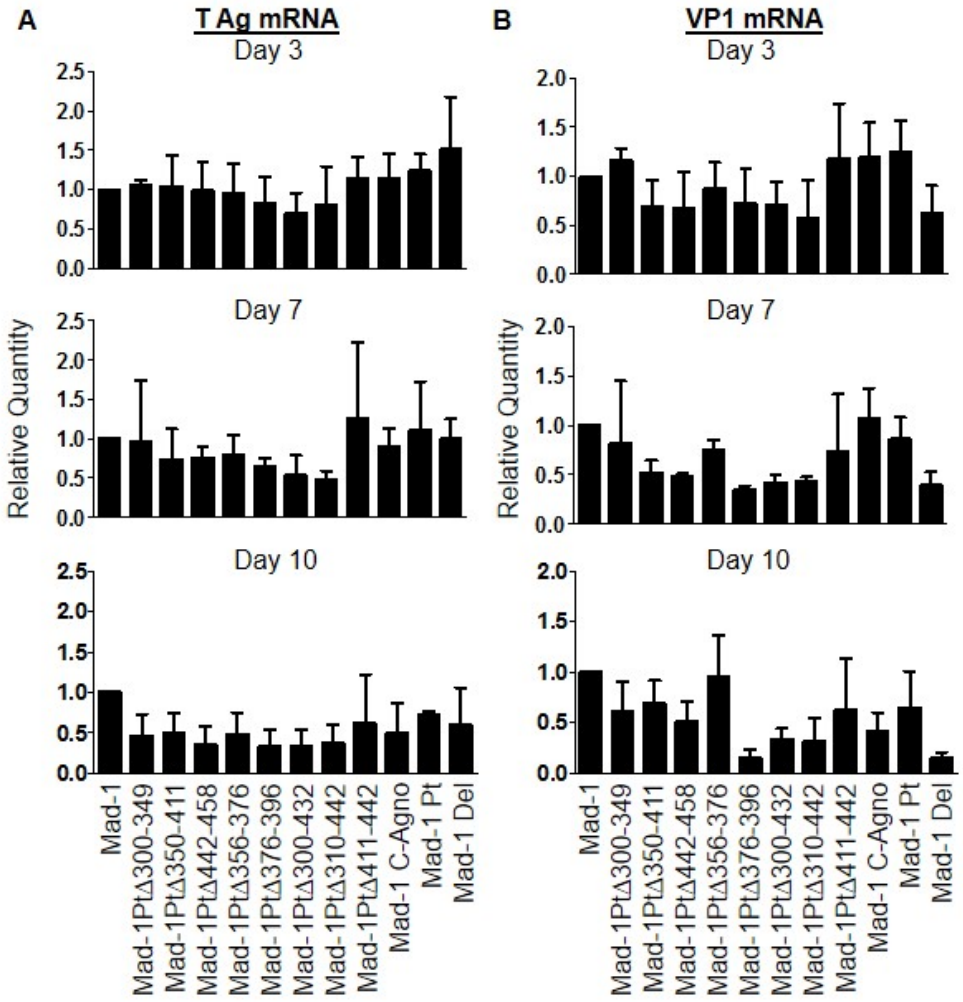

Figure 3.5 Deletion of nucleotides 376-396 results in a reduction of late mRNA expression. Cos-7 cells were transfected with linearized JCV genomes. Cell pellets were collect and RNA was extract and reverse transcribed into cDNA. qPCR was used to measure the levels of early (T Ag) and late (VP1) transcripts as well as the endogenous control TBP. Relative Quantity (RQ) was calculated using the ΔΔCt method, with TBP as the endogenous control and JCV_{Mad-1} as the calibrator sample. Data represents the average of 3 independent experiments. (A) While some decrease in T Ag mRNA is observed 10 days post-transfection, no significant differences were observed for any of the viruses tested. (B) Mad-1 PtΔ376-396 expressed decreased levels of VP1 mRNA 7 and 10 days post-transfection, with levels similar to Mad-1 Del. Mad-1 PtΔ300-432 and Mad-1 PtΔ310-442 also have some decrease in VP1 mRNA expression. None of these differences reached statistical significance. Mock transfected samples remained negative for JCV mRNAs. Error Bars represent standard deviation. P values were calculated for all viruses compared to JCV_{Mad-1} with Student's t test using univariate analysis.

Nucleotides 376-396 are critical for VP1 expression. Western blotting was done for VP1 expression in cell lysate collected from Cos-7 cells 14 and 21 days post-transfection. As previously published, JCV_{Mad-1} (Lane 1) and Mad-1 Pt (Lane 11) express detectable levels of VP1 protein, while Mad-1 C-Agno (Lane 10) and Mad-1 Del (Lane 12) do not (Figure 3.6) (23). Interestingly, all of the additional agnogene deletion mutants except Mad-1 PtΔ376-396 (Lane 6) express VP1, although at somewhat decreased levels. Mad-1 PtΔ376-396 does not express detectable levels of VP1 14 or 21 days post-transfection. This indicates that nucleotides 376-396 are crucial for VP1 protein expression.

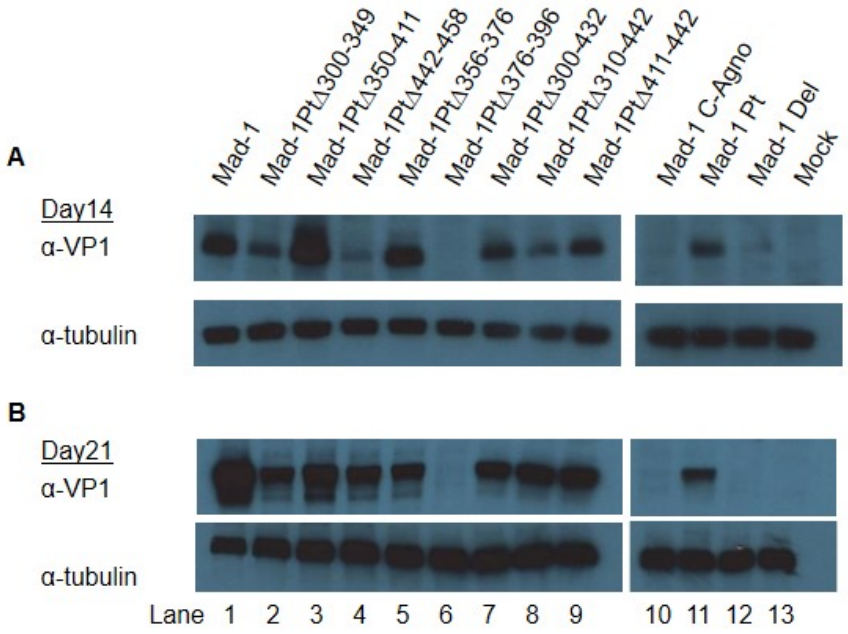

Figure 3.6 Deletion of nucleotides 376-396 prevents VP1 expression. Western blots were done with PAB597 (anti-VP1) (upper panels) using cell lysate collected from Cos-7 cells (A) 14 and (B) 21 days post-transfected. VP1 is detectable with most of the viruses tested, exept Mad-1 PtΔ376-396 (Lane 6), Mad-1 C-Agno (Lane 10) and Mad-1 Del (Lane 12). Anti-tubulin is used as a loading control (lower panels). Blots are representative of results observed in 3 independent experiments.

293T cells can be infected with JCV. Based on these results, we sought to identify the host cell proteins which bind to the agnogene of JCV by MS. Of the cell lines used in previous experiments, Cos-7 cells replicate the highest levels of JCV. However, this is an African green monkey cell line and is therefore not the ideal cell line for use in MS analysis. We tested 293T cells, a human kidney cell line transformed with SV40 T Ag, for the ability to replicate JCV. 293T cells were transfected with either JCV_{Mad-1} or JCV_{CPN}. DNA was extracted from cell lysates and supernatant and levels of DNA were determined using qPCR. We found that JCV can infect 293T cells (Figure 3.7). JCV_{Mad-1} was able to establish a persistent infection in these cells. JCV_{CPN} initially had high levels of JCV DNA present, but these levels dropped off at later times post-transfection. Based on these results, we decided to use 293T cells for initial MS studies.

DNA-IP MS to identify candidate agnogene binding proteins. To identify host cell proteins binding to the JCV agnogene DNA we used a DNA-IP approach. We generated biotinylated DNA probes of either the JCV_{Mad-1} or JCV_{CPN} agnogene through PCR using biotinylated primers. The biotinylated DNA probes were bound to streptavidin conjugated magnetic beads and incubated with nuclear proteins extracted from JCV_{Mad-1} positive 293T cells to pull down candidate agnogene binding proteins. Eluted proteins were run on an SDS-PAGE gel, and the bands of interest were excised and submitted for MS analysis. Submitted bands are indicated in Figure 3.8. Band 1 was excised from the Coomassie stained gel (Figure 3.8B), Band 2 from the silver stained gel (Figure 3.8A) and Band 3 from the Coomassie Stained gel (Figure 3.8B). Additionally, TCA precipitated samples were run a short distance in to the gel, stained with Commassie blue and the section containing

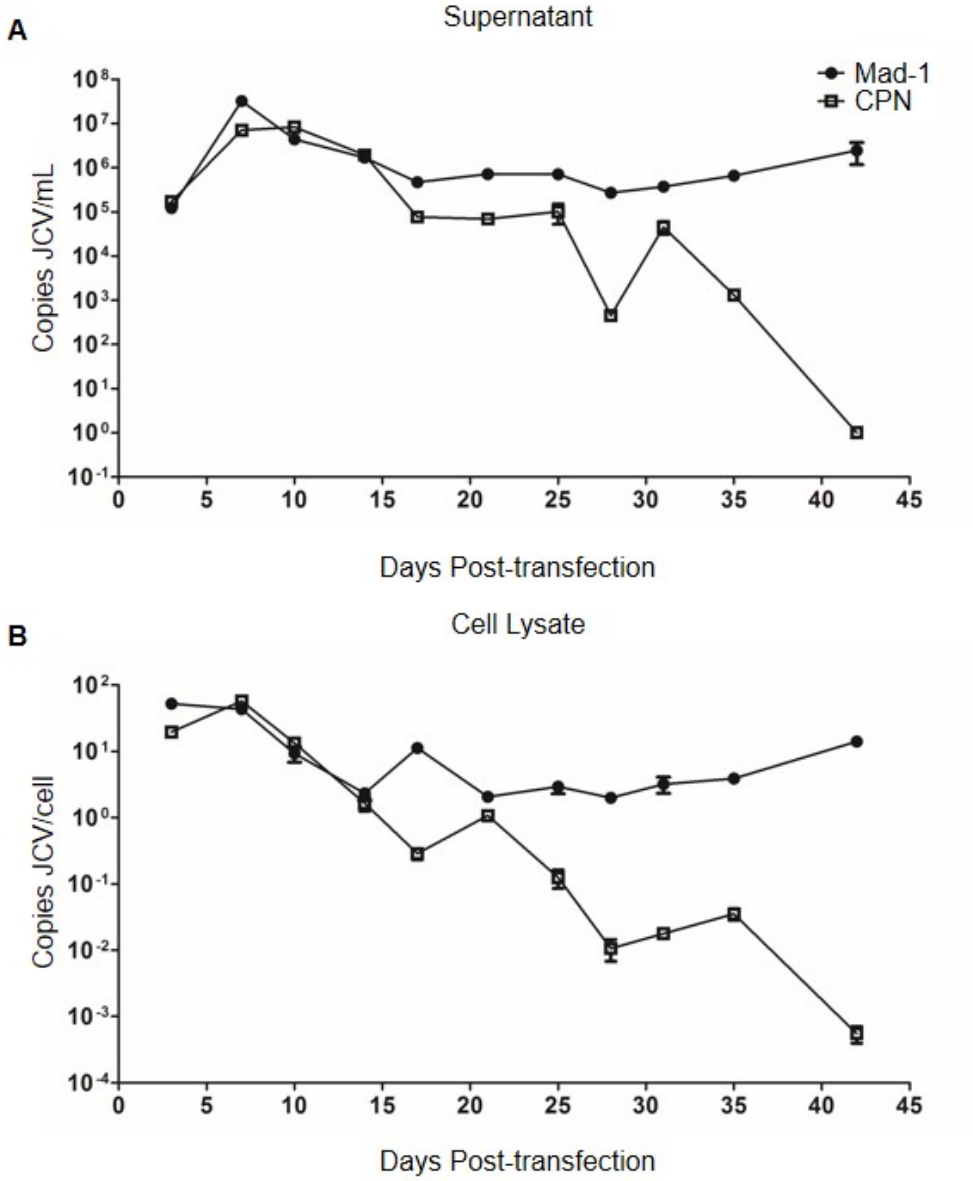

Figure 3.7 JCV_{Mad-1} and JCV_{CPN} replicate in 293T cells. 239T cells were transfected with either JCV_{Mad-1} or JCV_{CPN} as described in Figure 3.3. DNA was extracted from supernatant and cell pellets and JCV DNA levels were quantified using qPCR.

all the proteins in the sample was excised and submitted for MS analysis. Results were obtained and possible candidate binding proteins were identified. Band 1 was identified as poly (ADP-ribose) polymerase 1 (PARP-1), Band 2 as Ku70 and Ku80 and Band 3 was not definitively identified from the results. Band 3 was resubmitted from additional experiments, but we were unable to identify it. The MS results from

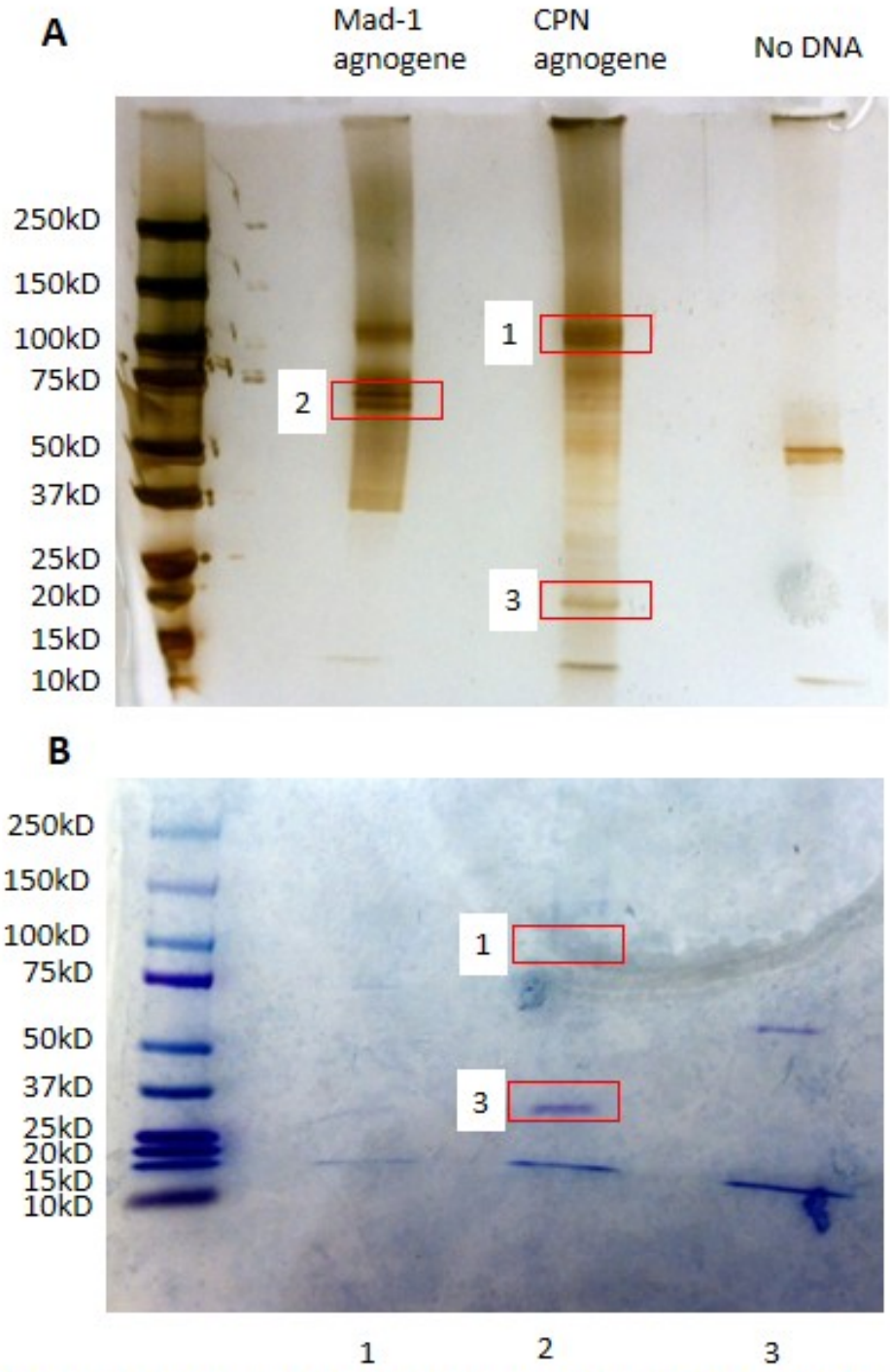

Figure 3.8 Protein Bands sent for Mass Spectrometry Analysis. A) Silver Stain of proteins bound to JCV_{Mad-1} agnogene DNA (Lane 1), JCV_{CPN} agnogene DNA (Lane 2) or no DNA control (Lane 3). Band 2 was excised and submitted of Mass Spectrometry (MS) analysis. B) Coomassie stain of the same samples concentrated by TCA precipitation. Bands 1 and 3 were excised and submitted for MS analysis.

the total JCV_{Mad-1}, JCV_{CPN} and no DNA total samples were compared to identify any proteins that were present at higher frequencies in either both JCV_{Mad-1} and JCV_{CPN} r in only JCV_{Mad-1} or JCV_{CPN}. Replication protein A 70 kDa DNA-binding subunit (RPA1) and Replication protein A 32 kDa subunit (RPA2) were present in the JCV_{Mad-1} but not JCV_{CPN} or no DNA control samples. General transcription factor II-I (GTF2I) was present in JCV_{Mad-1} and JCV_{CPN} but not the no DNA control sample.

Testing candidate binding proteins. Two additional probes were made from the Ampicillin Resistance gene of pUC18. A 220-bp (JCV_{Mad-1} agnogene size) and a 75-bp (JCV_{CPN} agnogene size) probe were generated. These DNAs were used as controls for proteins binding non-specifically to any DNA fragment. A silver stained gel of all proteins bound to each probe is seen in Figure 3.9A. Western Blots for specificity of binding of candidate proteins were done. Despite what was seen with silver staining, PARP-1 was not found to bind specifically to JCV agnogene DNA in DNA-IPs done using either 293T or IMR-32 nuclear proteins (Figure 3.9B). We also tested Ku70, RPA1 and GTF2I, all of which lacked specific binding to the agnogene DNA (Figure 3.9C).

The PARP-1 inhibitor 3-AB does not inhibit JCV replication. While the specificity of binding was being tested, we also tested whether the inhibition of PARP-1 enzymatic activity had an effect on JCV replication. To do so, we used 3-aminobenzamide (3-AB), an inhibitor of the enzymatic activity of PARP-1. Concentrations from 0.1 mM to 5 mM of 3-AB were added to JCV_{Mad-1} transfected 293T cells and the levels of DNA in the cell lysate and supernatant were monitored

(Figure 3.10). 3-AB treatment did no significantly change the levels of JCV DNA detected.

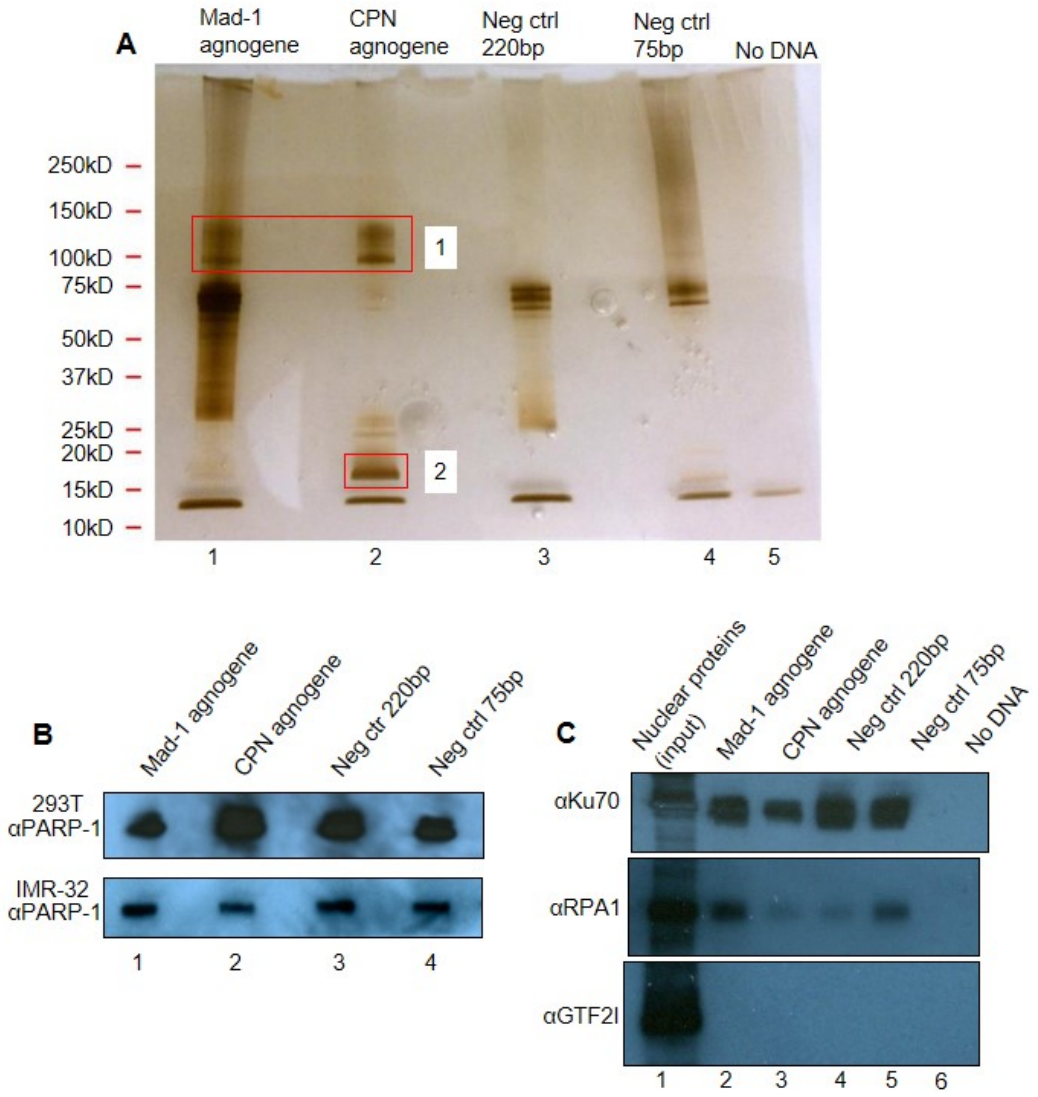

Figure 3.9 Confirmation of candidate binding proteins. A) Silver Stain of proteins bound to JCV_{Mad-1} agnogene DNA (Lane 1), JCV_{CPN} agnogene DNA (Lane 2), 220 bp negative control (Lane 3), 75bp negative control (Lane 4) or no DNA control (Lane 5). Band 1 was identified as PARP-1 by MS. We could not identify Band 2. B) Western blots for PARP1 from agnogene DNA IPs using 293T or IMR-32 nuclear proteins. PARP-1 binding to JCV agnogene is non-specific. C) Western blots to test binding of Ku70, RPA1 and GTF2I to JCV agnogene DNA using 293T nuclear proteins. Lane 1 contains the total nuclear proteins extracted before IP. Lanes 2-6 contain proteins bound to JCV_{Mad-1} agnogene DNA (Lane 2), JCV_{CPN} agnogene DNA (Lane 3), 220 bp negative control (Lane 4), 75bp negative control (Lane 5) or no DNA control (Lane 6). None of these were found to bind specifically to JCV agnogene DNA.

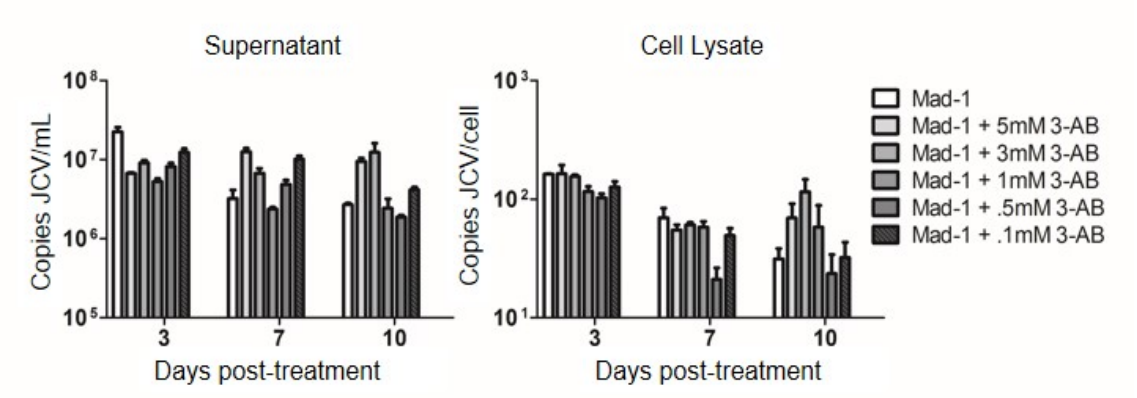

Figure 3.10 The PARP-1 inhibitor 3-AB does not inhibit JCV replication in 293T cells. JCV_{Mad-1} positive 293T cells were treated with increasing concentrations of 3-AB**.** At 3, 7 and 10 days post-treatment cells were subcultured and supernatant and cell samples were collected. The levels of JCV DNA were determined using QPCR.

DISCUSSION

Recent studies of the agnoprotein have identified a number of roles for the protein in JCV replication, but the exact mechanisms of action have yet to be worked out. Additionally, a cis-acting regulatory DNA element and host cell binding sites in the agnogene have been identified (22), although the mechanism of action is unclear. We have previously studied JCV_{CPN}, a naturally occurring isolate which contains a 143 nucleotide deletion, the first large agnogene deletion found in nature (23, 24). The agnogene deletion in JCV_{CPN} was found to impair VP1 expression and virion production, and this phenotype was primarily due to the loss of the agnogene DNA, rather than lack of a full length agnoprotein.

In this study, we generated a series of agnogene deletion mutants. In order to rule out any effects of mutations of the agnoprotein, these deletions were introduced into Mad-1 Pt, which has a start codon mutation preventing agnoprotein expression. We transfected these deletion mutants, along with a number of previously characterized control viruses, into Cos-7 cells and studied their replication by measuring levels of DNA replication, mRNA expression and VP1 protein production.

We have previously found that both Mad-1 Del and Mad-1 C-Agno have decreased levels of DNA replication at later times post-transfection and lack expression of VP1 protein. Mad-1 Pt has similar levels of DNA detected as JCV_{Mad-1}. Most of the new deletion mutants have similar phenotypes to Mad-1 Pt and JCV_{Mad-1}. The most striking phenotype was observed with Mad-1 PtΔ376-396, which had decreased levels of DNA replication at later time points post-transfection, and was the only new mutant which did not expression VP1. We initially chose these nucleotides to delete because they are highly conserved between JCV, BKV and SV40 (Figure 3.3). This may mean that the function of these nucleotides is

conserved among these three related viruses. Interestingly, some of the larger deletions that include these 20 nucleotides do express VP1. There are a number of possible mechanisms which may explain this phenomenon. Nucleotides 376-396 fall within the predicted binding site III for host cell factors. If there are multiple host cell proteins binding to the agnogene, Mad-1 Pt∆376-396 may have lost only one of them. This could change the interactions and effects of other host cell proteins binding to the agnogene. Alternatively, this deletion may have created a new binding site. It is also possible that these nucleotides are involved in proper splicing of the late mRNA, or that this deletion has created a new RNA secondary structure which affects translation of the VP1 protein. If future studies identify the mechanism of this phenotype, it will be of interested to determine if these nucleotides play the same role in either BKV or SV40.

Recently, Saribas et al published a study where they included an agnoprotein mutant with amino acids 34-36 deleted, named Mad-1 Agno ∆(34-36) (15). This region is within the deleted region of Mad-1 Pt∆376-396. In this study, they found that these residues are crucial for agnoprotein oligomerization and dimerization. They also see reduced viral DNA replication 15 days post-transfection, and decreased levels of late transcription and altered relative levels of the M1 and M2 late transcript splice variants with Mad-1 Agno ∆(34-36). Our results indicate that some of these phenotypes may be due to the loss of the DNA in the agnogene rather than expressing an agnoprotein which cannot form dimers and oligomers.

To further understand the role of the agnogene, we attempted to identify host cell proteins binding to the agnogene DNA. DNA-IPs followed by MS were done and the candidate proteins PARP-1, Ku70, RPA1 and GTF2-I were identified as possible binding factors. However, none of these proved to bind specifically to the JCV

agnogene. We can rule out these proteins as the host cell factors which bind the agnogene and influence viral replication. The small band specific to JCV_{CPN} samples was seen in multiple experiments (Figure 3.8, Band 3). Repeated attempts were made to determine the identity of this protein, but we were unsuccessful. Further studies of the host cell proteins interacting with the agnogene DNA are warranted. Transcription factors predicted to bind to the agnogene through sequence analysis could be tested for specific binding. The agnogene deletion mutants generated here could then be used to help narrow down the exact binding sites for any specific binding factors.

Nukuzuma et al. reported that the PARP-1 inhibitor 3-aminobenzamide (3-AB) can inhibit JCV replication in IMR-32 cells (30). We tested the effect of 3-AB on JCV replication in 293T cells, and did not see significant changes in the levels of JCV DNA detected in either the cell lysate or supernatant. PARP-1 was a candidate protein found bound to the JCV agnogene at high levels. However, this interaction was also found with other DNA sequences, indicating that the interaction was non-specific. Given that PARP-1 plays a role in double strand DNA break repair, it is not surprising that it was identified in our study but proved non-specific. While a lack of binding to the agnogene does not rule out other mechanisms of action for PARP-1 inhibition of JCV replication, we did not see an effect of 3-AB treatment in our experiments using 203T cells. The discrepancy between our results and those of Nukuzuma et al. may be due to the use of different cell lines and viral strains (30).

Our study adds to the body of evidence that there is a cis-acting DNA element in the agnogene. Studies to identify these proteins should continue to be carried out. Identification of the host cell proteins which bind to the agnogene would be valuable in understanding the role of the agnogene in JCV replication, and in the future

development of therapeutics for treatment of PML and other brain diseases caused by JCV infection.

REFERENCES

1. Koralnik IJ, Wuthrich C, Dang X, Rottnek M, Gurtman A, Simpson D, Morgello S. 2005. JC virus granule cell neuronopathy: A novel clinical syndrome distinct from progressive multifocal leukoencephalopathy. *Ann Neurol* 57: 576-80

2. Tan C, Koralnik I. 2010. Beyond progressive multifocal leukoencephalopathy: expanded pathogenesis of JC virus infection in the central nervous system. *Lancet Neurology* 9: 425-37

3. Wuthrich C, Dang X, Westmoreland S, McKay J, Maheshwari A, Anderson MP, Ropper AH, Viscidi RP, Koralnik IJ. 2009. Fulminant JC virus encephalopathy with productive infection of cortical pyramidal neurons. *Ann Neurol* 65: 742-8

4. Knowles WA, Pipkin P, Andrews N, Vyse A, Minor P, Brown DW, Miller E. 2003. Population-based study of antibody to the human polyomaviruses BKV and JCV and the simian polyomavirus SV40. *J Med Virol* 71: 115-23

5. Weber T, Trebst C, Frye S, Cinque P, Vago L, Sindic CJ, Schulz-Schaeffer WJ, Kretzschmar HA, Enzensberger W, Hunsmann G, Luke W. 1997. Analysis of the systemic and intrathecal humoral immune response in progressive multifocal leukoencephalopathy. *J Infect Dis* 176: 250-4

6. Berger JR, Kaszovitz B, Post MJ, Dickinson G. 1987. Progressive multifocal leukoencephalopathy associated with human immunodeficiency virus infection. A review of the literature with a report of sixteen cases. *Ann Intern Med* 107: 78-87

7. Molloy ES, Calabrese LH. 2009. Progressive multifocal leukoencephalopathy: a national estimate of frequency in systemic lupus erythematosus and other rheumatic diseases. *Arthritis Rheum* 60: 3761-5

8. Shimizu N, Imamura A, Daimaru O, Mihara H, Kato Y, Kato R, Oguri T, Fukada M, Yokochi T, Yoshikawa K, Komatsu H, Ueda R, Nitta M. 1999. Distribution of JC virus DNA in peripheral blood lymphocytes of hematological disease cases. *Intern Med* 38: 932-7

9. Gheuens S, Wuthrich C, Koralnik IJ. 2013. Progressive multifocal leukoencephalopathy: why gray and white matter. *Annu Rev Pathol* 8: 189-215

10. Jensen PN, Major EO. 2001. A classification scheme for human polyomavirus JCV variants based on the nucleotide sequence of the noncoding regulatory region. *J Neurovirol* 7: 280-7

11. Khalili K, White MK, Sawa H, Nagashima K, Safak M. 2005. The agnoprotein of polyomaviruses: a multifunctional auxiliary protein. *J Cell Physiol* 204: 1-7

12. Okada Y, Endo S, Takahashi H, Sawa H, Umemura T, Nagashima K. 2001. Distribution and function of JCV agnoprotein. *J Neurovirol* 7: 302-6

13. Sariyer IK, Akan I, Palermo V, Gordon J, Khalili K, Safak M. 2006. Phosphorylation mutants of JC virus agnoprotein are unable to sustain the viral infection cycle. *J Virol* 80: 3893-903

14. Sariyer IK, Khalili K, Safak M. 2008. Dephosphorylation of JC virus agnoprotein by protein phosphatase 2A: inhibition by small t antigen. *Virology* 375: 464-79

15. Saribas A, Abou-Gharbia M, Childers W, Sariyer IK, White MK, Safak M. 2013. Essential roles of Leu/Ile/Phe-rich domain of JC virus agnoprotein in dimer/oligomer formation, protein stability and splicing of viral transcripts. *Virology* 443: 161-76

16. Saribas AS, White MK, Safak M. 2012. JC virus agnoprotein enhances large T antigen binding to the origin of viral DNA replication: evidence for its involvement in viral DNA replication. *Virology* 433: 12-26

17. Safak M, Barrucco R, Darbinyan A, Okada Y, Nagashima K, Khalili K. 2001. Interaction of JC virus agno protein with T antigen modulates transcription and replication of the viral genome in glial cells. *J Virol* 75: 1476-86

18. Safak M, Sadowska B, Barrucco R, Khalili K. 2002. Functional interaction between JC virus late regulatory agnoprotein and cellular Y-box binding transcription factor, YB-1. *J Virol* 76: 3828-38

19. Sariyer IK, Saribas AS, White MK, Safak M. 2011. Infection by agnoprotein-negative mutants of polyomavirus JC and SV40 results in the release of virions that are mostly deficient in DNA content. *Virol J* 8: 255

20. Suzuki T, Semba S, Sunden Y, Orba Y, Kobayashi S, Nagashima K, Kimura T, Hasegawa H, Sawa H. 2012. Role of JC virus agnoprotein in virion formation. *Microbiol Immunol* 56: 639-46

21. Suzuki T, Orba Y, Okada Y, Sunden Y, Kimura T, Tanaka S, Nagashima K, Hall WW, Sawa H. 2010. The human polyoma JC virus agnoprotein acts as a viroporin. *PLoS Pathog* 6: e1000801

22. Akan I, Sariyer IK, Biffi R, Palermo V, Woolridge S, White MK, Amini S, Khalili K, Safak M. 2006. Human polyomavirus JCV late leader peptide region contains important regulatory elements. *Virology* 349: 66-78

23. Ellis LC, Norton E, Dang X, Koralnik IJ. 2013. Agnogene deletion in a novel pathogenic JC virus isolate impairs VP1 expression and virion production. *PLoS One* 8: e80840

24. Dang X, Wuthrich C, Gordon J, Sawa H, Koralnik IJ. 2012. JC virus encephalopathy is associated with a novel agnoprotein-deletion JCV variant. *PLoS One* 7: e35793

25. Frisque RJ, Bream GL, Cannella MT. 1984. Human polyomavirus JC virus genome. *J Virol* 51: 458-69

26. Gluzman Y. 1981. SV40-transformed simian cells support the replication of early SV40 mutants. *Cell* 23: 175-82

27. Major EO, Miller AE, Mourrain P, Traub RG, de Widt E, Sever J. 1985. Establishment of a line of human fetal glial cells that supports JC virus multiplication. *Proc Natl Acad Sci U S A* 82: 1257-61

28. Tumilowicz JJ, Nichols WW, Cholon JJ, Greene AE. 1970. Definition of a continuous human cell line derived from neuroblastoma. *Cancer Res* 30: 2110-8

29. Schmittgen TD, Livak KJ. 2008. Analyzing real-time PCR data by the comparative C(T) method. *Nat Protoc* 3: 1101-8

30. Nukuzuma S, Kameoka M, Sugiura S, Nakamichi K, Nukuzuma C, Takegami T. 2013. Suppressive effect of PARP-1 inhibitor on JC virus replication in vitro. *J Med Virol* 85: 132-7

CHAPTER 4: DISCUSSION

SUMMARY

JCV infection of the brain can cause the fatal diseases PML, JCV GCN and JCVE. This list is likely to grow as new diseases continue to be identified. These diseases usually occur in individuals with some form of immune suppression. In healthy individuals, JCV infection remains latent in the kidneys. The disease pathogenesis and mechanisms of viral reactivation are not well understood. The RR form of the virus determines the location, type and number of transcription factor binding sites in the early and late promoters, and is thought to play a role in JCV pathogenesis and tropism. The agnogene, which encodes the agnoprotein, is located in the late region, and its functions are still unclear. A better understanding of the basic biology of JCV replication is crucial for the future development of therapeutics for the treatment of PML, JCV GCN and JCVE.

In Chapter 2, we studied the replication of JCV_{CPN} in cell culture. The 143-nucleotide deletion in the JCV_{CPN} agnogene is the first large deletion in the agnogene found in a naturally occurring isolate of JCV. The RR of JCV_{CPN} is archetype-like, a type which is generally found in the kidneys and urine and is considered non-pathogenic. We used kidney, glial and neuronal cell lines to compare the replication of JCV_{CPN} and JCV_{Mad-1} in different cell types. We initially hypothesized that JCV_{CPN} would have a replication advantage in neuronal cells because it was isolated from the first patient found to have JCV infection of cortical pyramidal neurons. While JCV_{CPN} was able to replicate in all cell lines tested, it did not show a replication advantage in the neuronal cell line tested. We found that, while JCV_{Mad-1} was able to establish a persistent high level infection, JCV_{CPN} was unable to maintain high levels of DNA in

either transfected cell lysate or supernatant. JCV_{CPN} failed to express detectable levels of VP1 capsid protein and produced very low levels of infectious virions only at early time points post-transfection. The agnogene and RR are the two main regions of difference between JCV_{CPN} and JCV_{Mad-1}. To determine which region was the main cause of the JCV_{CPN} phenotype, we generated a series of chimeras between JCV_{CPN} and JCV_{Mad-1} and additional agnogene and agnoprotein deletion mutants. We found that the predominant cause of the lack of VP1 expression and virion production was the deletion in the agnogene. This phenotype was due primarily to the loss of the agnogene DNA and not the lack of a full length agnoprotein. Introduction of a full length agnogene with a point mutation preventing agnoprotein expression was able to rescue JCV_{CPN}. These findings support a role for the agnogene DNA in VP1 expression and virion production.

In Chapter 3, we further examined the role of the agnogene DNA in JCV replication. We introduced a series of smaller agnogene deletions on a JCV_{Mad-1} backbone with the agnoprotein start codon mutated to prevent protein expression. This allowed us to study the role of the agnogene DNA without confounding effects from mutations in the agnoprotein. We characterized the levels of DNA replication, early and late mRNA transcription and VP1 protein production of these mutants. We found that the deletion of nucleotides 376-396 resulted in a lack of VP1 capsid protein. We then sought to determine the host cell proteins which bind to the agnogene DNA. We identified a number of candidate proteins, including PARP1, Ku70, GTFII-I and RPA1, but none were found to bind specifically to the agnogene.

Overall, we have used a naturally occurring, pathogenic isolate of JCV to better understand the basic biology of replication of the virus. We have used a cell culture model to study the newly discovered ability of JCV to infect neurons. The deletion in the JCV_{CPN} virus and our additional agnogene deletions have allowed us to better characterize the role of the agnogene DNA is JCV replication. We have also studied the effect of the archetype-like RR of JCV_{CPN}, a form more common found in the kidneys than the CNS, on replication in cell culture.

DISCUSSION

JCV infection in neurons.

Since the isolation of JCV in 1971, it has been thought that JCV can only infect oligodendrocytes and astrocytes in the brain. Over the past decade, the Koralnik laboratory has shown that JCV is also able to infect neurons, which results in newly discovered diseases other than PML. This was seen for the first time in a patient with PML who also had JCV-infection of granule cell neurons (1). JCV GCN can also occur independently from PML and cases have now been identified all over the world (1-5). More recently, JCV was found to infect cortical pyramidal neurons in the first patient with JCVE (6). The discoveries of JCV GCN and JCVE indicate a broadened pathogenesis of JCV infection in the brain, and we are only beginning to understand the prevalence and role in pathogenesis of neuronal infection by JCV.

Since the identification of JCV GCN and JCVE, histological studies have been done to determine the prevalence of JCV infection of neurons. The Koralnik laboratory studied archival brain samples from 49 PML patients and 109 healthy control subjects to determine the prevalence of gray matter lesions and JCV infection of cortical pyramidal neurons. 96% of the PML patients had demyelinating lesions at the gray-white junction and 57% had lesions in the gray matter. Histological studies revealed that, while most JCV infected cells were oligodendrocytes, infected neurons in PML lesions were present in 54% and 50% of the gray-white junction and gray matter lesions, respectively. Outside of PML lesions, 11% were found to have isolated cortical neurons expressing JCV proteins. None of the control subjects had detectable JCV-infected cells. This indicates that cerebral cortical neurons are infected by JCV in a significant

portion of PML patients (7). A similar study using archival samples from 43 PML patients to examine the frequency of JCV infection of cerebral granule cell neurons found that, of the 70% of samples in which JCV infected cells were detected, 93% had JCV positive cells in the granule cell layer. 19 samples were tested specifically for JCV infection of granule cell neurons, and 15 of them were found to be positive for infection. Only 1 of 72 control subjects without PML had JCV infection in granule cell neurons. This patient was HIV-positive (8). In both of these studies, infected neurons expressing Large T Ag were more frequent than those expressing VP1, suggesting most of these neurons are not productively infected (7, 8). Finally, there is evidence of JCV infection of neurons in the brains of individuals without any clinically apparent JCV-associated disease. A study using laser capture microdissection of different cell types in non-PML brain samples, followed by PCR amplification found JCV DNA in oligodendrocytes, astrocytes and cerebral granule cell neurons, suggesting that JCV may also latently infect neurons in individuals without PML (9).

It is now clear that JCV can infect neurons, both in patients with PML, JCV GCN and JCVE, as well as possibly individuals without any apparent JCV-related disease. The role of JCV infection of neurons in disease pathogenesis is still being determined. One study found JCV DNA in cerebral granule cell neurons of 7 of 17 archival non-PML brain samples tested by laser capture microdissection and PCR (9). Most, but not all, of these individuals were HIV-positive or had some other form of immune suppression (9). Another only found 1 of 72 archival brain samples from HIV-infected individuals without PML had JCV protein expression in cerebral granule cell neurons (8). This may indicate that these cells are a site of latent JCV infection. This infection could happen with initial

infection with JCV, making these infected neurons a possible source of JCV reactivation under conditions of immune suppression.

Studying neuron infection in cell cultures is challenging. Neurons are difficult to grow and differentiate and the brain has a complex architecture that cannot be accurately replicated in cell cultures. Additionally, JCV replicates in very few cell lines, most of which express a polyomavirus T Ag, and has a slow replication cycle. It may be possible to address these issues by studying JCV infection *ex vivo* in cultured brain slices. However, brain samples are generally only available from individuals who either have a disease requiring the removal or biopsy of brain tissue or from individuals who are deceased, making it difficult to obtain healthy brain tissue for study. Additionally, the long replication cycle of JCV may make it difficult to sustain an infection in a brain slice culture long enough to gather sufficient data.

Another complication to studying JCV infection in neurons is the lack of an animal model. However, SV40 has been shown to sometimes cause a PML like disease in immunocompromised rhesus monkeys (10, 11). When two immunocompromised monkeys were inoculated with an SV40 strain isolated from the CNS of another monkey with PML-like disease and meningoencephalitis, both developed meningoencephalitis and were found to have productive infection of cortical neurons (12). A study of archival brain samples from rhesus monkeys found that neuron infection is present in 60% of immunocompromised monkeys with disease in the CNS due to SV40 infection (13). Further studies of SV40 infection in neurons in rhesus macaques may add to our understanding of the role of neuronal infection in SV40 and JCV neuropathogenesis. Studying primary infection in rhesus macaques would allow

us to determine if neurons are infected with SV40 during primary infection, and then latently infected until reactivation associated with immune suppression. Mutations could be introduced into SV40 which equivalent to those seen in the strains of JCV isolated from JCV GCN and JCVE patients and these viruses could be used to determine the impact of these mutations on SV40 and its cellular tropism.

JCV_{CPN} and JCVE

JCV_{CPN} was isolated from the brain of a patient with JCVE. We were interested in studying this virus due to both the unique agnogene deletion as well as the fact that it was isolated in association with the infection of a new cell type, cortical pyramidal neurons. We had initially hypothesized that the mutations in JCV_{CPN} would allow it to infect neurons, and that it would have a replication advantage over JCV_{Mad-1} in neurons. Our cell culture studies in Chapter 2 did not indicate an increased ability of JCV_{CPN} to replicate in the neuronal cell line tested, IMR-32 cells. However, these cells are a neuroblastoma cell line, and the results seen in them may not be representative of what occurs in the human brain. First, they are a neuroblastoma cell line, not cortical pyramidal neurons. JCV cellular tropism is highly dependent on the transcription factors present in a cell. IMR-32 cells may lack the expression of a transcription factor that is present in cortical pyramidal neurons that is important for JCV_{CPN} replication. Second, neurons in the brain are surrounded by astrocytes, oligodendrocytes and other types of neurons. These interactions may be important for the replication or spread of the virus, and are lacking in a cell culture model. While we have not found any evidence for an

increased ability of JCV_{CPN} to replicate in neuronal cells, we cannot rule out that this occurred in the brain of the JCVE patient.

To date, there have been no additional cases of JCVE reported. This makes it difficult to determine if the agnogene deletion of JCV_{CPN} is the cause of this new disease, or if these are two independent phenomena. JCV_{CPN} was not the only strain of JCV present in the brain of the JCVE patient. This strain co-existed with a strain of JCV with an intact agnogene (14). The strain with the intact agnogene was found in the DNA from all parts of the brain tested, as well as in the blood and CSF. PCR screen indicated that the majority of the JCV present was JCV_{CPN}, while the intact-agno strain was the minority species. One possible explanation for the high levels of JCV_{CPN} found in the brain of the JCVE patient is that the presence of this strain expressing the full length agnoprotein helped the JCV_{CPN} strain replicate. A second strain of JCV with a large deletion in the agnogene has been identified in a PML patient who was not diagnosed with JCVE (14). It may be that JCV variants with deletions occur with some regularity during natural infection, just as cortical pyramidal neurons are frequently infected in PML patients, as described above. Further studies are needed to determine if this deletion actually plays a role in cortical pyramidal neuron infection in other cases. Laser capture microdissection of infected cortical pyramidal neurons from PML patients could be used to determine if these cells actually harbor a strain of JCV with a deletion in the agnogene, or an intact agnogene. If they have intact agnogenes, then it is unlikely that the JCV_{CPN} deletion is actually giving the virus the ability to infect cortical pyramidal neurons. If additional cases of JCVE are diagnosed in the future, these

patients could also be studied to determine whether they also have a deletion in the agnogene in the JCV in their brain.

While it is impossible to know exactly what happened in the JCVE patient, the results of our studies allow us to hypothesize about what may have occurred. JCV excreted in the urine usually contains an archetype RR, making this the form which is most likely to be present during initial infection. Both the JCV strains with the deleted agnogene and the intact agnogene isolated from the brain of the JCVE patient had an archetype-like RR. The sequence of the RR present in the urine of this patient is unknown. It is possible that the JCV_{CPN} archetype-like RR sequence was present in the virus which first infected the patient, or that this sequence arose in the virus before it infected the brain. PCR analysis of the JCV present in the CSF and plasma indicated that they contained only JCV with a full length agnogene. Based on these results, it is most likely that the brain was infected by JCV with this archetype-like RR and an intact agnogene, and the deletion in the agnogene arose in the brain of the patient. JCV typically infects oligodendrocytes, and the infection of cortical pyramidal neurons was seen for the first time in the JCVE patient. Most likely, the JCV with an intact agnogene reached the brain, where if first infected a limited number of oligodendrocytes without causing clinically apparent PML. Over the course of time, the deletion in the agnogene occurred, and the virus was then able to infect the cortical pyramidal neurons. In our cell culture studies, JCV_{CPN} replicated poorly, and produced only very low levels of infectious virions. While this led to poor replication in cell culture, it may have been advantageous in the patient, allowing the viruses to remain undetected and accumulated in the neurons over years or decades. Then, when the JCVE patient was

treated with chemotherapy, the right conditions occurred for JCV_{CPN} to cause the patient to develop JCVE (14).

JCV_{CPN} biology and the function of the agnogene

While the cell culture studies of JCV_{CPN} did not confirm our initial hypothesis, we were able to use this unique virus to study the functions of both the RR and the agnogene and agnoprotein. Levels of viral DNA in the cell lysate and supernatant were not significantly different between JCV_{CPN} and $JCV_{Mad\text{-}1}$ until 10-14 days post-transfection. Given that one replication cycle takes about 7 days and the initial levels of JCV DNA transfected were equal, this indicates that the JCV_{CPN} virus can replicate viral DNA normally (15). The drop in viral DNA after this first round of replication is indicative of an inability to produce infectious virions to initiation further rounds of infection in the cell culture. The drastic decrease in late mRNA expression and the lack of detectable VP1 protein are evidence that the block in the replication cycle is due to insufficient levels of VP1 to produce virions. Our model is that the low levels of late mRNA production leads to very low levels of VP1 production (Figure 4.1). Although there is plenty of viral DNA, the amount of VP1 protein available to form the virion capsid is extremely limited, resulting in very few infectious virions being formed and released from the JCV_{CPN} transfected cells. Given the low level of infection observed after inoculation of Cos-7 cells with JCV_{CPN} supernatant collected 7 and 14 days post-transfection, it seems that some virions are produced, but not enough to sustain an infection in our cell culture model. The fact that we can observe some DNA after

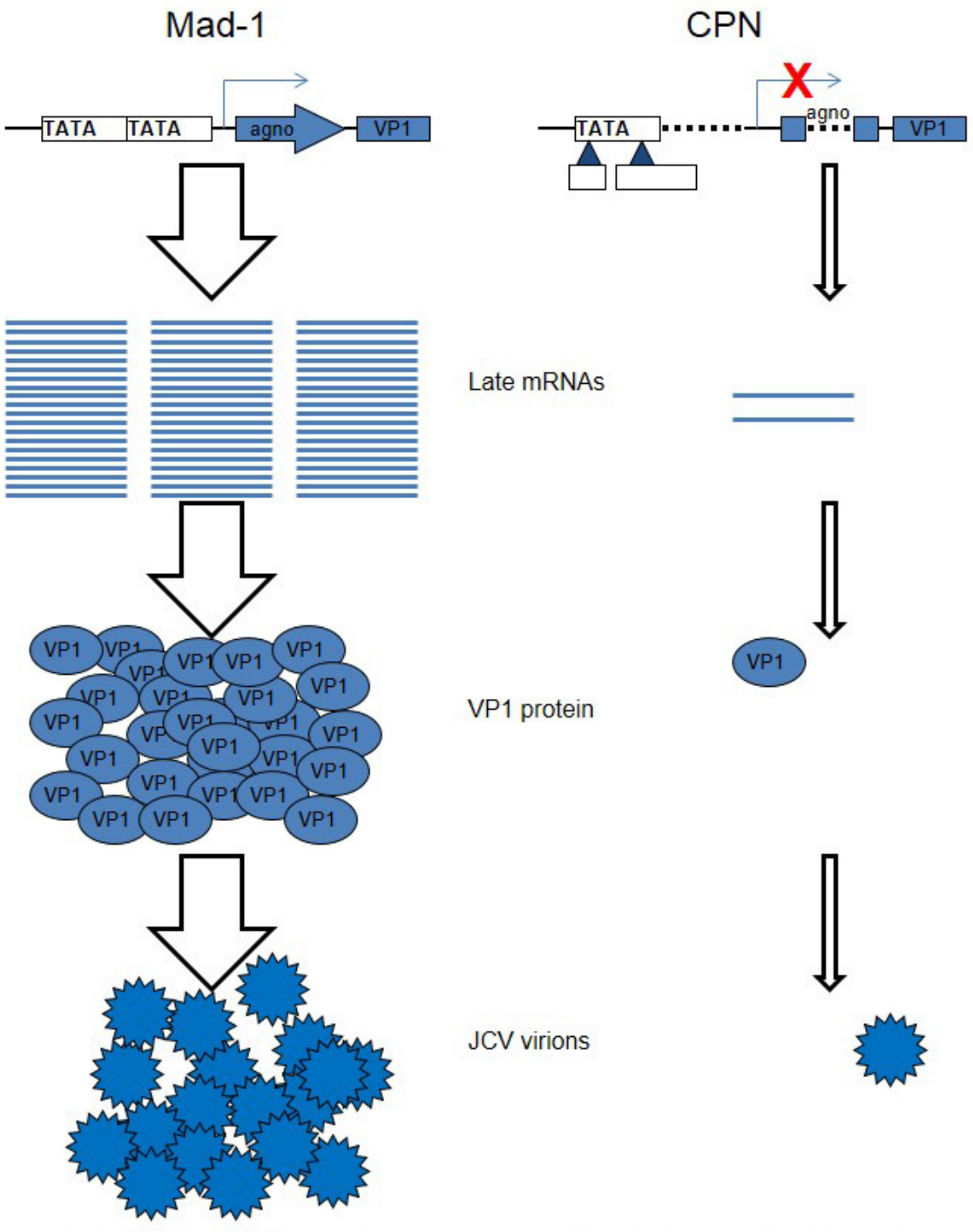

Figure 4.1 Model of JCV_{CPN} VP1 expression and virion production impairment. JCV_{CPN} has lower levels of late transcription, resulting in low VP1 expression. This leads to very low levels of virion formation compared to JCV_{Mad-1}.

inoculation with this supernatant supports the idea that DNA replication of JCV_{CPN} is not affected by the agnogene deletion or archetype-like RR.

While it has long been thought that the RR of JCV needed to rearrange to allow infection of the CNS, there has been increasing evidence that archetype and archetype-like RR forms can be found in the brain (16). Based on our studies using chimeric viruses, it does not appear that the archetype-like RR of JCV_{CPN} prevents VP1 protein expression and the production of infectious virions. This suggests that the archetype-like RR of JCV_{CPN} does not impair replication of the virus when compared to the prototype rearranged strain, JCV_{Mad-1}. Our results also provide support for the idea that archetype and archetype-like RRs are not limited to replication in the kidneys, and can be found in the brain.

The agnoprotein was initially given its name due to the unknown nature of its function. This protein is not essential for replication of JCV, and recent studies have begun to determine the role it plays during JCV replication. Our studies of the chimeric viruses indicated that the phenotype of JCV_{CPN} was due to the deletion in the agnogene, and more specifically loss of the DNA sequence in the agnogene. We found that adding the full length gene with the start codon mutation preventing agnoprotein expression was sufficient to partially rescue the virus. All of our data together indicate that the JCV agnogene plays a role in the expression of VP1 protein.

It has been previously reported that deletion of the agnogene DNA has a greater impact on JCV replication than a start codon mutation preventing expression of the agnoprotein, suggesting that a DNA regulatory element is present in the agnogene (17). Further experiments indicated the presence of 3 host cell factor binding sites in the

agnogene. This study and the results of our JCV_{CPN} studies led us to generate additional small deletions in the agnogene to determine which nucleotides are critical for JCV replication. The most striking finding of these studies was that deleting only nucleotides 376-396 prevents VP1 expression, while the viruses with all of the other larger deletions expressed VP1 protein. This region was chosen for deletion because it is highly conserved between JCV, BKV and SV40. This result was surprising given that this small deletion was encompassed by a number of larger ones, which had VP1 expression. There are many possible explanations for this. The small deletion may disrupt an interaction between two binding factors by deleting the binding site for only one of them. If this is the case, the presence of only one of these binding factors may have a different effect than the presence of both together. If a large complex is being formed on the agnogene DNA, this small deletion may alter the proteins which are present by deleting one binding site, while larger deletions may lose the binding of multiple factors. It may be altering late mRNA structure or splicing. Another alternative explanation is the creation of a new binding site at the newly formed sequence. To truly understand the mechanism of action of the agnogene, it is necessary to identify the host cell proteins which bind to it. It would then be interesting to see whether these same nucleotides play a similar role in BKV and/or SV40.

We used a DNA-IP and MS approach to try to identify the host cell proteins which bind to the agnogene. We have so far been unsuccessful in identifying a specific agnogene binding protein. We have ruled out PARP1, Ku70, Ku80, RPA1 and GTFII-I as proteins which bind to the agnogene. Further experiments must be conducted to determine the identity of the proteins binding. Altering the conditions used in the DNA-

IP may be necessary to successfully pull down the proteins of interest. Alternatively, a different method such as a gel shift followed by MS analysis could be used to identify these proteins. If the binding factors are transcription factors, then these interactions may be transient and difficult to pick up with our DNA-IP. More targeted experiments, such as Chromatin Immunoprecipitations, to test for binding of transcription factors which are predicted to bind by computer algorithms could be used. Regardless of method, identifying these proteins is an important area of research which will clarify the mechanism of the effect of deleting the agnogene.

While the list of human polyomaviruses has increased in recent years, decades passed between the discovery of JCV and BKV, and the discovery of additional human polyomaviruses. It is interesting to note that of the human polyomaviruses, only JCV and BKV have an agnogene and express an agnoprotein. The presence of an agnoprotein may have been advantageous for replication, and subsequent identification, of these viruses in cell culture using the techniques available at the time. While many of the new polyomaviruses have yet to be associated with a disease, MCPyV and TSPyV have been linked to Merkel cell carcinoma and Trichodysplasia Spinulosa, respectively. This indicates that the lack of an agnoprotein does not prevent these viruses from causing human disease. In addition to the JCV_{CPN} strains, BKV with deletions of the 5' end of the agnogene preventing agnoprotein expression have been isolated from 2 renal transplant patients (18, 19). Both of these patients were also found to be infected with a BKV strain with an intact agnogene (18, 19). While it is clear that naturally occurring JCV and BKV strains with agnogene deletions exist, it is possible that they require the presence of another strain with an intact agnogene.

Additional human polyomaviruses encoding agnoproteins may be discovered in the future, and aid in our understanding of the roles of the agnoprotein and agnogene in JCV replication.

Challenges of studying JCV in cell culture

Studying JCV in cell culture presents a number of challenges. First, there are few cell lines in which JCV robustly replicates. Many of the cell lines which are available for use are transformed with a polyomavirus, usually SV40, T Ag. Second, the replication cycle of JCV is low, taking approximately 7 days for one replication cycle (15). In our studies, we used Cos-7, SVG and IMR-32 cells. Cos-7 is an African Green Monkey kidney cell line which express SV40 T Ag (20). SVG is a human fetal glial cell line, also transformed with SV40 T Ag (21). IMR-32 is a cell line derived from a human neuroblastoma tumor, and does not express any polyomavirus T Ag (22). In some experiments, we also used the 293T cell line, which is a human kidney cell line which expresses SV40 T Ag. All of these are cell lines which are commonly used to JCV in cell culture. The difficulties of studying neuron infection have been discussed above.

Understanding JCV replication in glial cells is crucial, as these are the cells which are lytically infected in patients with PML. However, studying infection of glial also presents a challenge. We used the SVG cell line to model glial cell infection. SVG-A cells are also commonly used to study JCV infection. This cell line is derived from the SVG cell line, and expresses the astrocyte specific marker glial fibrillary acidic protein (GFAP) (23) These cells are different than oligodendrocytes, the primary target of JCV in the brain. This cell line also has the disadvantage of already expressing SV40 T Ag.

U-87 MG glioblastoma cells and TC620 oligodendroma cells have also been used to study JCV replication (24-27). While these cells do not express a polyomavirus T Ag, they have the disadvantage of being derived from tumors. Given the importance of transcription factor expression profiles in determining susceptibility to JCV infection, the altered cellular environments in these cancer cell lines may not be ideal for the study of JCV infection in glial cells.

It has also been suggested that the used of progenitor derived astrocytes (PDAs) would be a better system for the study of JCV replication in glial cells. These cells are derived from human neural progenitor cells (NPCs) from fetal CNS tissue, and do not express any polyomavirus T Ag (28-30). They have been used in multiple studies of JCV, including a study of susceptibility factors for JCV infection, and to look at the effect of 1-O-hexadecyloxypropyl-cidofovir (CMX001) on JCV replication (28, 29). One advantage to the use of PDAs is that they are more likely to accurately mimic the conditions present in the glial cells in the brain. However, they require the use of fetal CNS tissue, and may be more difficult to obtain and culture than transformed cell lines. Nevertheless, it may be beneficial to repeat our experiments done in cell lines in PDAs.

Currently, there is not a single perfect system for studying JCV in cell culture. Both the currently available cell lines and PDAs have advantages and disadvantages. Cell lines either express T Ag or are derived from tumors, but they grow well in culture and provide robust replication of JCV. PDAs may be difficult to obtain and grow, but are more likely to represent the conditions present in glial cells in the brain. The best utilization of these reagents is most likely using a combination of different cell lines and PDAs. A study of the effect of CMX001 on JCV replication used both Cos-7 and PDA

cells, and found the results were consistent between the two cell types (29). It would be beneficial to follow up the studies we have done here using cell lines in PDAs and possibly also in NPCs which have been differentiated into neuronal cells.

CONCLUSION

Infection with JCV is prevalent, with 39-91% of the population worldwide being seropositive for antibodies against the virus, depending on the population studied and assay used (31-35). Individuals infected with JCV are at risk for the development of PML, JCV GCN and JCVE if they develop some form of immunosuppression. Additionally, with the use of immunomodulatory monoclonal antibody therapies, more of which are being developed for a variety of ailments, the population at risk for the development of these diseases is increasing. Currently, there is no effective therapy for PML or other diseases caused by JCV infection in the brain. The management consists of treating the underlying cause of immune suppression to boost the patient's immune response to JCV, or, if possible, discontinuation of immunosuppressive medications. The development of a drug which inhibits JCV replication would be extremely valuable for the treatment of these patients. A better understanding of JCV replication and pathogenesis may aid in such a breakthrough. The agnoprotein was given its name due to the unknown nature of its function. While recent research has begun to elucidate the functions of the agnoprotein and agnogene, the mechanisms of action remain unknown. Interestingly, of the human polyomaviruses, only JCV and BKV have an agnogene. All of the more recently discovered viruses, including MCPyV, do not have an agnogene encoding an agnoprotein. A better understanding of the role of the agnogene in the viral replication cycle will increase our understanding of JCV replication, and may help in the development of treatments for PML and other diseases caused by JCV infection in the brain.

In this thesis, we have explored the role of the agnogene, agnoprotein and RR in JCV replication. JCV_{CPN} was isolated from the brain of the first patient found to have JCV infection of cortical pyramidal neurons. It is a pathogenic, naturally occurring strain of JCV which contains a 143 nucleotide deletion in the agnogene and has an archetype-like RR. Although our cell culture studies did not find evidence of a replication advantage for JCV_{CPN} in neuronal cells, it is possible that JCV_{CPN} is responsible for the broadened pathogenesis of JCV seen in JCVE. Using JCV_{CPN} to study the agnoprotein and agnogene we found that the agnogene DNA is necessary for the expression of VP1 capsid protein and the successful production of infectious virions. Additionally, the phenotype of JCV_{CPN} can be attributed to the deletion of the nucleotides in the agnogene, rather than the loss of a full length agnoprotein. We generated additional deletions in the agnogene and found that nucleotides 376-396 within the agnogene are critical for VP1 protein production. Finally, we attempted to identify host cell proteins which bind to the agnogene DNA. We have not yet identified a specific binding factor, but future efforts to identify binding factors and their functions in JCV replication will help to clarify the mechanism of action of the agnogene. Overall, these studies have added considerably to our understanding of the role of the agnogene in JCV replication.

REFERENCES

1. Du Pasquier RA, Corey S, Margolin DH, Williams K, Pfister LA, De Girolami U, Mac Key JJ, Wuthrich C, Joseph JT, Koralnik IJ. 2003. Productive infection of cerebellar granule cell neurons by JC virus in an HIV+ individual. *Neurology* 61: 775-82

2. Schippling S, Kempf C, Buchele F, Jelcic I, Bozinov O, Bont A, Linnebank M, Sospedra M, Weller M, Budka H, Martin R. 2013. JC virus granule cell neuronopathy and GCN-IRIS under natalizumab treatment. *Ann Neurol* 74: 622-6

3. Hecht JH, Glenn OA, Wara DW, Wu YW. 2007. JC virus granule cell neuronopathy in a child with CD40 ligand deficiency. *Pediatr Neurol* 36: 186-9

4. Granot R, Lawrence R, Barnett M, Masters L, Rodriguez M, Theocharous C, Pamphlett R, Hersch M. 2009. What lies beneath the tent? JC-virus cerebellar granule cell neuronopathy complicating sarcoidosis. *J Clin Neurosci* 16: 1091-2

5. Tan IL, Brew BJ. 2009. Possible JCV granular cell neuronopathy in a patient with HIV infection. *Neurology* 73: 1598-9

6. Wuthrich C, Dang X, Westmoreland S, McKay J, Maheshwari A, Anderson MP, Ropper AH, Viscidi RP, Koralnik IJ. 2009. Fulminant JC virus encephalopathy with productive infection of cortical pyramidal neurons. *Ann Neurol* 65: 742-8

7. Wuthrich C, Koralnik IJ. 2012. Frequent infection of cortical neurons by JC virus in patients with progressive multifocal leukoencephalopathy. *J Neuropathol Exp Neurol* 71: 54-65

8. Wuthrich C, Cheng YM, Joseph JT, Kesari S, Beckwith C, Stopa E, Bell JE, Koralnik IJ. 2009. Frequent infection of cerebellar granule cell neurons by polyomavirus JC in progressive multifocal leukoencephalopathy. *J Neuropathol Exp Neurol* 68: 15-25

9. Bayliss J, Karasoulos T, McLean CA. 2012. Frequency and large T (LT) sequence of JC polyomavirus DNA in oligodendrocytes, astrocytes and granular cells in non-PML brain. *Brain Pathol* 22: 329-36

10. Simon MA, Ilyinskii PO, Baskin GB, Knight HY, Pauley DR, Lackner AA. 1999. Association of simian virus 40 with a central nervous system lesion distinct from

progressive multifocal leukoencephalopathy in macaques with AIDS. *Am J Pathol* 154: 437-46

11. Axthelm MK, Koralnik IJ, Dang X, Wuthrich C, Rohne D, Stillman IE, Letvin NL. 2004. Meningoencephalitis and demyelination are pathologic manifestations of primary polyomavirus infection in immunosuppressed rhesus monkeys. *J Neuropathol Exp Neurol* 63: 750-8

12. Dang X, Wuthrich C, Axthelm MK, Koralnik IJ. 2008. Productive simian virus 40 infection of neurons in immunosuppressed Rhesus monkeys. *J Neuropathol Exp Neurol* 67: 784-92

13. Kaliyaperumal S, Dang X, Wuethrich C, Knight HL, Pearson C, MacKey J, Mansfield KG, Koralnik IJ, Westmoreland SV. 2013. Frequent infection of neurons by SV40 virus in SIV-infected macaque monkeys with progressive multifocal leukoencephalopathy and meningoencephalitis. *Am J Pathol* 183: 1910-7

14. Dang X, Wuthrich C, Gordon J, Sawa H, Koralnik IJ. 2012. JC virus encephalopathy is associated with a novel agnoprotein-deletion JCV variant. *PLoS One* 7: e35793

15. Sariyer IK, Akan I, Palermo V, Gordon J, Khalili K, Safak M. 2006. Phosphorylation mutants of JC virus agnoprotein are unable to sustain the viral infection cycle. *J Virol* 80: 3893-903

16. Tan CS, Ellis LC, Wuthrich C, Ngo L, Broge TA, Jr., Saint-Aubyn J, Miller JS, Koralnik IJ. 2010. JC virus latency in the brain and extraneural organs of patients with and without progressive multifocal leukoencephalopathy. *J Virol* 84: 9200-9

17. Akan I, Sariyer IK, Biffi R, Palermo V, Woolridge S, White MK, Amini S, Khalili K, Safak M. 2006. Human polyomavirus JCV late leader peptide region contains important regulatory elements. *Virology* 349: 66-78

18. Olsen GH, Andresen PA, Hilmarsen HT, Bjorang O, Scott H, Midtvedt K, Rinaldo CH. 2006. Genetic variability in BK Virus regulatory regions in urine and kidney biopsies from renal-transplant patients. *J Med Virol* 78: 384-93

19. Myhre MR, Olsen GH, Gosert R, Hirsch HH, Rinaldo CH. 2010. Clinical polyomavirus BK variants with agnogene deletion are non-functional but rescued by trans-complementation. *Virology* 398: 12-20

20. Gluzman Y. 1981. SV40-transformed simian cells support the replication of early SV40 mutants. *Cell* 23: 175-82

21. Major EO, Miller AE, Mourrain P, Traub RG, de Widt E, Sever J. 1985. Establishment of a line of human fetal glial cells that supports JC virus multiplication. *Proc Natl Acad Sci U S A* 82: 1257-61

22. Tumilowicz JJ, Nichols WW, Cholon JJ, Greene AE. 1970. Definition of a continuous human cell line derived from neuroblastoma. *Cancer Res* 30: 2110-8

23. Gee GV, Manley K, Atwood WJ. 2003. Derivation of a JC virus-resistant human glial cell line: implications for the identification of host cell factors that determine viral tropism. *Virology* 314: 101-9

24. Wollebo HS, Safak M, Del Valle L, Khalili K, White MK. 2011. Role for tumor necrosis factor-alpha in JC virus reactivation and progressive multifocal leukoencephalopathy. *J Neuroimmunol* 233: 46-53

25. Romagnoli L, Wollebo HS, Deshmane SL, Mukerjee R, Del Valle L, Safak M, Khalili K, White MK. 2009. Modulation of JC virus transcription by C/EBPbeta. *Virus Res* 146: 97-106

26. Devireddy LR, Kumar KU, Pater MM, Pater A. 1996. Evidence for a mechanism of demyelination by human JC virus: negative transcriptional regulation of RNA and protein levels from myelin basic protein gene by large tumor antigen in human glioblastoma cells. *J Med Virol* 49: 205-11

27. Wollebo HS, Woldemichaele B, Khalili K, Safak M, White MK. 2013. Epigenetic regulation of polyomavirus JC. *Virol J* 10: 264

28. Monaco MC, Maric D, Bandeian A, Leibovitch E, Yang W, Major EO. 2012. Progenitor-derived oligodendrocyte culture system from human fetal brain. *J Vis Exp*

29. Gosert R, Rinaldo CH, Wernli M, Major EO, Hirsch HH. 2011. CMX001 (1-O-hexadecyloxypropyl-cidofovir) inhibits polyomavirus JC replication in human brain progenitor-derived astrocytes. *Antimicrob Agents Chemother* 55: 2129-36

30. Messam CA, Hou J, Gronostajski RM, Major EO. 2003. Lineage pathway of human brain progenitor cells identified by JC virus susceptibility. *Ann Neurol* 53: 636-46

31. Knowles WA, Pipkin P, Andrews N, Vyse A, Minor P, Brown DW, Miller E. 2003. Population-based study of antibody to the human polyomaviruses BKV and JCV and the simian polyomavirus SV40. *J Med Virol* 71: 115-23

32. Egli A, Infanti L, Dumoulin A, Buser A, Samaridis J, Stebler C, Gosert R, Hirsch HH. 2009. Prevalence of polyomavirus BK and JC infection and replication in 400 healthy blood donors. *J Infect Dis* 199: 837-46

33. Kean JM, Rao S, Wang M, Garcea RL. 2009. Seroepidemiology of human polyomaviruses. *PLoS Pathog* 5: e1000363

34. Antonsson A, Green AC, Mallitt KA, O'Rourke PK, Pawlita M, Waterboer T, Neale RE. 2010. Prevalence and stability of antibodies to the BK and JC polyomaviruses: a long-term longitudinal study of Australians. *J Gen Virol* 91: 1849-53

35. Matos A, Duque V, Beato S, da Silva JP, Major E, Melico-Silvestre A. 2010. Characterization of JC human polyomavirus infection in a Portuguese population. *J Med Virol* 82: 494-504

APPENDIX A (copy)

Ellis LC, Norton E, Dang X, Koralnik IJ (2013) Agnogene Deletion in a Novel Pathogenic JC Virus Isolate Impairs VP1 Expression and Virion Production. PLoS ONE 8(11): e80840. doi:10.1371/journal.pone.0080840

OPEN ACCESS Freely available online

PLOS ONE

Agnogene Deletion in a Novel Pathogenic JC Virus Isolate Impairs VP1 Expression and Virion Production

Laura C. Ellis[1,2,3], Elizabeth Norton[1,2¤], Xin Dang[1,2], Igor J. Koralnik[1,2*]

1 Division of Neurovirology, Department of Neurology, Beth Israel Deaconess Medical Center, Harvard Medical School, Boston, Massachusetts, United States of America, **2** Center for Virology and Vaccine Research, Department of Medicine, Beth Israel Deaconess Medical Center, Harvard Medical School, Boston, Massachusetts, United States of America, **3** Harvard Program in Virology, Harvard Medical School, Boston, Massachusetts, United States of America

Abstract

Infection of glial cells by the human polyomavirus JC (JCV) causes progressive multifocal leukoencephalopathy (PML). JCV Encephalopathy (JCVE) is a newly identified disease characterized by JCV infection of cortical pyramidal neurons. The virus JCV_{CPN} associated with JCVE contains a unique 143 base pair deletion in the agnogene. Contrary to most JCV brain isolates, JCV_{CPN} has an archetype-like regulatory region (RR) usually found in kidney strains. This provided us with the unique opportunity to determine for the first time how each of these regions contributed to the phenotype of JCV_{CPN}. We characterized the replication of JCV_{CPN} compared to the prototype virus JCV_{Mad-1} in kidney, glial and neuronal cell lines. We found that JCV_{CPN} is capable of replicating viral DNA in all cell lines tested, but is unable to establish persistent infection seen with JCV_{Mad-1}. JCV_{CPN} does not have an increased ability to replicate in the neuronal cell line tested. To determine whether this phenotype results from the archetype-like RR or the agnogene deletion, we generated chimeric viruses between JCV_{CPN} of JCV_{Mad-1}. We found that the deletion in the agnogene is the predominant cause of the inability of the virus to maintain a persistent infection, with the introduction of a full length agnogene, either with or without agnoprotein expression, rescues the replication of JCV_{CPN}. Studying this naturally occurring pathogenic variant of JCV provides a valuable tool for understanding the functions of the agnogene and RR form in JCV replication.

Citation: Ellis LC, Norton E, Dang X, Koralnik IJ (2013) Agnogene Deletion in a Novel Pathogenic JC Virus Isolate Impairs VP1 Expression and Virion Production. PLoS ONE 8(11): e80840. doi:10.1371/journal.pone.0080840

Editor: Robert Shin Fujinami, University of Utah School of Medicine, United States of America

Received August 1, 2013; **Accepted** October 16, 2013; **Published** November 12, 2013

Funding: This study was supported in part by NIH grants R01 NS 074995 and 047029 and K24 NS 060950 to IJK; grants.nih.gov. The funders had no role in study design, data collection and analysis, decision to publish, or preparation of the manuscript.

Competing Interests: The authors have declared that no competing interests exist.

* E-mail: ikoralni@bidmc.harvard.edu

¤ Current address: employee at Biogen Idec, Weston, Massachusetts, United States of America

Introduction

The human polyomavirus JC (JCV) has a circular double stranded DNA genome which can be divided into 3 regions. The early coding region encodes the regulatory proteins small t antigen and large T antigen (T Ag). The late coding region encodes the VP1, VP2 and VP3 structural proteins, and the agnoprotein [1]. The regulatory region (RR) contains the origin of replication, as well as the early and late promoters [2,3]. While the coding regions are well conserved, the RR is hypervariable, with different sequences being isolated from individuals [1]. Archetype RR, which has one 98-bp element and contains a 23-bp and a 66-bp insert, is generally found in the kidneys or urine of healthy and immunosuppressed individuals [4]. RRs from the brain or CSF of PML patients are generally of the rearranged type, containing two 98-bp tandem repeats with additional mutations, insertions and deletions [1,2].

JCV is the etiological agent of Progressive Multifocal Leukoencephalopathy (PML), an often fatal demyelinating disease caused by lytic infection of oligodendrocytes by the virus [5]. Infection with JCV is widespread in the population, but remains asymptomatic in healthy people [6,7]. Development of PML is associated with immune suppression, such as in patients with AIDS [8], organ transplants [9] or hematological malignancies [10]. We have identified two additional syndromes caused by JCV infection in the brain, JCV Granule Cell Neuronopathy (JCV GCN) [11,12,13] and JCV Encephalopathy (JCVE) [14]. The viruses isolated from patients with these syndromes contain previously unreported unique mutations. JCV GCN is associated with deletions in the C-terminus of the VP1 protein [15,16] and JCVE with a deletion in the agnogene [17]. These naturally occurring pathogenic variants provide a unique tool for studying the basic biology of JCV replication and pathogenesis.

JCVE was described in an HIV-negative patient with a history of lung cancer treated with chemotherapy, who presented with cortical lesions, aphasia and progressive cognitive decline. Post-mortem analysis of the brain showed cortical lesions with productive infection of cortical pyramidal neurons [14]. Isolation and sequencing of the JCV DNA present in the brain of this patient identified a virus with an archetype-like RR and a 143 base pair deletion in the agnogene [17]. This virus was named JCV Cortical Pyramidal Neuron 1 (JCV_{CPN1}). The deleted agnogene encodes a 10 amino acid truncated peptide. Further analysis found that multiple forms of JCV_{CPN} were present, and that these strains co-existed with a virus containing a full length agnogene. Immunostaining analysis indicated that the majority of the cortical cells infected with JCV contained the truncated form of the agnoprotein [17].

JCV agnoprotein is a highly basic, 71 amino acid, non-essential protein that is expressed late in infection, but not incorporated into virions [18]. It is primarily expressed in the cytoplasm, particularly in the perinuclear region, with a small amount found in the nucleus [19]. Agnoprotein has been shown to form homodimers and oligimers [20]. Agnoprotein contains 3 phosphorylation sites, which can be phosphorylated by protein kinase C [21] and dephosphorylated by protein phosphatase 2A [22]. The phosphorylation state may impact agnoprotein localization [19]. Agnoprotein has been shown to bind to T Ag, down regulating DNA replication [23] and enhancing T Ag origin binding [24]. Agnoprotein may also influence viral gene expression and splicing of viral transcripts [25]. Loss of agnoprotein expression has been associated with loss of early and late mRNA expression [19]. Agnoprotein has also been shown to suppress activity of the late promoter [23], and to interact with the transcription factor YB-1, inhibiting its ability to activate the early and late promoters [26]. Prevention of agnoprotein expression also has been shown to result in decreased levels of T Ag and VP1 protein expression [27]. Viruses lacking agnoprotein are less efficient at packaging DNA and virion formation, with infected cells releasing empty particles [27,28]. The agnoprotein may also function as a viroporin, aiding in the release of virions from infected cells [29]. These studies have added to our knowledge of agnoprotein function in recent years, but the exact mechanisms by which this protein influences the viral life cycle remain unclear.

In addition to agnoprotein function, the DNA of the agnogene has been shown to contain 3 host cell factor binding sites. Deletion of the agnogene DNA has a greater effect on replication than prevention of agnoprotein expression by mutation of the start codon [30]. In the agnogene deletion present in JCV_{CPN}, 1 of the 3 sites is completely deleted, and a second is shortened by 1 nucleotide.

We hypothesized that the agnogene deletion of JCV_{CPN} allowed the virus to infect cortical pyramidal neurons. We used cell culture models to study the replication of JCV_{CPN} compared to the prototype strain $JCV_{Mad\text{-}1}$ [31] in different cell types. We generated chimeric viruses of JCV_{CPN} and $JCV_{Mad\text{-}1}$, swapping both the agnogene and RR, to determine the specific effects of the agnogene deletion and the archetype-like RR on viral replication in cell culture. In these experiments we characterized the replication of JCV_{CPN} in different cell types, and determined the relative contributions of the agnogene deletion and archetype-like RR to the JCV_{CPN} replication phenotype. Studying these novel naturally occurring changes in JCV_{CPN} provided unique insights into our understanding of the function of the agnogene and RR form in JCV replication.

Materials and Methods

Cell Culture

Cos-7 [32], SVG [33] and IMR-32 [34] cells were purchased from the ATCC. Cos-7 cells were maintained in Dulbecco's Modified Eagle Medium (DMEM) supplemented with 10% fetal bovine serum (FBS), Penicillin (500 units/mL) and Streptomycin (500 μg/mL). SVG cells were maintained in Minimum Essential Medium (MEM) supplemented with Sodium Bicarbonate (1.5 g/L), 10% FBS, Penicillin (500 units/mL) and Streptomycin (500 μg/mL). IMR-32 cells were maintained in MEM supplemented with Sodium Bicarbonate (1.5 g/L), Sodium Pyruvate (1 mM), Non-Essential Amino Acids (NEAA) (Invitrogen), 10% FBS, Penicillin (500 units/mL) and Streptomycin (500 μg/mL).

Plasmids

Construction of the JCV_{CPN} and $JCV_{Mad\text{-}1}$ plasmids was previously described by Dang et al. [17]. To generate the agnogene chimeric viruses Mad-1 C-Agno and CPN M-Agno, the agnogene region was excised using the restriction enzymes ApaI and PciI (New England Biolabs), and the digested DNA was run on an agarose gel. The agnogene DNA and the virus minus the agnogene DNA bands were excised and purified using the QIAquick Gel Extraction Kit (QIAGEN). Agnogene DNA segments were ligated into the viral backbone using T4 ligase (New England Biolabs). The resulting plasmids were transformed into TOP10 (Invitrogen) or XL1-Blue cells (Agilent). Plasmid DNA was maxi prepped (QIAGEN), and plasmids were fully sequenced. The RR chimeras were generated with the same protocol, using the restriction enzymes BamHI and PciI (NEB) to excise the RR. Mad-1 Pt and Mad-1 Del plasmids were previously described [30], and obtained as a generous gift from Dr Safak. The agnogene from these viruses was introduced into our $JCV_{Mad\text{-}1}$ or JCV_{CPN} plasmid using the ApaI and PciI restriction sites as previously described.

Transfection

Full-length JCV genomes were digested out of the plasmid backbone using EcoRI (NEB) and run on a 0.8% agarose gel. The 5 kb virus band was purified using the QIAquick Gel Extraction Kit (QIAGEN). Cells were transfected with 1 μg (for IMR-32 and SVG cells) or 2 μg (for Cos-7 cells) of purified JCV DNA using FuGENE6 transfection reagent (Roche or Promega) in 6 well plates. 3 days post-transfection, cells were passaged 1:3 to T25 flasks, and subsequently every 3–4 days 1:4 in T25 flasks. At each passage, supernatant was collected and cells were collected, pelleted and stored at −80°C until further analysis.

DNA Extraction and Quantitative PCR (QPCR)

DNA was extracted from cell pellets and supernatant samples using the QIAamp DNA Blood Mini Kit (QIAGEN). QPCR was performed as previously described [15]. An RNAase P primer/probe set (Applied Biosystems) was used in a multiplex assay with the JCV primer/probe set on cell lysate samples. Copies RNAse P per reaction was determine and divided by 2 to determine the number of input cells for each reaction. Copies JCV/cell was calculated by dividing the copies JCV per reaction by the number of cells per reaction. All samples were run in triplicate.

RNA Extraction and qRT-PCR

RNA was extracted using the RNEasy Mini Kit (QIAGEN). RNA samples were digested with rDNAse I (Ambion) to remove any contaminating DNA. Reverse transcription was done using the High Capacity RNA-to-cDNA Kit (Applied Biosystems). QPCR was performed on a 7300 Real-time PCR System using Gene Expression Master Mix (Applied Biosystems). For amplification of the early transcript mRNA, a primer probe set spanning the Large T Ag splice site was used. The primers were JCT208F (5′-CATCAGCCTGATTTTGGTACATG-3′, reverse complement of position 4784–4806) and JCT 279R (5′-CCAGGATTCCCATTCATCTGTT-3′, position 4392–4412). The probe used was JCT-232p (6FAM-5′-AAT AGT TCA GAG GTG CCA AC-3′-MGB, reverse complement of position 4419–4426 and 4771–4482). For detection of late transcript mRNA we used the primers JCVP1-745F (5′-GGTGACAACTTATACTTGTCAGCTGTT-3′, position 2213–2239) and JCVP1-812R (5′-TGCTGGGAACCAGACCTGTT-3′, reverse complement of position 2261–2280) and the probe JCVP1-773p (6FAM-

5′-ATG TCT GTG GCA TGT TTA-3′-MGB, position 2241–2248). A TATA-box binding protein (TBP) primer/probe set (Invitrogen) was used as the endogenous control for determination of relative quantity by the comparative C_T method (also known as the ΔΔCt method) [35]. All samples were run in triplicate wells.

Western Blotting

Cells were lysed in TNN lysis buffer (50 mM Tris-HCl pH 7.5, 150 mM NaCl, 0.1% NP40) with 0.2 mM Na-Orthovanadate and 1% protease inhibitor cocktail for 30 minutes on ice. Samples were centrifuged at 8000 rpm for 4 min to remove cell debris. Laemmli Buffer (Bio-Rad) was added to whole cell lysate. Samples were boiled for 10 min and run on a 10% SDS-PAGE gel in Tris/Glycine/SDS running buffer (Bio-Rad). Samples were transferred for 2 hours at 150 mAmps to a nitrocellose membrane in Transfer Buffer (Tris/Glycine with 20% methanol) or to a nitrocellulose membrane using the iBlot system (Invitrogen). Membranes were blocked using 5% milk in PBST and incubated overnight at 4°C with VP1 antibody pAB597 (1 mg/mL) diluted 1:1000 or loading control anti-alpha tubulin [DM1A] (abcam) in 2% milk in PBST. An HRP conjugated goat-anti mouse IgG secondary antibody (Bio-Rad) was used and detection was done with ECL Plus reagent (Thermo Scientific). Signal was detected on film.

Flow Cytometry Analysis of JCV-Positive Cells

Cells were trypsinized, collected and washed with 2% FBS in PBS. Cells were passed through a 30 μm filter (Miltenyi Biotec) and incubated for 20 minutes at 4°C with Aqua Amine to stain dead cells, and then washed with PBS. Cells were fixed with Cytofix/Cytoperm (BD Biosciences) for 20 minutes at 4°C then washed with PBS. Staining with the primary antibody PAB597 (mouse monoclonal anti-VP1) in Perm/Wash Buffer (BD Biosciences) was done for 2 hours at 4°C. Cells were washed with Perm/Wash Buffer, then PBS and then stained with Alexa 488 conjugated Anti-Mouse IgG (Invitrogen) secondary antibody in Perm/Wash Buffer for 1 hour at 4°C. Cells were washed, and then analyzed using a BD LSR II Flow Cytometer (BD Biosciences).

JCV Infectivity Test

Cos-7 cells were plated in 6 well plates at low density and allowed to adhere overnight. Cell free supernatant collected from transfected cells was put on the Cos-7 cells, and incubated 2 hours at room temperature with rocking. Supernatant was not digested with DNAse to remove free JCV DNA, as previous experiments have shown that digesting with DNAse does not affect the levels of JCV DNA detected in the supernatant by qPCR, or the percentage of cells subsequently infected from the supernatant (data not shown). The infection was allowed to proceed for 7 days. Cells were then collected and analyzed for either VP1 expression by flow cytometry or JCV DNA by QPCR as previously described.

Statistical Analyses

Analyses were done using SAS Software version 9.3. Data was tested for normality before statistical analysis. P-values for DNA levels were determined using the non-parametric Wilcoxon Rank Test. P-values for mRNA levels were done using univariate analysis, and taking the student's t p value. Flow cytometry p-values were determined using Student's t test.

Results

JCV_{CPN} has a 143 base pair deletion in the agnogene and an archetype-like RR

The JCV_{CPN1} RR is archetype-like, lacking a duplication of the TATA-box and containing a 66 bp and 80 bp insert, which contain portions of the 23 bp and 66 bp inserts present in archetype RR (Fig. 1A) [17]. A 143 bp deletion in the agnogene is also present in JCV_{CPN1} (Fig. 1B) [17]. This deletion creates a premature stop codon, and is predicted to code for a truncated 10 amino acid agnoprotein. Multiple forms of JCV_{CPN} were identified, including $JCV_{CPN1.1}$ and $JCV_{CPN1.2}$ which both contain the same regulatory region and agnogene deletion. In addition, $JCV_{CPN1.2}$ contains a 75 bp duplication between the agnogene and the VP2 gene, encompassing the start of the VP2 gene (Fig. 1B). This form is predicted to encode for both a truncated and a full length VP2. Our studies determined that $JCV_{CPN1.1}$ and $JCV_{CPN1.2}$ are phenotypically equivalent in our cell cultures model (data not shown). Therefore, we chose to conduct the experiments in this study using the $JCV_{CPN1.2}$ strain, because it was the predominant strain in the JCVE patient's brain. $JCV_{CPN1.2}$ is referred to as JCV_{CPN} for the remainder of this work.

JCV_{CPN} can replicate DNA in cell culture, but at a lower level than $JCV_{Mad\text{-}1}$

To determine the cellular tropism of JCV_{CPN}, we studied its replication in cell culture. We used multiple cell lines to model the replication of the virus in three different types of cells, kidney cells, glial cells and neurons. Cos-7 cells are African Green Monkey kidney cells which express SV40 T Ag, and are known to replicate JCV well [32]. SVG cells are human fetal glial cells, also transformed with SV40 T Ag [33]. IMR-32 cells are a human neuroblastoma cell line, derived from a tumor isolated from the abdominal cavity of a child, which do not express any polyomavirus T Ag [34]. We first wanted to determine if JCV_{CPN} is capable of genome replication. To do so, linearized genomes of JCV_{CPN} and $JCV_{Mad\text{-}1}$ were transfected into Cos-7, SVG and IMR-32 cells. DNA from cell lysate, representing JCV DNA replicated in the transfected cells, and supernatant, representing DNA released from the transfected cells, was extracted and digested with DpnI to remove any remaining input plasmid DNA. JCV genome copy number was determined by QPCR. We found that JCV_{CPN} replicated DNA after transfection in all 3 cell lines tested (Fig. 1C–H). However, the levels of DNA were not equivalent to those seen with the prototype strain $JCV_{Mad\text{-}1}$.

In Cos-7 kidney cells, $JCV_{Mad\text{-}1}$ establishes a high level infection that persists over 3 weeks, as measured by copies JCV DNA in the cell lysate and supernatant (Fig. 1C and 1D). JCV_{CPN} has equivalently high levels of JCV genomes present in the cell lysate and supernatant during the first week post-transfection, but does not maintain such a high viral load, with the copy number decreasing with time. In SVG glial cells, both $JCV_{Mad\text{-}1}$ and JCV_{CPN} establish persistent infections (Fig 1E and 1F). Levels of JCV_{CPN} genome copies in cell lysate and supernatant at later time points post-transfection are significantly lower than those of $JCV_{Mad\text{-}1}$, but with a smaller magnitude of difference than observed in Cos-7 cells. In IMR-32 neuronal cells, $JCV_{Mad\text{-}1}$ DNA decreased over the first 2 weeks after transfection, and then leveled off, remaining detectable over 3 weeks (Fig. 1G and 1H). In contrast, JCV_{CPN} decreased and dropped below the limit of detection at 14 days post-transfection in cell lysate and 17 days post-transfection in the supernatant. These results indicate that JCV_{CPN} is able to replicate its genome after transfection into Cos-7, SVG and IMR-32 cells, but may have a decreased capacity to

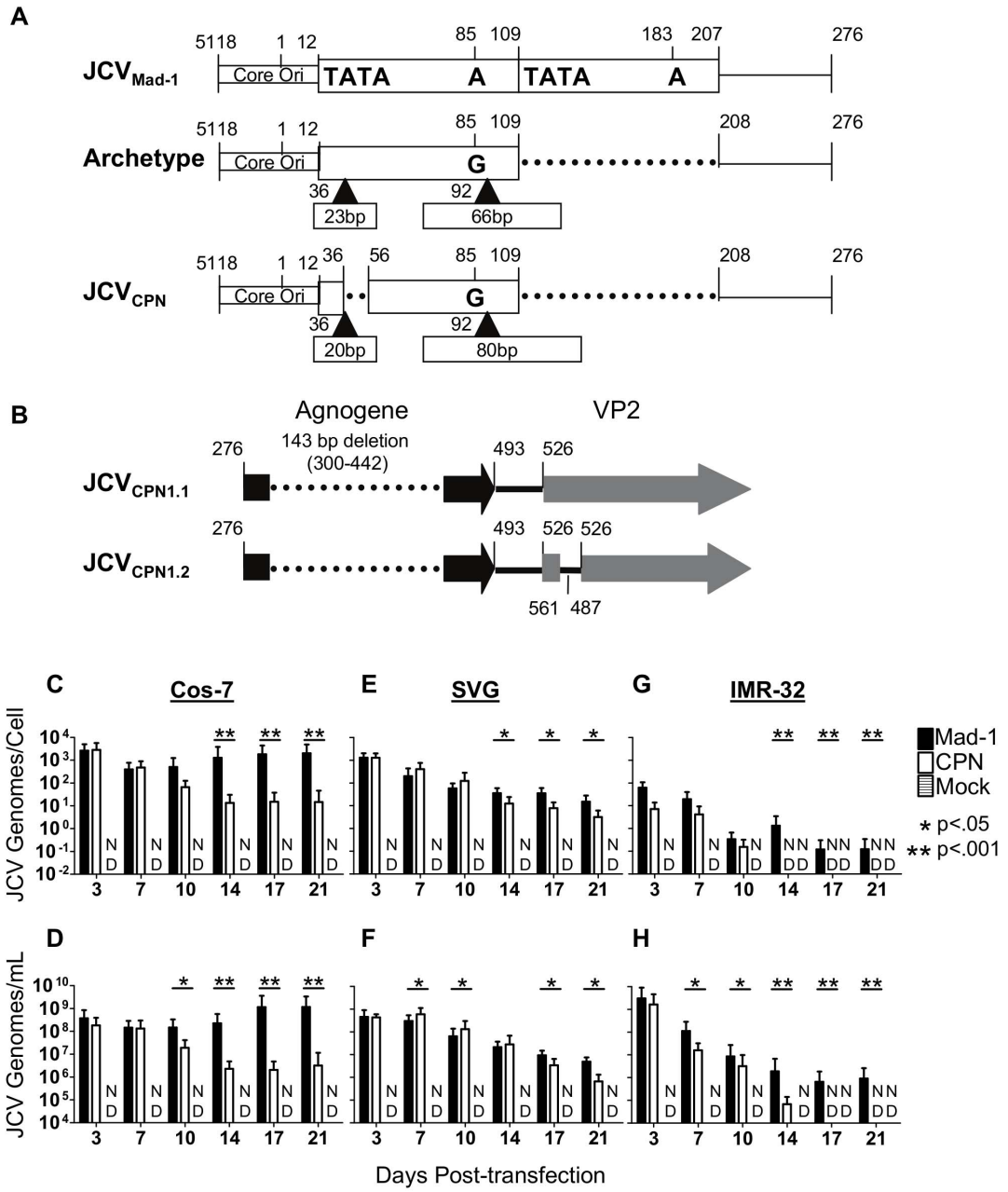

Figure 1. JCV_{CPN} replicates viral DNA, but at lower levels than JCV_{Mad-1}. (A) JCV_{CPN} RR is archetype-like (adapted from (17)). (B) $JCV_{CPN1.2}$ (hereafter referred to as simply JCV_{CPN}) agnogene contains a 143 base pair deletion followed by a 75 base pair duplication at the beginning of the VP2 gene. (C–H) Cos-7, SVG and IMR-32 cells were transfected with linearized JCV genomes, or mock transfected. Cells were subcultured every 3–4 days and cell and supernatant samples were collected. DNA was extracted from the samples, digested with DpnI to remove input plasmid DNA, and analyzed by QPCR. Data represents the average of 4–10 independent experiments. In Cos-7 cell lysate (C) and supernatant (D) JCV_{Mad-1} but not JCV_{CPN} establishes a persistent infection. In SVG cell lysate (E) and supernatant (F) JCV_{Mad-1} and JCV_{CPN} both establish persistent infections. In IMR-32 cells, JCV_{Mad-1} infection persists for 21 days, while JCV_{CPN} becomes undetectable in cell lysate (G) and in supernatant (H). Error bars represent standard deviation. P-values were calculated using the Wilcoxon Rank Test. ND is not detected.
doi:10.1371/journal.pone.0080840.g001

persist and spread within the culture compared to prototype JCV_{Mad-1}. Additionally, JCV_{CPN} does not display a replication advantage in the neuronal cell culture line tested.

JCV_{CPN} expresses both early and late transcripts, but at decreased levels compared to JCV_{Mad-1}

Knowing that JCV_{CPN} is able to replicate viral DNA, but not establish a persistent high level infection, we wanted to determine if JCV_{CPN} is able initiate transcription of mRNAs from the early and late promoters. To do so, we used qRT-PCR on RNA from transfected cells using primer and probe sets located in T Ag to detect early transcripts, and in VP1 to detect late transcripts. In Cos-7, SVG and IMR-32 cells, JCV_{CPN} expresses detectable levels of both the early and late transcripts (Fig. 2). In Cos-7 cells, the level of early transcripts is significantly lower than those seen with JCV_{Mad-1} 3 and 10 days post-transfection (Fig. 2A). In SVG cells,

the level of early transcripts is similar between JCV_{CPN} and JCV_{Mad-1} 3 and 7 days post-transfection, and significantly lower 10 days post-transfection (Fig. 2B). In IMR-32 cells, level of early transcripts produced by JCV_{CPN} is significantly lower than those of JCV_{Mad-1} at 3, 7 and 10 days post-transfection (Fig. 2C). In all three cell lines, the level of late transcripts is markedly lower in JCV_{CPN} transfected cells compared to JCV_{Mad-1} transfected cells (Fig. 2D–F). These results indicate that, although both the early and late promoter of JCV_{CPN} are transcriptionally active, they function at a level lower than JCV_{Mad-1}. The decrease in transcript levels is larger for the late than the early promoter.

JCV_{CPN} fails to produce detectable levels of VP1 protein in Cos-7 cells

We then wanted to determine if JCV_{CPN} produces VP1 protein from the late mRNA. JCV_{Mad-1} transfected cells produce VP1 protein, with the amount of VP1 present increasing with later times post-transfection (Fig. 2G). JCV_{CPN} does not produce detectable levels of VP1 protein, even with long exposure times (Fig. 2G).

To determine if there is VP1 present in a small number of JCV_{CPN} transfected cells, which cannot be detected by Western Blot, we developed a protocol to analyze transfected Cos-7 cells for VP1 expression using flow cytometry. JCV_{Mad-1} transfected cells were positive for VP1 expression, with an increase in the percentage of cells positive for VP1 over time, with the highest percentage of VP1 positive cells seen 21 days post-transfection (Fig. 2H). The percentage of JCV_{Mad-1} VP1 positive cells is significantly higher than the background observed in Mock transfected cells. JCV_{CPN} transfected cells are not positive for VP1 by flow cytometry at a level significantly higher than Mock transfected cells (Fig 2H). This supports the results seen in using Western blotting, that JCV_{CPN} does not express detectable levels of VP1 protein.

JCV_{CPN} produces low levels of infectious virions

Although we could not detect VP1 expression by Western Blot or flow cytometry in transfected cells, there may be a very low level of expression below our limit of detection. We therefore wanted to determine if JCV_{CPN} transfected cells are producing virions capable of infecting a new round of cells. To do so, supernatant

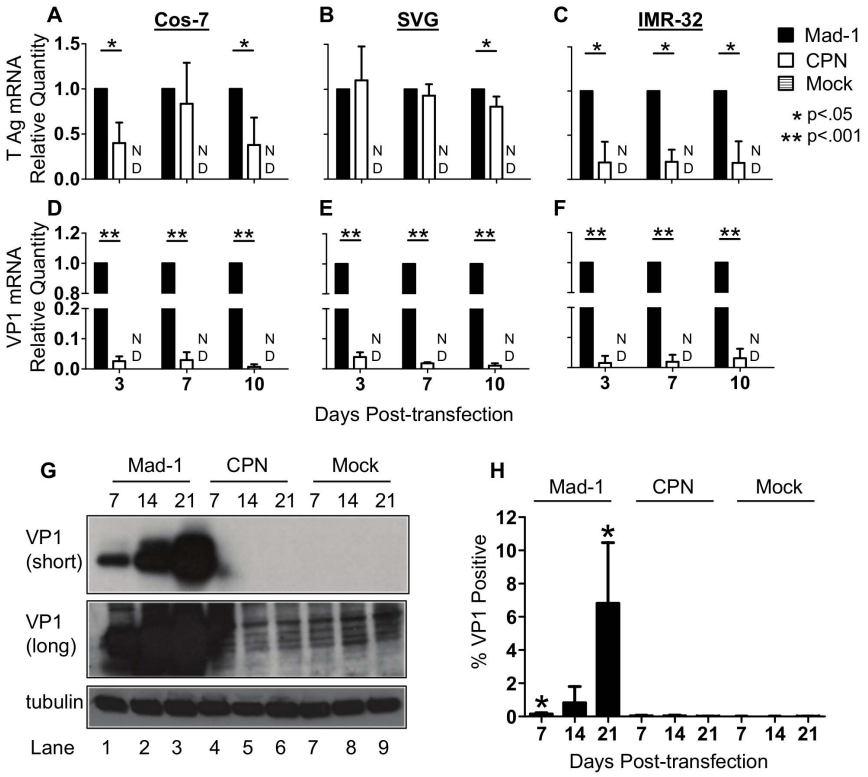

Figure 2. JCV_{CPN} expresses less early and late mRNA and VP1 protein than JCV_{Mad-1}. (A–F) Cos-7, SVG and IMR-32 cells were transfected with JCV_{Mad-1}, JCV_{CPN} or mock transfected and samples collected as described in Figure 1. qRT-PCR was used to determine the levels of early (T Ag) and late (VP1) transcripts. Relative Quantity (RQ) was calculated using the ΔΔCt method, using TATA-Box Binding Protein (TBP) as the endogenous control and JCV_{Mad-1} as the calibrator sample. Data represents the average of 5–6 independent experiments. (A and D) In Cos-7 cells, JCV_{CPN} expresses significantly lower levels of T Ag (A) and VP1 (D) mRNA. (B and E) In SVG cells, levels of T Ag (B) mRNA expressed by JCV_{CPN} are similar to JCV_{Mad-1}, while VP1 (E) mRNA is significantly lower. (C and F) JCV_{CPN} expresses significantly less T Ag (C) and VP1 (F) mRNA in IMR-32 cells. Error Bars represent standard deviation. P values were calculated for Student's t test using univariate analysis. ND is not detected. (G) Western blots were done with PAB597 (anti-VP1) using cell lysate from Cos-7 cells transfected with either JCV_{Mad-1} (Lanes 1–3), JCV_{CPN} (Lanes 7–9) or mock transfected cells (Lanes 4–6) collected 7 (Lanes1,4,7), 14 (Lanes 2,5,8) or 21 (Lanes 3,6,9) days post-transfection. VP1 can be detected in JCV_{Mad-1} transfected cells at all time points, but not at any time with JCV_{CPN}, with either a short (upper panel) or long (middle panel) exposure. Anti-tubulin antibody was used for loading control (lower panel). Blots are representative of 3 independent experiments (H) JCV_{Mad-1}, JCV_{CPN} or mock transfected Cos-7 cells were analyzed for VP1 expression by flow cytometry. JCV_{Mad-1} but not JCV_{CPN} transfected cells have significantly higher levels of VP1 positive cells than Mock transfected samples. Results are the average of 4 independent experiments. Error bars represent standard deviation. P values were calculated using students t test, comparing JCV_{Mad-1} and JCV_{CPN} to mock.
doi:10.1371/journal.pone.0080840.g002

was collected from transfected Cos-7, SVG and IMR-32 cells 7, 14 and 21 days post-transfection and was used to infect Cos-7 cells. Infection was allowed to proceed for 7 days. Cells were collected, and analyzed for JCV DNA by QPCR or stained for VP1 and analyzed by flow cytometry.

JCV_{Mad-1} containing supernatant from Cos-7 cells was able to establish an infection in the new cells, with the viral load and the percentage of cells infected increasing with supernatant collected at later time points post-transfection (Fig. 3A and B). The percentage of VP1 positive cells was significantly higher than in the samples treated with supernatant from mock transfected cells (Fig. 3B). In contrast, cells infected with JCV_{CPN} containing supernatant had significantly lower levels of viral DNA detected, which decreased over time, becoming undetectable in samples infected with supernatant collected 21 days post transfection (Fig. 3A). The percentage of JCV_{CPN} VP1 positive cells was not significantly higher than observed with Mock supernatant (Fig. 3B), which is most likely due to the lack of detectable expression of VP1 protein in JCV_{CPN} transfected cells.

Similar results were seen using supernatant from transfected SVG and IMR-32 cells, with low levels JCV DNA detected in cells infected with JCV_{CPN} containing supernatant collected 7 days post-transfection, and then decreasing (Fig. 3C and D). Using supernatant from SVG cells, JCV_{CPN} DNA remains detectable with supernatant collected 14, but not 21, days post-transfection and JCV_{Mad-1} infected cells had DNA levels that were significantly higher than those observed with JCV_{CPN} at all time points (Fig. 3C). In contrast to the results observed using Cos-7 supernatant, the viral loads in JCV_{Mad-1} infected cells decreased with later collection points using SVG supernatant (Fig. 3C). Cells infected with supernatant collected 14 and 21 days post-transfection from IMR-32 cells had undetectable JCV_{CPN} DNA levels (Fig. 3D). JCV_{Mad-1} DNA was detected in cells infected with supernatant collected from IMR-32 cells at 7 and 21 days, but not 14 days, post-transfection (Fig. 3D). This is most likely due to the levels of JCV DNA being below the limit of detection of our assay.

Generation of chimeras and agnogene mutants

The results of the above experiments comparing JCV_{CPN} and JCV_{Mad-1} suggest that JCV_{CPN} has a block preventing late gene expression and protein production, as well as in the production and release of infectious virions. The two major regions of difference between JCV_{CPN} and JCV_{Mad-1} are the RR and the agnogene. To determine which area of the virus is the major contributor to the phenotype of JCV_{CPN}, we generated chimeric viruses of JCV_{CPN} and JCV_{Mad-1} (Fig. 4). We swapped the agnogene genes of the two viruses to generate Mad-1 C-Agno and CPN M-Agno. Mad-1 C-RR and CPN M-RR were generated by exchanging the RRs of the two viruses. We obtained two agno deletion mutations, Mad-1 Pt, which has a start codon point mutation which prevents the expression of agnoprotein, and Mad-1 Del, which has the entire agnogene deleted. CPN M-Pt contains the full length agnogene with the start codon point mutation from

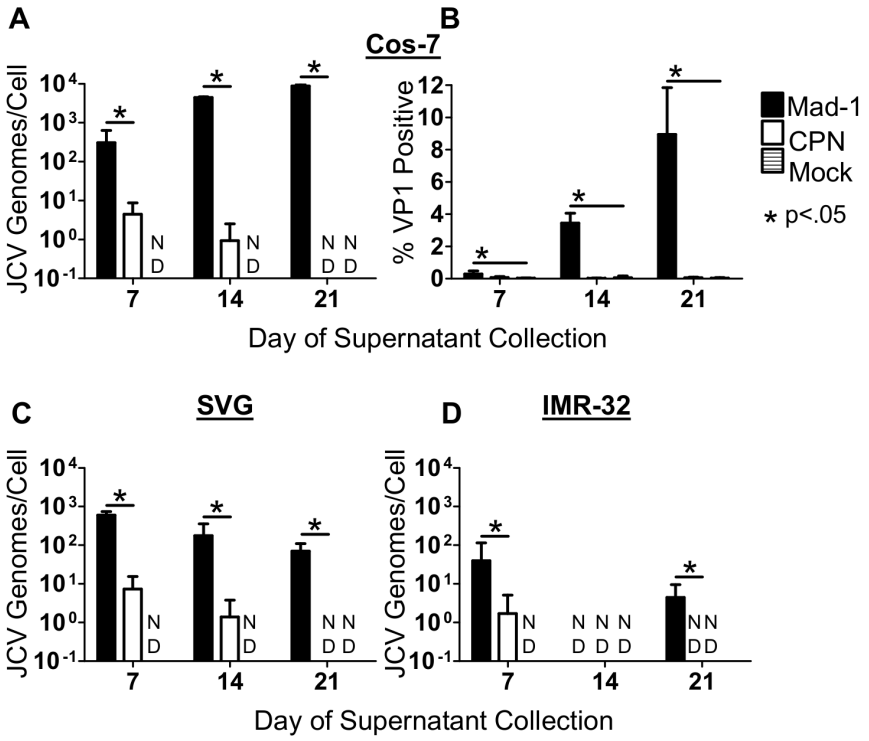

Figure 3. JCV_{CPN} transfected IMR-32, SVG and Cos-7 cells produce low levels of infectious virions. Supernatant from transfected Cos-7, SVG and IMR-32 cells was collected 7, 14 and 21 days post-transfection, and used to infect naive Cos-7 cells. At 7 days post-infection, cells were collected and either analyzed for JCV DNA using QPCR (A, C and D) or stained for VP1 and analyzed using flow cytometry (B). Supernatant collected 7 days post-transfection from JCV_{CPN} transfected Cos-7 (A), SVG (C) or IMR-32 (D) cells can establish an infection in naïve Cos-7 cells, as measured by the presence of JCV DNA 7 days post-infection. Levels of DNA detected with JCV_{CPN} infection are significantly lower than with JCV_{Mad-1} infection (A, C and D). (B) VP1 positive cells are detected after infection with JCV_{Mad-1}, but not JCV_{CPN} containing supernatant. Data is the average of 3–4 independent experiments. Error bars represent standard deviation. P vales were calculated using Wilcoxon rank test for QPCR data, comparing JCV_{CPN} to JCV_{Mad-1}. P-values for flow cytometry data were calculated using students t test, comparing JCV_{Mad-1} and JCV_{CPN} to mock at each time point. ND is not detected.

doi:10.1371/journal.pone.0080840.g003

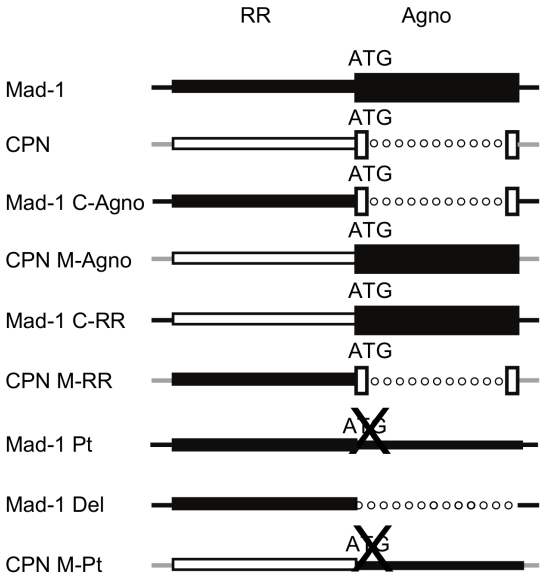

Figure 4. JCV_{Mad-1} and JCV_{CPN} chimeras and agno deletion mutants. This diagram shows the various chimeric viruses and deletion mutants generated. Black represents sequences from JCV_{Mad-1} and white represents sequences from JCV_{CPN}. Lines represent DNA sequences. Dotted Lines represent deletions. Boxes represent genes. An X through ATG represents mutation of the start codon to eliminate protein expression. Mad-1 C-Agno is JCV_{Mad-1} with the JCV_{CPN} agnogene introduced. CPN M-Agno is JCV_{CPN} with a full length agnogene from JCV_{Mad-1} introduced. Mad-1 C-RR is JCV_{Mad-1} with the JCV_{CPN} RR and CPN M-RR is JCV_{CPN} with the JCV_{Mad-1} RR. Mad-1 Pt is JCV_{Mad-1} with a mutated start codon which prevents the expression of the agnoprotein and Mad-1 Del is JCV_{Mad-1} with the entire agnogene deleted. CPN M-Pt is JCV_{CPN} with the agnogene of Mad-1 Pt.
doi:10.1371/journal.pone.0080840.g004

Mad-1 Pt. We studied these additional mutants in Cos-7 cells, because these cells displayed the greatest difference in phenotype between JCV_{Mad-1} and JCV_{CPN}.

The agnogene deletion is the major contributor to the phenotype of JCV_{CPN}

To begin characterizing the phenotypes of the viruses shown in Figure 4, linearized DNA was transfected into Cos-7 cells, and JCV DNA levels in cell lysate and supernatant were monitored for 3 weeks using QPCR (Fig. 5). Mad-1 C-Agno has significantly lower levels of DNA from 10–21 days post-transfection compared to Mad-1, while Mad-1 C-RR has DNA levels similar to Mad-1 (Fig. 5A and 5C). This indicates that introducing the agnogene deletion of JCV_{CPN} into Mad-1 results in a decrease in DNA replication. In contrast, the introduction of the JCV_{CPN} RR does not. This suggests that the major cause of the replication kinetics seen with JCV_{CPN} are due to the agnogene deletion, and the not the archetype-like RR. When comparing the agno deletion viruses to JCV_{Mad-1}, Mad-1 Pt has similar DNA levels, while Mad-1 Del had decreased levels late in infection similar to JCV_{CPN} (Fig. 5A and 5C). This provides evidence the gene deletion is more important than the loss of the agnoprotein for the observed phenotype.

Furthermore, the results seen with the viruses on the JCV_{CPN} backbone support these conclusions. CPN M-Agno, with the full length agnogene and agnoprotein, and CPN M-Pt, with just a full length agnogene, have the greatest increase of JCV DNA levels compare to JCV_{CPN}, and in both cases the level of DNA increase is similar (Fig. 5B and 5D). This supports the conclusion that the deletion in the agnogene causes the decreased replication ability of JCV_{CPN}. CPN M-RR, with the JCV_{Mad-1} RR, also show some increase in DNA levels, but to a lesser extent than CPN M-Agno (Fig. 5B and 5D).

Deletion in the agnogene prevents expression of VP1 protein

We then sought to determine if the levels of VP1 protein expression would correspond with levels of viral DNA in cells transfected with the chimeras and agno deletion mutants. Western blots were done for VP1 expression in JCV transfected Cos-7 cells. At 14 days post-transfection, only JCV_{Mad-1}, Mad-1 Pt, Mad-1 C-RR and CPN M-Agno have detectable levels of VP1 (Fig. 6A). At 21 days post-transfection, all of these viruses and CPN M-Pt have detectable VP1 protein expression (Fig. 6B). All of these viruses have full length agnogenes, but Mad-1 Pt does not have agnoprotein expression. Compared to JCV_{Mad-1}, Mad-1 Pt shows some decrease in VP1 expression, while Mad-1 Del has a complete lack of VP1 expression. All of the viruses with the JCV_{CPN} agnogene deletion, JCV_{CPN}, Mad-1 C-Agno and CPN M-RR lack VP1 expression (Fig. 6A and 6B). Taken together, these results indicate that the deletion in the agnogene results in decreased or undetectable levels of VP1 protein expression, and that the levels of DNA replication correspond with the presence of VP1 protein expression.

Deletions in the agnogene reduce the production of infectious virions

Finally, we sought to determine if the ability to produce infectious virions of the chimeric and agno deletion viruses also corresponds with DNA levels and VP1 protein production in these cells. Supernatant collected from Cos-7 cells 21 days post-transfection was used to infect naïve Cos-7 cells, and the DNA levels (Fig. 7A) and percentage of cells expressing VP1 (Fig. 7B) were determined by QPCR and flow cytometry, respectively, at day 7. Compared to JCV_{Mad-1}-infected cells, both Mad-1 C-agno and Mad-1 Del –infected cells have significantly lower viral loads, showing a 1.5–2 log decrease (Fig. 7A). Mad-1 Pt and Mad-1 C-RR-infected cells also have significantly lower viral loads than JCV_{Mad-1}-infected cells, but tended to have a smaller magnitude of decrease (Fig. 7A). Mad-1 C-agno and Mad-1 Del-infected cells have significantly lower percentages of cells expressing VP1, while Mad-1 Pt and Mad-1 C-RR-infected cells do not (Fig. 7B). CPN M-Agno, CPN M-RR and CPN M-Pt-infected cells all have detectable DNA levels, with significantly higher viral loads compared to JCV_{CPN} (Fig. 7A). Compared with JCV $_{CPN}$-infected cells, CPN M-Agno-infected cells have a significantly higher percentage cells expressing VP1, and CPN M-Pt-infected cells tended to have more cells expressing VP1. Interestingly, introduction of only the full length gene without protein expression in CPN M-Pt is enough to rescue the DNA levels, and show some increase in percent of cells expressing VP1.

The results of these infection experiments suggest that the deletion in the agnogene is the primary cause of the phenotype observed with JCV_{CPN}. However, CPN M-RR, with the JCV_{Mad-1} RR does show some increase in DNA replication and production of infectious virions compare to JCV_{CPN}, which may indicate that the RR composition is also affecting replication of the virus, but to a lesser degree than the agnogene deletion. It is likely that the combination of the agnogene deletion together with archetype-like RR is the cause of the overall phenotype of JCV_{CPN}. Overall, these experiments have used the unique naturally occurring JCV_{CPN} agnogene deletion and archetype-like RR to clarify the

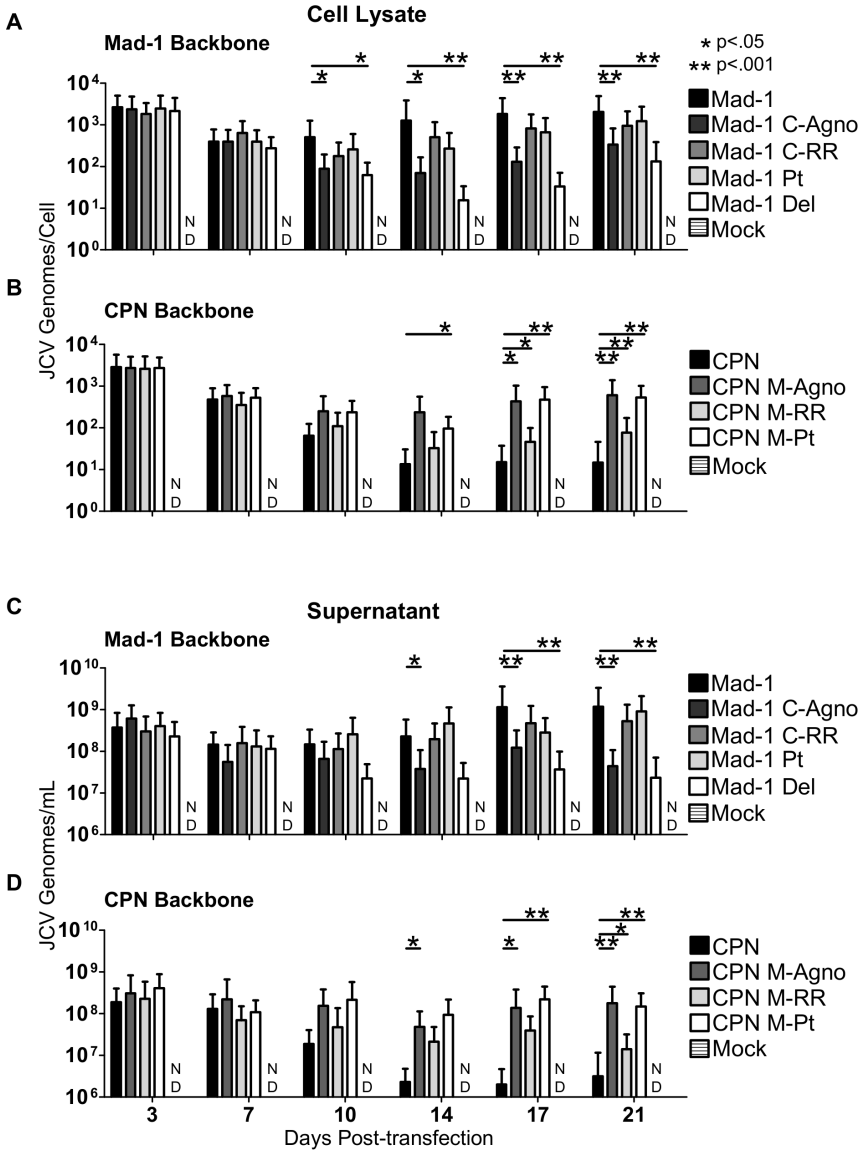

Figure 5. The agnogene deletion of JCV_{CPN} is the primary cause of its replication defect. Linearized JCV DNA of JCV_{Mad-1}, Mad-1 C-Agno, Mad-1 C-RR, Mad-1 Pt, Mad-1 Del, JCV_{CPN}, CPN M-Agno, CPN M-RR, and CPN M-Pt were transfected into Cos-7 cells and DNA levels were quantified over 3 weeks, as described in Figure 1. (A and C) Levels of DNA with JCV_{Mad-1} and the chimeras and agno deletion viruses on the JCV_{Mad-1} backbone were measured in the cell lysate (A) and supernatant (C). Mad-1 C-Agno and Mad-1 Del show significantly lower levels of DNA late in infection. (B and D) Levels of DNA with JCV_{CPN} and the chimeras and agno deletion viruses on the JCV_{CPN} backbone were measured in the cell lysate (B) and supernatant (D). Introduction of a full length agnogene causes the greatest increase in DNA levels. Data represents the average of 4–10 independent experiments. Error bars represent standard deviation. P-values were calculated with the Wilcoxon Rank Test. ND is not detected.
doi:10.1371/journal.pone.0080840.g005

role of the agnogene and RR forms in JCV replication in cell culture.

Discussion

JCV_{CPN} was isolated from the brain of the first patient to be diagnosed with JCVE, a novel syndrome characterized by infection of cortical pyramidal neurons. JCV_{CPN} is the first naturally occurring isolate with a large deletion in the agnogene, which was originally called agno due to the unknown nature of its function. While studies have begun to shed light on the function of the agnoprotein and agnogene, there is still much to be learned. JCV_{CPN} presents the opportunity to study the function of the agnogene and agnoprotein in a naturally occurring pathogenic variant of JCV, isolated in association with infection of a new cell type.

In this study, we compared the replication of JCV_{CPN} to that of the prototype virus JCV_{Mad-1}. We used Cos-7 cells to model infection in kidney cells and SVG cells as a glial cell model. Both of these cell lines are widely used to study the replication of JCV in kidney and glial cells, and it is commonly thought that the results obtained in them are applicable to what would occur in these cell types during JCV infection in humans. Studying the replication of JCV in cortical pyramidal neurons is challenging, as there are no cortical pyramidal neuron cell lines available. We therefore used IMR-32 neuroblastoma cells to model neuronal infection. Using these cell lines allowed us to study the replication of JCV_{CPN} in

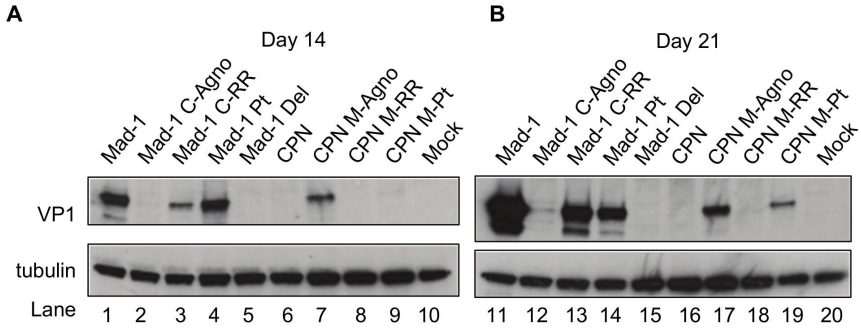

Figure 6. Deletion in the agnogene prevents VP1 expression. Western blots for VP1 were done as described in Figure 2. (A) VP1 levels in Cos-7 cell lysate 14 days post-transfection. (B) VP1 levels in Cos-7 cells 21 days post-transfection. Levels of VP1 expression are drastically reduced in Mad-1 C-Agno, and expression is rescued by the full length agnogene in CPN M-Agno. Deletion of the agnogene Mad-1 Del results in a greater decrease in VP1 expression than just the prevention of the protein expression in Mad-1 Pt. Blots are representative of 3 or 4 independent experiments.
doi:10.1371/journal.pone.0080840.g006

different cell types in cell culture. We found that JCV_{CPN} was capable of replicating its genome in cell culture. However, it could not establish an infection at the same level observed with JCV_{Mad-1} over time and did not display any replication advantage over JCV_{Mad-1} in any cell line. Levels of JCV_{CPN} DNA replication in Cos-7 and IMR-32 cells were similar to JCV_{Mad-1} at early time points, and then decreased at later time points, indicating that the virus is able to replicate viral DNA after transfection but the infection could not spread and persist in the cell culture at the same level as JCV_{Mad-1}. In addition, mRNA and VP1 protein analyses showed some decrease in early transcription and a marked decrease in late transcription, with no detectable VP1 protein production. In all three cell lines, low levels of infection were observed using supernatant from JCV_{CPN} transfected cells, but only using supernatant collected at early times post-transfection, and at levels significantly lower than seen with JCV_{Mad-1}. These data indicate that the virus has a block in late gene expression and protein production, which results in low levels of infectious virions being released, and an inability to sustain a persistent high level infection in cell culture. Furthermore, since agnoprotein has been implicated in late stages of viral maturation, there may be an additional block at the level of virion formation and/or release independent of the lack of VP1 production.

JCV_{CPN} and JCV_{Mad-1} are different in two regions, the RR and the agnogene. This provided us with the unique opportunity to determine for the first time how each of these regions contributed to the phenotype of JCV_{CPN}. We therefore studied a series of chimeric viruses of the RR and agnogene. Interestingly, the agnogene deletion in JCV_{CPN} was the predominant cause of its phenotype, not the archetype-like RR. Moreover, the loss of the agnogene DNA had a larger effect on the replication of the virus than the loss of agnoprotein expression. Finally, the archetype-like RR also showed a detrimental effect on JCV_{CPN} replication, but of a smaller magnitude than that of the agnogene deletion. For these experiments we used Cos-7 cells, because they displayed the largest difference in phenotype between JCV_{CPN} and JCV_{Mad-1} and allowed us to use the greatest number of techniques to study these viruses. We believe that the results obtained in these experiments are representative of what would be observed with the other cell lines used in this study.

Previous studies have implied that agnoprotein had a role in viral DNA replication [23,24]. However, JCV_{CPN} is able to

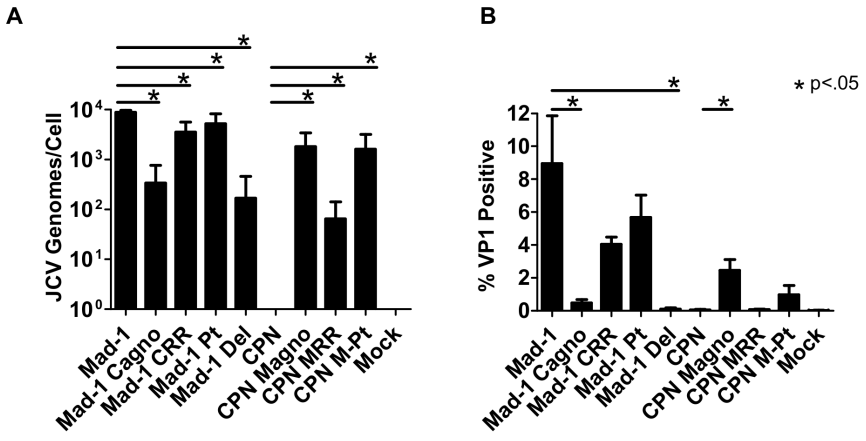

Figure 7. Loss of the agnogene results in decreased production of infectious virions. Supernatant was collected from Cos-7 cells 21 days post-transfection and used to infect naive Cos-7 cells. After 7 days, the cells were analyzed for (A) JCV DNA by QPCR or (B) VP1 expression by flow cytometry. Deletions in the agnogene in JCV_{Mad-1}-infected cells resulted in a significant decrease in JCV genomes/cell and percentage of cells expressing VP1, while introduction of a full length agnogene into JCV_{CPN} results in a significant increase in the viral load and percentage of cells expressing VP1. Data is the average of 3 independent experiments. Error bars represent standard deviation. P values were calculated using Wilcoxon rank test for QPCR data, comparing each virus to its parent virus, either JCV_{Mad-1} or JCV_{CPN}. P-vales for flow cytometry data were calculated using students t test using the same sets of comparisons. ND is not detected.
doi:10.1371/journal.pone.0080840.g007

produce levels of DNA similar to JCV_{Mad-1} early after transfection, with DNA levels decreasing with time. These results suggest that an agnogene-deletion mutant can indeed replicate DNA, but levels drop off due to blocks at later steps in infection, thereby preventing spread within the cell culture. Conflicting studies have associated agnoprotein with gene expression, with both the loss of agnoprotein [19,30] or its presence [23,26] suppressing activity of the late promoter of JCV in different experimental systems. Additionally, deletion of the full agnogene causes a greater decrease in VP1 expression than prevention of agnoprotein expression without deletion of the agnogene DNA [30]. Our data shows that the deletion in the agnogene of JCV_{CPN} results in a block in late gene expression, impairing the release of virions capable of infecting new cells and propagating the infection in cell culture. This is consistent with the results of Akan et al [30] and highlights the importance of the agnogene DNA in addition to the protein it codes for. Further studies are needed to determine the mechanism of the block in VP1 expression. One possibility is that a host cell factor which binds to one of the sites in the agnogene, identified by Akan et al [30], is involved in expression of the late transcript. Further investigations to identify these cellular proteins are warranted to determine the mechanism by which they act during JCV replication. Another potential mechanism is that deletions in the agnogene somehow alter the splicing or translation of VP1 from the late mRNA.

Previous studies of JCV deletion mutants lacking agnoprotein expression have implicated the agnoprotein in genome packaging and/or virion formation and release, with empty capsids being produced by viruses lacking the agnoprotein [27,28]. In our study however, the agnoprotein start codon point mutant was able to replicate its DNA and produce infectious virions at a level similar to JCV_{Mad-1}in Cos-7 cells, which suggests that at least in these cells, the agnoprotein is not necessary for formation and release of virions containing viral genomes.

Archetype RR is typically found in the urine, but the JCV_{CPN} RR isolated from the brain of the JCVE patient is archetype-like. Studies of the replication of different forms of RR have shown that archetype RR form has less active early and late promoters [36]. Surprisingly, our study did not find the archetype-like RR of JCV_{CPN} to be the primary cause of the decreased levels of late transcription and VP1 protein expression. Introducing the archetype-like RR of JCV_{CPN} into JCV_{Mad-1} had little effect on the ability of the virus to replicate. JCV_{Mad-1} RR introduced into JCV_{CPN} partially rescues replication, but had a lesser impact than introduction of a full length agnogene. In fact the archetype-like RR only has a significant impact on the virus once it has already been impaired by a deletion in the agnogene, indicating that not all archetype-like RR forms found in nature lead to lower levels of viral replication.

While JCV_{CPN} was unable to establish a persistent infection in our cell culture model, it was found at high levels in the brain of the JCVE patient. JCV_{CPN} does produce some infectious virions in cell culture, but at much lower levels than JCV_{Mad-1}. This does not, however, mean that the virus was unable to establish an infection in the brain of the JCVE patient. There are limitations to the cell culture model we utilized in this study. First, the infection in a person can take place on the timescale of years to decades, while our experiments were done over weeks. Second, this individual was also infected with a strain of JCV with a full length agnogene and agnoprotein, which may have influenced the replication of JCV_{CPN}. Third, it may be that having low levels of replication in the brain was actually advantageous to the virus while faced with a healthy immune system, allowing it to accumulate until the immune system became compromised and JCVE developed.

After observing the infection of granule cell neurons in JCV GCN and cortical pyramidal neurons in JCVE, we conducted studies to determine if infection of neurons by JCV was limited to these syndromes, or if it is more widespread. Based on staining of PML brain samples, it is predicted that up to 51% of patients have granule cell neurons infected by JCV [37]. Additionally, infection of cortical neurons by JCV in classic PML cases has been observed with infection present in the gray white junction and gray matter [38]. These studies demonstrate that infection of neurons occurs in a large number of PML patients, and is not limited to patients with JCV GCN or JCVE. Further studies of the molecular composition of JCV in neurons of patients with classic PML are needed to determine whether these cells are also infected by JCV-deletion mutants.

The study of unique pathogenic isolates of JCV, such as JCV_{CPN} or JCV_{GCN} allows us to decipher the basic biology of JCV replication using mutations that have arisen naturally during infection in humans. Our studies of JCV_{CPN} have provided valuable insights into both the function of the agnogene and agnoprotein, as well as a naturally occurring variation of the regulatory region, on JCV replication. Our results have helped clarify the role of the agnogene and agnoprotein in DNA replication, transcription and protein expression, demonstrating that a deletion in the agnogene has a dramatic effect on the expression of VP1 protein and the production of infectious virions. Further studies of naturally occurring variants of JCV will continue to add clarity to our understanding of the biology of JCV replication and pathogenesis.

Acknowledgments

We would like to thank Dr. Long Ngo for advice in statistical analysis. We would like to thank Dr. Mahmut Safak for the generous gift of Mad-1 Pt and Mad-1 Del plasmids.

Author Contributions

Conceived and designed the experiments: LCE EN XD IJK. Performed the experiments: LCE EN. Analyzed the data: LCE IJK. Contributed reagents/materials/analysis tools: LCE EN XD. Wrote the paper: LE XD IJK.

References

1. Gheuens S, Wuthrich C, Koralnik IJ (2013) Progressive multifocal leukoencephalopathy: why gray and white matter. Annu Rev Pathol 8: 189–215.
2. Jensen PN, Major EO (2001) A classification scheme for human polyomavirus JCV variants based on the nucleotide sequence of the noncoding regulatory region. J Neurovirol 7: 280–287.
3. Tan CS, Ellis LC, Wuthrich C, Ngo L, Broge TA, Jr., et al. (2010) JC virus latency in the brain and extraneural organs of patients with and without progressive multifocal leukoencephalopathy. J Virol 84: 9200–9209.
4. Ferenczy MW, Marshall LJ, Nelson CD, Atwood WJ, Nath A, et al. (2012) Molecular biology, epidemiology, and pathogenesis of progressive multifocal leukoencephalopathy, the JC virus-induced demyelinating disease of the human brain. Clin Microbiol Rev 25: 471–506.
5. Tan CS, Koralnik IJ (2010) Beyond progressive multifocal leukoencephalopathy: expanded pathogenesis of JC virus infection in the central nervous system. Lancet Neurol 9: 425–437.
6. Knowles WA, Pipkin P, Andrews N, Vyse A, Minor P, et al. (2003) Population-based study of antibody to the human polyomaviruses BKV and JCV and the simian polyomavirus SV40. J Med Virol 71: 115–123.
7. Weber T, Trebst C, Frye S, Cinque P, Vago L, et al. (1997) Analysis of the systemic and intrathecal humoral immune response in progressive multifocal leukoencephalopathy. J Infect Dis 176: 250–254.

8. Berger JR, Kaszovitz B, Post MJ, Dickinson G (1987) Progressive multifocal leukoencephalopathy associated with human immunodeficiency virus infection. A review of the literature with a report of sixteen cases. Ann Intern Med 107: 78–87.
9. Molloy ES, Calabrese LH (2009) Progressive multifocal leukoencephalopathy: a national estimate of frequency in systemic lupus erythematosus and other rheumatic diseases. Arthritis Rheum 60: 3761–3765.
10. Shimizu N, Imamura A, Daimaru O, Mihara H, Kato Y, et al. (1999) Distribution of JC virus DNA in peripheral blood lymphocytes of hematological disease cases. Intern Med 38: 932–937.
11. Koralnik IJ, Wuthrich C, Dang X, Rottnek M, Gurtman A, et al. (2005) JC virus granule cell neuronopathy: A novel clinical syndrome distinct from progressive multifocal leukoencephalopathy. Ann Neurol 57: 576–580.
12. Du Pasquier RA, Corey S, Margolin DH, Williams K, Pfister LA, et al. (2003) Productive infection of cerebellar granule cell neurons by JC virus in an HIV+ individual. Neurology 61: 775–782.
13. Hecht JH, Glenn OA, Wara DW, Wu YW (2007) JC virus granule cell neuronopathy in a child with CD40 ligand deficiency. Pediatr Neurol 36: 186–189.
14. Wuthrich C, Dang X, Westmoreland S, McKay J, Maheshwari A, et al. (2009) Fulminant JC virus encephalopathy with productive infection of cortical pyramidal neurons. Ann Neurol 65: 742–748.
15. Dang X, Vidal JE, Oliveira AC, Simpson DM, Morgello S, et al. (2012) JC virus granule cell neuronopathy is associated with VP1 C terminus mutants. J Gen Virol 93: 175–183.
16. Dang X, Koralnik IJ (2006) A granule cell neuron-associated JC virus variant has a unique deletion in the VP1 gene. J Gen Virol 87: 2533–2537.
17. Dang X, Wuthrich C, Gordon J, Sawa H, Koralnik IJ (2012) JC virus encephalopathy is associated with a novel agnoprotein-deletion JCV variant. PLoS One 7: e35793.
18. Khalili K, White MK, Sawa H, Nagashima K, Safak M (2005) The agnoprotein of polyomaviruses: a multifunctional auxiliary protein. J Cell Physiol 204: 1–7.
19. Okada Y, Endo S, Takahashi H, Sawa H, Umemura T, et al. (2001) Distribution and function of JCV agnoprotein. J Neurovirol 7: 302–306.
20. Saribas AS, Arachea BT, White MK, Viola RE, Safak M (2011) Human polyomavirus JC small regulatory agnoprotein forms highly stable dimers and oligomers: implications for their roles in agnoprotein function. Virology 420: 51–65.
21. Sariyer IK, Akan I, Palermo V, Gordon J, Khalili K, et al. (2006) Phosphorylation mutants of JC virus agnoprotein are unable to sustain the viral infection cycle. J Virol 80: 3893–3903.
22. Sariyer IK, Khalili K, Safak M (2008) Dephosphorylation of JC virus agnoprotein by protein phosphatase 2A: inhibition by small t antigen. Virology 375: 464–479.
23. Safak M, Barrucco R, Darbinyan A, Okada Y, Nagashima K, et al. (2001) Interaction of JC virus agno protein with T antigen modulates transcription and replication of the viral genome in glial cells. J Virol 75: 1476–1486.
24. Saribas AS, White MK, Safak M (2012) JC virus agnoprotein enhances large T antigen binding to the origin of viral DNA replication: evidence for its involvement in viral DNA replication. Virology 433: 12–26.
25. Sami Saribas A, Abou-Gharbia M, Childers W, Sariyer IK, White MK, et al. (2013) Essential roles of Leu/Ile/Phe-rich domain of JC virus agnoprotein in dimer/oligomer formation, protein stability and splicing of viral transcripts. Virology 443: 161–176.
26. Safak M, Sadowska B, Barrucco R, Khalili K (2002) Functional interaction between JC virus late regulatory agnoprotein and cellular Y-box binding transcription factor, YB-1. J Virol 76: 3828–3838.
27. Sariyer IK, Saribas AS, White MK, Safak M (2011) Infection by agnoprotein-negative mutants of polyomavirus JC and SV40 results in the release of virions that are mostly deficient in DNA content. Virol J 8: 255.
28. Suzuki T, Semba S, Sunden Y, Orba Y, Kobayashi S, et al. (2012) Role of JC virus agnoprotein in virion formation. Microbiol Immunol 56: 639–646.
29. Suzuki T, Orba Y, Okada Y, Sunden Y, Kimura T, et al. (2010) The human polyoma JC virus agnoprotein acts as a viroporin. PLoS Pathog 6: e1000801.
30. Akan I, Sariyer IK, Biffi R, Palermo V, Woolridge S, et al. (2006) Human polyomavirus JCV late leader peptide region contains important regulatory elements. Virology 349: 66–78.
31. Frisque RJ, Bream GL, Cannella MT (1984) Human polyomavirus JC virus genome. J Virol 51: 458–469.
32. Gluzman Y (1981) SV40-transformed simian cells support the replication of early SV40 mutants. Cell 23: 175–182.
33. Major EO, Miller AE, Mourrain P, Traub RG, de Widt E, et al. (1985) Establishment of a line of human fetal glial cells that supports JC virus multiplication. Proc Natl Acad Sci U S A 82: 1257–1261.
34. Tumilowicz JJ, Nichols WW, Cholon JJ, Greene AE (1970) Definition of a continuous human cell line derived from neuroblastoma. Cancer Res 30: 2110–2118.
35. Schmittgen TD, Livak KJ (2008) Analyzing real-time PCR data by the comparative C(T) method. Nat Protoc 3: 1101–1108.
36. Ault GS (1997) Activity of JC virus archetype and PML-type regulatory regions in glial cells. J Gen Virol 78 (Pt 1): 163–169.
37. Wuthrich C, Cheng YM, Joseph JT, Kesari S, Beckwith C, et al. (2009) Frequent infection of cerebellar granule cell neurons by polyomavirus JC in progressive multifocal leukoencephalopathy. J Neuropathol Exp Neurol 68: 15–25.
38. Wuthrich C, Koralnik IJ (2012) Frequent infection of cortical neurons by JC virus in patients with progressive multifocal leukoencephalopathy. J Neuropathol Exp Neurol 71: 54–65.

APPENDIX B (copy)

JC Virus Latency in the Brain and Extraneural Organs of Patients with and without Progressive Multifocal Leukoencephalopathy.

Chen S. Tan, Laura C. Ellis, Christian Wüthrich, Long Ngo, Thomas A. Broge Jr., Jenny Saint-Aubyn, Janice S. Millerand Igor J. Koralnik *J. Virol.* 2010, 84(18):9200. DOI: 10.1128/JVI.00609-10.

JOURNAL OF VIROLOGY, Sept. 2010, p. 9200–9209 Vol. 84, No. 18
0022-538X/10/$12.00 doi:10.1128/JVI.00609-10

JC Virus Latency in the Brain and Extraneural Organs of Patients with and without Progressive Multifocal Leukoencephalopathy▽

Chen S. Tan,[1,2,3] Laura C. Ellis,[2,3,4] Christian Wüthrich,[2,3] Long Ngo,[5] Thomas A. Broge, Jr.,[2,3] Jenny Saint-Aubyn,[2,3] Janice S. Miller,[2,3] and Igor J. Koralnik[2,3]*

Division of Infectious Disease,[1] Division of Viral Pathogenesis,[2] Department of Medicine,[5] Division of Neurovirology, Department of Neurology,[3] Beth Israel Deaconess Medical Center, and Program in Virology, Harvard University,[4] Boston, Massachusetts

Received 19 March 2010/Accepted 29 June 2010

JC virus (JCV) is latent in the kidneys and lymphoid organs of healthy individuals, and its reactivation in the context of immunosuppression may lead to progressive multifocal leukoencephalopathy (PML). Whether JCV is present in the brains or other organs of healthy people and in immunosuppressed patients without PML has been a matter of debate. We detected JCV large T DNA by quantitative PCR of archival brain samples of 9/24 (38%) HIV-positive PML patients, 5/18 (28%) HIV-positive individuals, and 5/19 (26%) HIV-negative individuals. In the same samples, we detected JCV regulatory region DNA by nested PCR in 6/19 (32%) HIV-positive PML patients, 2/11 (18%) HIV-positive individuals, and 3/17 (18%) HIV-negative individuals. In addition, JCV DNA was detected in some spleen, lymph node, bone, and kidney samples from the same groups. *In situ* hybridization data confirmed the presence of JCV DNA in the brains of patients without PML. However, JCV proteins (VP1 or T antigen) were detected mainly in the brains of 23/24 HIV-positive PML patients, in only a few kidney samples of HIV-positive patients, with or without PML, and rarely in the bones of HIV-positive patients with PML. JCV proteins were not detected in the spleen or lymph nodes in any study group. Furthermore, analysis of the JCV regulatory region sequences showed both rearranged and archetype forms in brain and extraneural organs in all three study groups. Regulatory regions contained increased variations of rearrangements correlating with immunosuppression. These results provide evidence of JCV latency in the brain prior to severe immunosuppression and suggest new paradigms in JCV latency, compartmentalization, and reactivation.

JC virus (JCV) is the etiologic agent of the often fatal brain-demyelinating disease progressive multifocal leukoencephalopathy (PML) (23a). JCV remains latent in the kidneys, lymph nodes, and bone marrow of healthy and immunosuppressed individuals without PML (2, 21, 24) and, upon reactivation, can cause a lytic infection of oligodendrocytes in the brain, leading to PML (14). Although JCV is often found in the urine of healthy individuals (12, 18), it is not usually detected in the blood of patients without PML (15). The pathway leading to viral reactivation and replication in the brains of immunosuppressed individuals is not well defined. Molecular analysis of JCV has prompted hypotheses on how the virus emerges from latency and becomes pathogenic. JCV has a double-stranded, circular DNA of 5,130 bp. While the coding region is well conserved, the noncoding regulatory region (RR) of JCV is hypervariable. The kidneys and urine usually contain JCV with a well-conserved, nonpathogenic RR which is called the "archetype" (30). The JCV RR detected in the brains and the cerebrospinal fluid (CSF) of PML patients usually has duplications, tandem repeats, and deletions and has been called "rearranged" compared to the archetype. Although it is not clear which form of JCV RR is propagated at the time of primary infection, it has been hypothesized that JCV with the archetype RR remains confined in the kidneys of most healthy individuals and that rearrangements which confer neurotropism need to occur prior to viral migration to the brain to destroy the myelin-producing glial cells. Whether JCV can reach the brain and establish latency in the central nervous systems (CNS) of otherwise-healthy individuals are matters of debate. While some investigators detected JCV DNA in 28 to 68% of frozen (8, 27) and 18 to 71% of formalin-fixed, paraffin-embedded (FFPE) (4, 7, 20) brain samples of patients without PML, others reported negative results (3, 6, 10, 23). Clearly, characterizing JCV sites of latency is imperative in the prevention of viral reactivation and PML. Recently, a group of PML patients has emerged among those treated with monoclonal antibodies, including natalizumab (13, 17, 26), efalizumab (16, 19a), and rituximab (5), for multiple sclerosis, psoriasis, hematological malignancies, and rheumatologic diseases. Mechanisms of JCV reactivation in these patients has yet to be defined. To better understand JCV organ tropism and characterize the types of JCV RRs in different compartments, we used archival pathology samples to detect JCV DNA and proteins and to analyze JCV RRs in various organ systems in HIV-positive individuals with and without PML and in HIV-negative subjects.

MATERIALS AND METHODS

Specimens. Formalin-fixed, paraffin-embedded (FFPE) samples of brain, kidney, vertebral bone, spleen, and lymph nodes from HIV-positive patients with or without PML and HIV-negative patients without PML were obtained from the National NeuroAIDS Tissue Consortium (NNTC). All brain samples in the HIV-positive and HIV-negative groups were sections from the cerebrum. Brain

* Corresponding author. Mailing address: Beth Israel Deaconess Medical Center, E/CLS 1005, 330 Brookline Ave., Boston, MA 02215. Phone: (617) 735-4460. Fax: (617) 735-4527. E-mail: ikoralni@bidmc.harvard.edu.

▽ Published ahead of print on 7 July 2010.

TABLE 1. Quantification of JCV DNA by qPCR in the brain, brain stem, kidney, spleen, and lymph node extracted from a PML patient

Sample type[a]	No. of JCV copies/μg of DNA in:				
	Brain	Brain stem	Kidney	Spleen	Lymph node
FFPE	194	6×10^8	249	725	1.41×10^3
Frozen	1.00×10^8	4.70×10^9	1.10×10^4	8,309	1.57×10^3

[a] Frozen, frozen at −80°C; FFPE, formalin fixed, paraffin embedded.

sections containing PML lesions were studied from the HIV-positive PML group. Of the 24 samples, 13 were from the cerebellum and 11 from the cerebrum.

Samples of brain, brain stem, kidney, spleen, and lymph nodes from a PML patient were obtained at autopsy. Half of the tissues were frozen for further analysis, and the other half were fixed in formalin and paraffin embedded for further analysis. Prior consent was obtained for the study protocol, approved by the Beth Israel Deaconess Medical Center Institutional Review Board of Human Studies.

DNA extraction from formalin-fixed, paraffin-embedded samples. Ten 5-μm-thick slices from FFPE blocks were collected into an Eppendorf tube, and a new microtome blade was used for each block. DNA was extracted after deparaffinization in 100% xylene for 10 min and then in 50% xylene and 50% ethanol for 10 min, followed by 100% ethanol for 10 min twice, all performed at 56°C. The dried sample was dissolved in 200 μl of tissue lysis solution, part of the Qiagen DNeasy blood and tissue kit (Qiagen). DNA was extracted by following the instructions of the manufacturer.

DNA extraction from frozen samples. Freshly frozen autopsy samples were kept frozen at −80°C until use. DNA extraction was performed with a Qiagen DNeasy blood and tissue kit (Qiagen).

qPCR. We used quantitative JCV PCR (qPCR) to detect and quantify JCV DNA in all samples as previously described (22). The limit of detection of the assay was 10 copies of JCV/μg of cellular DNA. All samples underwent two qPCR analyses with the same primers and conditions. The amount of DNA used per reaction ranged from 6 to 500 ng, and the results are expressed in numbers of copies of JCV/μg of cellular DNA. In the first qPCR analysis, we tested all samples in duplicate, and a sample was considered positive if at least one of the two wells had detectable DNA. In the second qPCR analysis, we tested the same samples in triplicate and considered positive those for which at least two of the three wells had detectable DNA. We then combined data from both analyses and considered positive those samples where JCV DNA could be detected in both the duplicate- and the triplicate-qPCR analysis.

Cloning and sequencing of the JCV RR. We amplified the JCV RR sequences by nested PCR using outer primers JRE1 (nucleotides [nt] 4989 to 5009) and LP2 (nt 537 to 518) and inner primers RREV (nt 310 to 291) and RFOR (nt 5085 to 5104) as described elsewhere (19). For each PCR, 20 pmol of primers was used in 30 cycles of amplification, with an annealing temperature of 63°C. The amount of DNA used in the reaction mixture ranged from 2 to 789 ng. The PCR products corresponding to the expected size were cloned with a TOPO-TA cloning kit (Invitrogen, Carlsbad, CA). Up to 10 clones for each PCR product were analyzed by restriction enzyme digestion and electrophoresis. We sequenced up to 10 clones of amplified fragments with the expected length. The DNA sequence was obtained on an ABI 3730xl sequencer (Applied Biosystems). Sequence analyses were performed using the Lasergene software MegAlign 7.1 (DNAStar, Madison, WI).

IHC. The expression of JCV proteins was determined by immunohistochemistry (IHC) staining using the anti-JCV antibody VP1 PAB597 (a generous gift from Walter Atwood) and the anti-large T antigen (T Ag) (simian virus 40 [SV40] Tag v-300; Santa Cruz Biotechnology), which cross-reacts with JCV, as previously described (28).

ISH. The presence of JCV DNA was determined by *in situ* hybridization (ISH), using a biotinylated JCV DNA probe (Enzo Life Sciences) as described previously (29), with modifications of the tissue preparation with antigen-retrieval solution (Dako) at 95°C for 20 minutes, followed by a 0.3% hydrogen peroxidase wash (Sigma) at room temperature for 60 minutes and then by proteinase K (50 ng/ml; Enzo Life Sciences) digestion at room temperature for 5 min. GenPoint (Dako), a catalyzed-signal amplification system, was used for staining.

Histological examination. All slides were stained with hematoxylin and Luxol fast blue solution to determine cellular structures and PML lesions. After deparaffinization and hydration in up to 95% ethanol, slides were placed in Luxol fast blue solution at 56°C overnight.

Statistical analysis. Correlation between JCV DNA detection in each patient and organ group was determined using Fisher's two-tailed exact test.

RESULTS

JCV DNA detection in FFPE tissues compared to frozen tissues. To determine the sensitivity of qPCR in detecting JCV large T DNA in formalin-fixed, paraffin-embedded (FFPE) tissues, we analyzed several organs from a PML patient that were either FFPE or frozen at −80°C (Table 1). All of the organs tested, including the brain, brain stem, kidney, spleen, and lymph nodes of this PML patient, contained detectable JCV DNA in samples obtained from both types of tissue preparations. Brain stem, spleen, and lymph node extractions had comparable quantities of detected JCV DNA in both preparations. However, the JCV DNA extracted from brain and kidney of FFPE tissues had 6-log- and 2-log-smaller viral loads, respectively, than their frozen counterparts. These results indicate that while FFPE tissues can be used for qualitative assessment of JCV DNA in tissues, quantitative measures may underestimate the actual viral burden in these specimens.

JCV DNA detection in brain and other organs. To determine the prevalence of JCV in different body compartments, we first performed qPCR detection of JCV large T DNA in the brain tissue of HIV-positive PML patients, as well as of HIV-positive and HIV-negative subjects (Table 2). We detected JCV large T DNA in 9/24 (38%) of the HIV-positive PML group, compared to 5/18 (28%) of the HIV-positive and 5/19

TABLE 2. Detection of JCV DNA in the large T and regulatory regions (RR) of HIV-positive PML, HIV-positive, and HIV-negative patients' brains, kidneys, bones, spleens, and lymph nodes

DNA type	Group	No. positive/total no. of specimens tested (%)				
		Brain	Kidney	Bone	Spleen	Lymph node
Large T Ag	HIV positive/PML	9/24 (38)	1/11 (9)	0/15	4/10 (40)	1/4 (25)
	HIV positive	5/18 (28)	0/11	2/11 (18)	1/9 (11)	3/7 (43)
	HIV negative	5/19 (26)	0/12	1/12 (8)	2/9 (22)	NA[a]
RR	HIV positive/PML	6/19 (32)	2/5 (40)	3/4 (75)	4/10 (40)	2/2 (100)
	HIV positive	2/11 (18)	0/3	3/4 (75)	7/7 (100)	4/6 (67)
	HIV negative	3/17 (18)	0/1	0/5	3/9 (33)	NA

[a] NA, not available.

TABLE 3. Detection of JCV large T Ag and capsid protein VP1 in brain, kidney, bone, spleen, and lymph node FFPE samples from HIV-positive PML, HIV-positive, and HIV-negative individuals

Sample type	Group	No. positive/total no. of samples tested (%)[a]		
		Large T Ag	Capsid protein VP1	T Ag or VP1
Brain	HIV positive/PML	21/24 (88)	20/24 (83)	23/24 (96)
	HIV positive	1/18 (6)	0/18	1/18 (6)
	HIV negative	1/19 (5)	0/19	1/19 (5)
Kidney	HIV positive/PML	1/11 (9)	0/11	1/11 (9)
	HIV positive	3/11 (27)	0/11	3/11 (27)
	HIV negative	0/12	0/12	0/12
Bone	HIV positive/PML	1/13 (8)	1/13 (8)	2/13 (15)
	HIV positive	0/11	0/11	0/11
	HIV negative	0/12	0/12	0/12
Spleen	HIV positive/PML	0/9	0/9	0/9
	HIV positive	0/9	0/9	0/9
	HIV negative	0/9	0/9	0/9
Lymph node	HIV positive/PML	NA	NA	NA
	HIV positive	0/7	0/7	0/7
	HIV negative	NA	NA	NA

[a] NA, not available.

(26%) of the HIV-negative groups ($P = 0.78$). The JC viral loads ranged between 38 and 3,464 (mean, 910) copies/μg of DNA in the HIV-positive PML group, 111 and 9,254 (mean, 3,033) copies/μg in the HIV-positive group, and 377 and 1,457 (mean, 768) copies/μg in the HIV-negative group.

Among the five HIV-positive patients who had detectable JCV large T DNA in their brain by qPCR, four had normal brain histology and one had a poorly differentiated metastatic tumor on pathological examination. Three of these patients had plasma HIV loads of 54,439, >75,000, and <400 copies/ml and corresponding CD4 counts of 8, 13, and 663 cells/μl. One other patient had a CD4 count of 25 cells/μl. Among the five HIV-negative subjects with detectable JCV DNA, three had amyotrophic lateral sclerosis (ALS) and the other two did not have any brain pathology on examination.

JCV large T DNA was detected in the kidney of only one HIV-positive PML patient and in the bone samples of one HIV-positive and one HIV-negative subject. JCV DNA was detected in the spleen and lymph nodes of few individuals in all available study groups. To further clarify JCV DNA detection in these FFPE tissues, we also amplified the JCV RR by nested PCR with available samples (Table 2). Detection of the amplified RR product by gel electrophoresis was confirmed by cloning and sequencing. In the brain tissues, detection of the JCV RR was comparable to detection of JCV large T, with prevalences of 6/19 (32%) in HIV-positive PML patients and 2/11 (18%) and 3/17 (18%) in HIV-positive and HV-negative patients, respectively ($P = 0.67$), but in the kidney, bone, spleen, and lymph nodes, RR detection by nested PCR exceeded that of large T DNA. However, only 1/11 brain, 1/5 kidney, 2/6 bone, and 1/26 spleen samples with detectable RRs by nested PCR had no large T detection by qPCR in any of the runs. The rest of the samples had at least one qPCR run that was positive for large T but did not meet the criteria for a positive qPCR result.

In a separate analysis, the large T and RR DNA detections showed no significant differences in the rates of detection of JCV DNA in the brains of HIV-positive PML patients compared to the HIV-positive and HIV-negative groups. Detection of large T DNA in the brain was not significantly more frequent than in the extraneural organs combined for any of the three groups ($P = 0.07$, 0.26, and 0.12). Similarly, the detection of regulatory region DNA in the brains of HIV-positive patients with PML and HIV-negative patients was also not significantly more frequent than in the extraneural organs combined ($P = 0.22$ and 1). In the HIV-positive group, however, the JCV regulatory region DNA was more frequently found in the combined extraneural organs than in the brain ($P = 0.009$). These results showed that JCV DNA is detectable in multiple organs and that JCV DNA is present in the brains of patients both with and without immunosuppression.

JCV VP1 and T Ag protein detection in brain and other organs. We performed IHC on all available tissues. We found that JCV large T antigen (T Ag), a regulatory protein expressed early in the viral life cycle, was detected in the brains of 21 of the 24 HIV-positive PML patients (Table 3) and that the major capsid protein VP1, indicating the presence of mature viral particles, was expressed in the lesions of 20/24 (83%) HIV-positive PML patient brain samples. All together, 23 of the 24 HIV-positive PML brain samples expressed either one or both of the JCV proteins tested. One brain sample showed extensive demyelination but did not stain for VP1 or T Ag protein. We also found T Ag in one brain sample each from the HIV-positive and -negative control groups. As expected, JCV proteins were significantly more frequently expressed in the brains of PML patients than in the HIV-positive and HIV-negative groups ($P = <0.001$). Furthermore, T Ag were detected at low levels in kidney samples from the HIV-positive PML and HIV-positive groups. T Ag and VP1 were rarely detected in the bone samples of the HIV-positive PML group only. T Ag was not detected in the extraneural organs of the

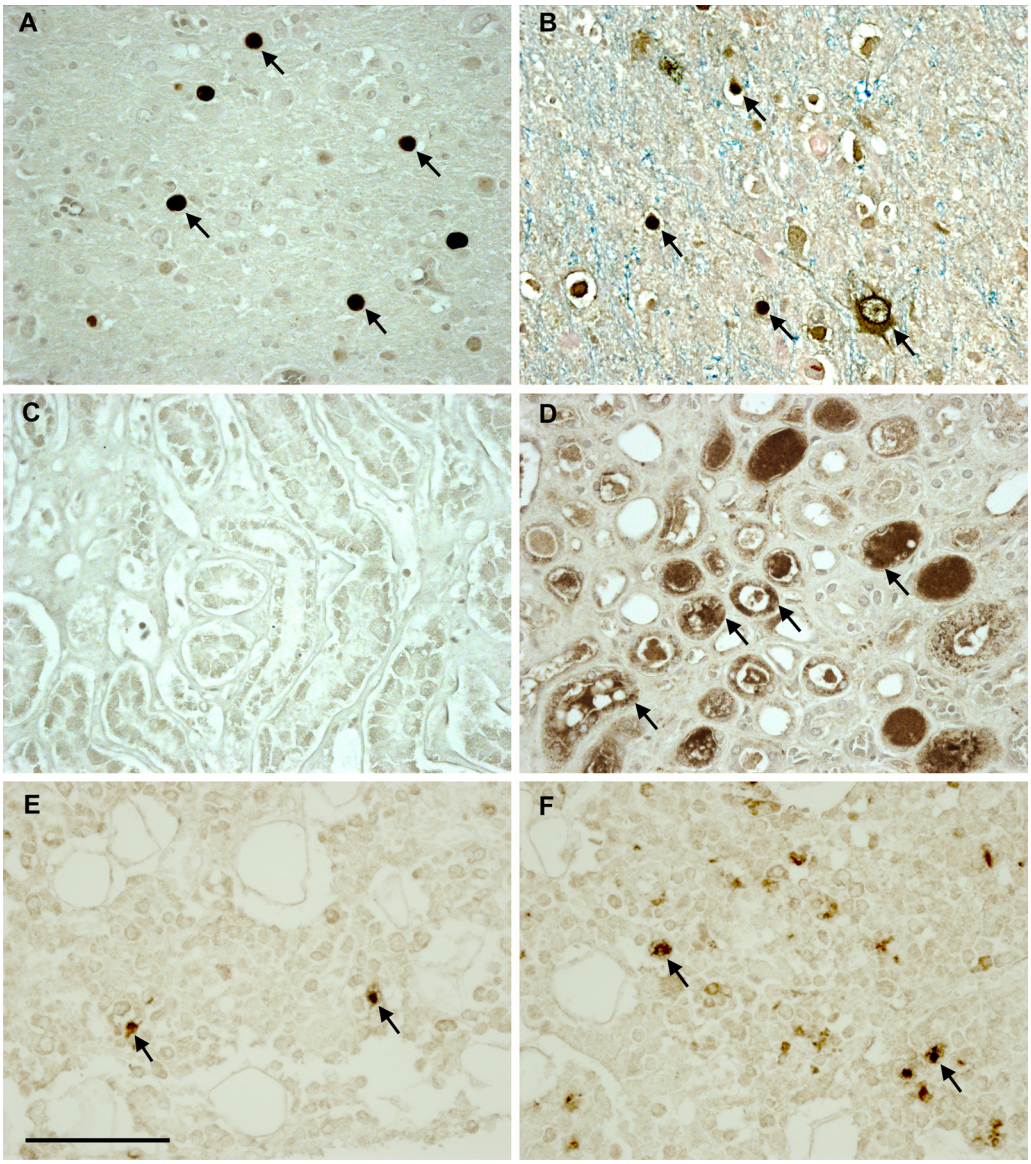

FIG. 1. Immunohistochemical staining of JCV proteins Vp1 and T Ag in brain, kidney, and bone in HIV-positive PML patients. Numerous cells (arrows) in the brain stained positive for VP1 (A) and TAg (B). While no VP1 protein was detected in the kidney (C), JCV-infected kidney tubular epithelium cells (arrows) stained positive for T Ag (D). In the bone, rare cells (arrows) stained positive for both VP1 (E) and T Ag (F). All the images are magnified 40-fold, and the scale bar is 100 μm.

HIV-negative group, and VP1 protein was not detected in any organs of this group (Fig. 1).

All five HIV-positive patients with detectable JCV DNA in the brain had negative staining for VP1, and the patient with an undifferentiated tumor had a brain sample which stained positive for T Ag. All five HIV-negative patients with detectable JCV DNA in the brain showed no expression of VP1 protein, and one of the five with normal brain pathology had rare cells expressing T Ag.

***In situ* hybridization of JCV DNA.** To further clarify the discrepant results between JCV DNA detection by qPCR and JCV protein detection by IHC, we performed *in situ* hybridization (ISH) for JCV DNA on a subset of the FFPE tissue sections (Fig. 2). In the HIV-positive control group, the brain tissue sections of 3 of the 5 patients who were positive for JCV by qPCR exhibited rare cells (1 to 2 cells per tissue section) which also stained JCV positive by ISH. As described above, only 1 of these 5 patients had rare cortical cells expressing T Ag, and the ISH was also positive in this case. Serving as controls, 5 of 5 other HIV-positive patients with negative qPCR and IHC results also showed negative ISH results (data not shown). In the HIV-negative control group, 3 of the 5 patients with positive qPCR results also had 1 to 10 cells per tissue section that stained positive by ISH, including one with positive IHC T Ag staining in the same distribution. Furthermore, three additional HIV-negative control patients with undetectable JCV DNA by qPCR and proteins detected by IHC also had negative ISH results (data not shown). In HIV-posi-

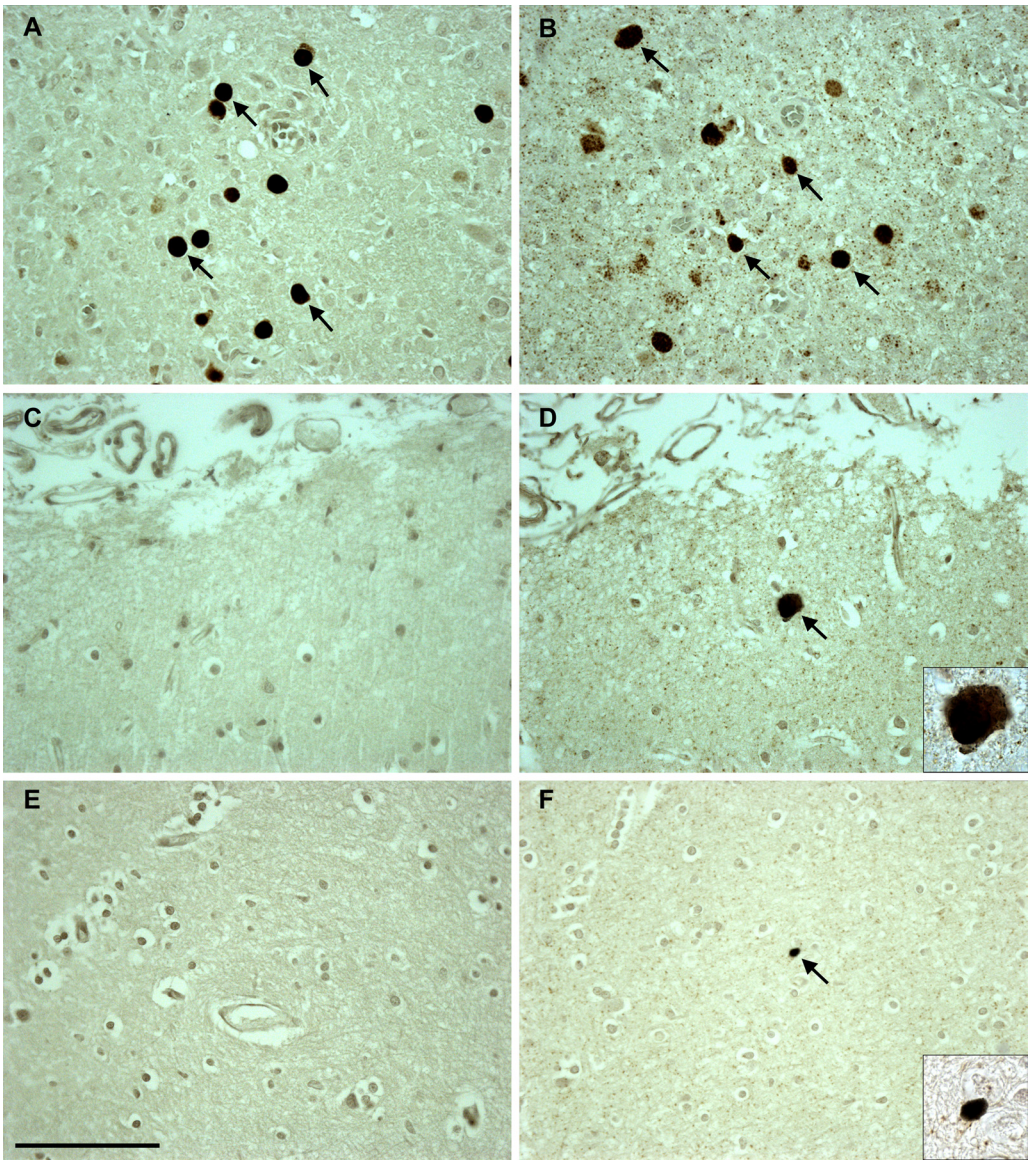

FIG. 2. *In situ* hybridization (ISH) detection of JCV-positive cells in the brain samples of HIV-positive PML, HIV-positive, and HIV-negative individuals compared to the immunohistochemical staining detection of JCV VP1 proteins in the same patients. Positive VP1 protein staining in JCV-infected cells (arrows) in an HIV-positive PML individual (A) corresponds to positive ISH for JCV DNA (arrows) in the same individual (B). (C) JCV VP1 protein is not detected in the brain of an HIV-positive individual. (D) However, ISH detected rare cells harboring JCV DNA (arrow) in this patient. (E) JCV VP1 protein is not detected in an HIV-negative individual. (F) However, ISH showed rare JCV DNA-positive cells (arrow). The images are magnified 40-fold, and the insets are magnified 100-fold. Scale bar = 100 μm.

tive patients with PML, samples that had detectable JCV DNA by qPCR and JCV proteins by IHC all had positive ISH results. Finally, there were 15/24 brain samples in this group with discrepant results; each sample had at least one cell staining positive for JCV protein by IHC staining but did not meet the criteria for qPCR positivity. Of those 15 samples, 8 were positive for JCV DNA by ISH; therefore, compared to that of IHC, the sensitivity of ISH to detect JCV in PML lesions was 8/15 (53%). The one HIV-positive PML patient brain sample with demyelinated lesions, but no VP1 or T Ag IHC staining and undetectable JCV DNA, was positive by ISH. Lastly, in all ISH-positive cases, JCV-infected cells were located in the brain parenchyma and not inside identifiable blood vessels.

JCV regulatory region analysis. Samples that were positive for JCV DNA on the first duplicate analysis by qPCR were selected to be tested for the JCV regulatory region (RR) in a nested PCR assay (Table 4). We obtained RR sequences from 39 samples (11 brains, 14 spleens, 6 bones, 6 lymph nodes, 2 kidneys) from 27 patients (12 PML, 10 HIV-positive, and 5 HIV-negative). Whenever possible, 10 clones from each nested-PCR-positive RR sample were sequenced, with an average of 8 clones per sample (311 clones total).

The RR forms were classified into four types as previously described (11). Type I-S has a single 98-base-pair unit, and type I-R has repeats of this 98-base-pair unit, with various deletions, as seen in the JCV Mad-1 and Mad-4 strains; both of

TABLE 4. Types of JCV RRs found in brain, kidney, bone, spleen, and lymph node FFPE samples from HIV-positive PML, HIV-positive, and HIV-negative individuals

Sample type	Group	No. of patients	No. of clones	No. of RRs of the indicated type/no. of clones sequenced (%)[a]			
				I-S	I-R	II-S	II-R
Brain	HIV positive/PML	6	28	3/28 (11)	13/28 (46)	12/28 (43)	0
	HIV positive	2	19	4/19 (21)	15/19 (79)	0	0
	HIV negative	3	21	9/21 (43)	12/21 (57)	0	0
Kidney	HIV positive/PML	2	19	0	19/19 (100)	0	0
	HIV positive	0	0	NA	NA	NA	NA
	HIV negative	0	0	NA	NA	NA	NA
Bone	HIV positive/PML	3	20	10/20 (50)	10/20 (50)	0	0
	HIV positive	3	25	0	6/25 (24)	9/25 (36)	10/25 (40)
	HIV negative	0	0	NA	NA	NA	NA
Spleen	HIV positive/PML	4	32	2/32 (6)	16/32 (50)	14/32 (44)	0
	HIV positive	7	65	10/65 (15)	43/65 (66)	12/65 (18)	0
	HIV negative	3	30	0	0	30/30 (100)	0
Lymph node	HIV positive/PML	2	19	0	9/19 (47)	10/19 (53)	0
	HIV positive	4	33	3/33 (9)	26/33 (79)	4/33 (12)	0
	HIV negative	NA	NA	NA	NA	NA	NA

[a] NA, not available.

these types have no inserts. Conversely, type II-S has a single 98-base-pair unit and one 23- and one 66-base-pair insert, as seen in the archetype, and type II-R has repeats of this 98-base-pair unit and inserts with various mutations, also called rearranged RRs. In the brains of HIV-positive PML patients, the RRs were significantly more frequently of the types I-R and II-S ($P = 0.007$) (Fig. 3). All the RRs from the kidneys of two HIV-positive PML patients were of type I-R. While the bone RRs were of all four types, the greatest numbers of patients and clones were obtained from the spleen. Finally, in the HIV-negative group, only one sequence representation was detected in each of the three RR types (I-S, I-R, II-S), whereas in both the HIV-positive PML and HIV-positive groups, both type I-R and type II-S clones with several different sequence rearrangements were detected. This indicates that JCV RR rearrangements occur more frequently with increased immunosuppression.

In 9 of the 27 patients, we were able to obtain RR sequences from more than one organ. We cloned and sequenced the RRs from three organs in three patients; in an HIV-positive patient with PML, we detected the I-S type in the brain and bone, the I-R type in the brain, and the II-S type in the lymph node. In an HIV-positive patient, we found type II-S in the bone and a mixture of types I-S and I-R in both the spleen and lymph node. Another HIV-positive individual had type II-R in the bone and both types I-R and II-S in the spleen and lymph nodes. We obtained sequences from two organs in six patients, including three HIV-positive PML patients. In one HIV-positive patient with PML, we found type I-R in both the brain and kidney. In two other HIV-positive PML cases, we detected RR sequences in the brain and spleen, including types I-R and II-S in the brain and type II-S in the spleen in one of them and type I-R in the brain and types I-S and I-R in the spleen in the other. We obtained sequences from two organs in two HIV-positive control patients. In both cases, we found JCV RRs in spleen and lymph node, with one patient having types I-R and II-S in both organs and the other having types I-R and I-S in both organs. Finally, RR sequences from two organs in one HIV-negative control patient showed types I-S and I-R in the brain and type II-S in the spleen. In all cases where both spleen and lymph node sequences were obtained from the same patient, the same types of RRs were present in both organs.

DISCUSSION

Our results suggest that JCV can spread throughout the body in immunosuppressed and immunocompetent individuals alike and that it is present in the brains of individuals without PML. Using FFPE tissues allowed us access to archival material from PML patients suitable for our study. However, to estimate the yields of JCV DNA extracted from FFPE samples, we first compared JCV DNA detection in freshly frozen tissues to that in FFPE tissues obtained at autopsy from the same PML patient seen at our institution. These experiments indicated that although the PCR results were concordant, JC viral load was 1 to 6 logs lower in FFPE tissues than in freshly frozen tissues. However, the main demyelinating lesions were located in the brain stem of this PML patient. The FFPE tissues from the brain stem showed only a 1-log decrease in JC virus load from that in the frozen sample, whereas the FFPE tissues from the brain had a 6-log decrease compared with the viral load in the frozen sample. This may be due to inhomogeneous spread of the virus within the brain areas sampled for frozen and FFPE tissue analysis.

Although the availability of FFPE tissues allowed us to test a large number of cases, the frequency of DNA detection was likely underestimated. This was demonstrated by finding either JCV large T Ag or RR DNA in only 50% of PML cases, while JCV proteins could be detected in 96% of them. The archival samples used in the study groups were available autopsy samples from patients with various lengths of survival after the diagnosis of PML. Therefore, the lower frequency of JCV

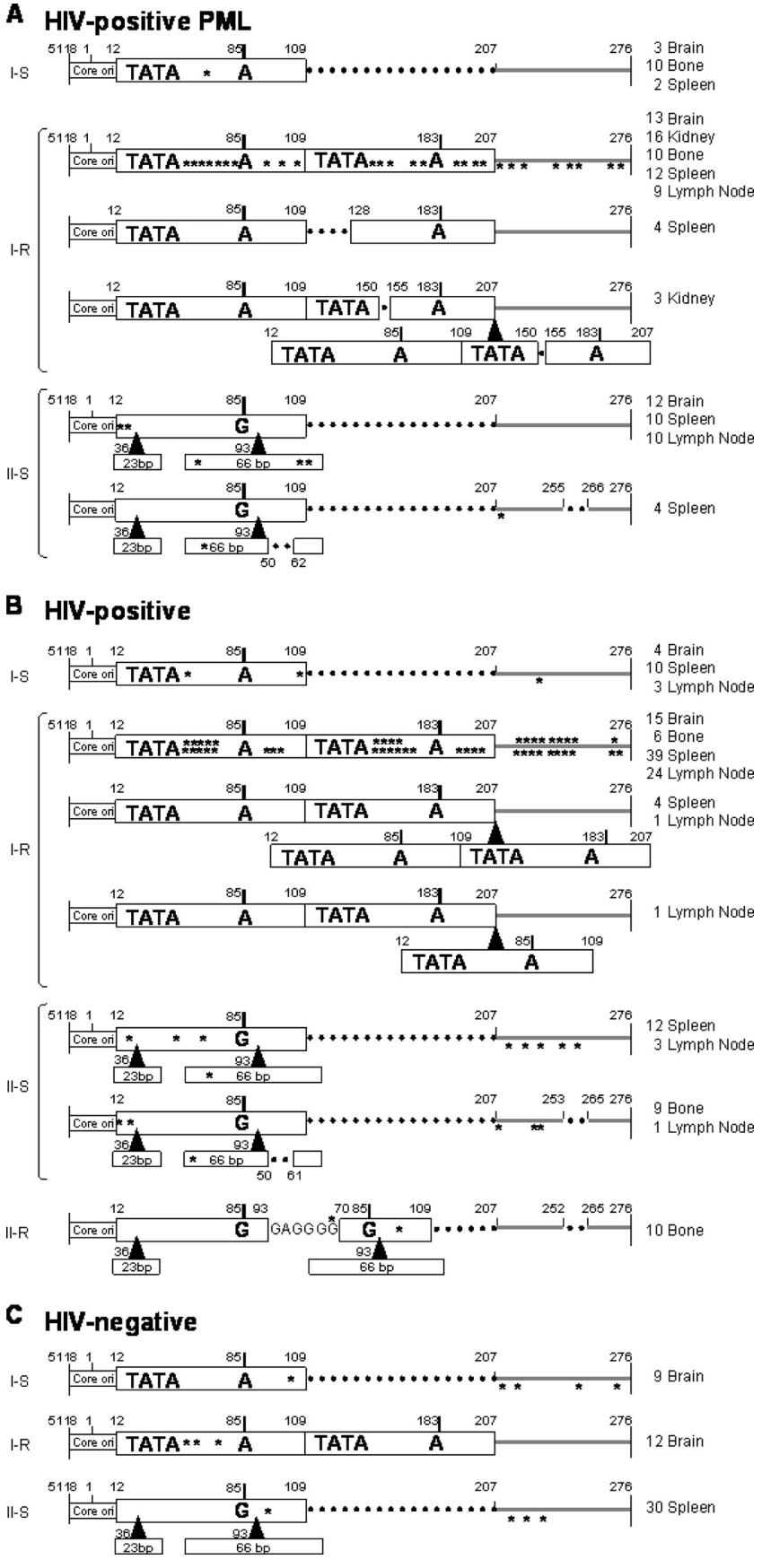

DNA detection by PCR can be due to the fact that the viral burden in the lesions decreased in time, commensurate with the destruction of glial cells and demyelination. Another possibility is that many of these autopsy samples had been in storage for as long as 13 years and had been incubated for extended periods of time in formalin prior to being embedded, which affects the integrity and quality of the extracted DNA. Using archival samples is not ideal, but it was the only way to study a rare and deadly disease such as PML.

The samplings of tissues used in our study represent a small portion of the organ, thus subjecting our analysis to sampling bias. Specifically, prior studies demonstrated detection of JCV DNA in the urine of up to 30% of healthy individuals (12, 18), far greater than the detection of JCV DNA in the kidneys (9% in the HIV-positive group with PML and none in the HIV-positive and HIV-negative groups without PML) in our study. This discrepancy is due to the fact that urine represents a sampling of the entire kidney instead of focal sites, as demonstrated by others (21). However, this bias is balanced by comparing only focal samples in all organs. Future studies should determine whether JCV spread is homogeneous in each organ.

We took several measures to ensure the integrity of our data and to eliminate the possibility of contaminations. All laboratory procedures were performed only after working surfaces were cleaned with DNase. DNA extractions from all specimens were performed in laboratory space entirely separate from areas of PCR amplification. All samples were deidentified and processed in batches by researchers. We also performed two separate qPCR experiments on each sample. In the first qPCR experiment, we analyzed the samples in duplicate. Samples were considered positive if one out of two tubes had detectable JCV DNA. We then repeated the qPCR experiment, analyzing all of the same samples in triplicate. In this experiment, samples were considered positive if two out of the three tubes had detectable JCV DNA. Combining the results of two separate qPCR experiments, we set the stringent criteria that a sample was considered to have detectable JCV DNA only if it was considered positive in both qPCR experiments and thus had JCV DNA in at least 3 of 5 replicates. These criteria may have contributed to a lower qPCR sensitivity. Furthermore, several PML patient lesions had extensive demyelination and only a few remaining JCV-infected cells, which may explain some of the negative PCR results. In these cases, ISH seemed to be a more robust method than PCR to demonstrate the presence of rare cells harboring JCV DNA in FFPE specimens from PML patient lesions. We therefore employed ISH as an additional technique to help us decipher JCV DNA detection in these tissues. Our data showed that stringent qPCR criteria for the detection of JCV DNA may have in some cases assigned negative results to samples. It is also likely that the JCV DNA from rare positive cells detected by ISH was diluted within genomic DNA and dropped below the detection level of the qPCR assay.

While ISH confirmed the results for all the qPCR-positive samples in the HIV-positive PML group, only 3 of the 5 large T DNA-positive brains from the HIV-positive and HIV-negative groups were positive by ISH staining. As shown in Fig. 2, ISH detected rare positive cells in the latter two groups. In the brains of PML patients, the higher sensitivity of ISH may have been due to the fact that JCV DNA was more abundant in these samples and could readily be detected by ISH. In the brain of non-PML patients, some qPCR-positive cases were ISH negative. Since the piece of tissue used to extract DNA for qPCR is not the same as the sections used for ISH, this apparent discrepancy may be caused by sampling in areas of low JCV burden. This most likely contributed to the lower sensitivity of ISH in the HIV-positive and HIV-negative groups than in the HIV-positive PML group.

We did not expect to detect JCV DNA in the brains of a third of the HIV-positive and negative patients without PML and therefore performed ISH to verify these findings. ISH confirmed the presence of rare JCV-infected cells in most of these cases. However, only one subject in each HIV-positive and HIV-negative group without PML had expression of JCV T Ag, but not VP1, in the brain. These results suggest that JCV DNA may remain latent in a limited number of cells in many immunocompetent and immunosuppressed individuals alike, which may lead to an abortive infection with occasional expression of the T Ag only, without the virus undergoing a full replicative cycle. We have recently reported 38 cases of PML occurring in individuals with minimal or occult immunosuppression (9). It is therefore possible that in those patients, JCV was already latent and reactivated from within the brain.

The similar prevalences of JCV DNA in the brains of all three study groups indicate that the presence of JCV DNA in the brain is not associated with immunosuppression. A prior study has also shown that JCV DNA is present in 44% of brain samples of HIV-positive patients without PML and 33% of brain samples of HIV-negative patients without PML (25).

To determine the extent of JCV spread in the body, we also tested kidney, bone, spleen, and lymph node samples. PCR analysis, including detection of JCV large T and RR DNA, indicated that JC virus may spread throughout the body in both immunocompetent and immunosuppressed individuals with and without PML. However, JCV protein expression was seldom found in the kidneys of HIV-positive patients, with or without PML, and only occasionally in bone samples from HIV-positive PML patients. Taken together, these data demonstrate that although JCV DNA is present in various organs,

FIG. 3. Sequencing results of the JCV RRs from the brains, kidneys, bones, spleens, and lymph nodes of HIV-positive patients with PML (A), HIV-positive patients (B), and HIV-negative patients (C). The nucleotide numbers are based on the prototype MAD-1 sequence. Each 98-bp unit is represented by an open box. The TATA box is represented by TATA. The 23-bp insert and 66-bp insert characteristic of archetype (II-S) sequences are represented as open boxes labeled "23 bp" and "66 bp," respectively. Gray lines represent the region downstream of the 98-bp units. Dotted lines represent deletions or regions not present. Asterisks represent single nucleotide point mutations or deletions. Letters indicate nucleotides. MAD-1 contains an adenine at positions 85 and 183, compared with all other sequences, which contain guanine at these positions. The types of RRs are indicated. These numbers represent total numbers of clones from all patients in the category and may include multiple clones of the type from a single patient. ori, origin of replication. The black triangles indicate the locations of the drawn fragment insert sites.

active JCV replication and protein expression occur preferentially in the brains of patients who develop PML.

Lastly, the sequencing of JCV RR from all groups contained multiple types and mutations, which further support isolation and amplification of real physiological samples and not laboratory strains. The RR of JCV, containing transcription control factor binding sites, is closely associated with pathogenesis. Although the exact mechanism of rearranging and the effects of rearrangements on pathogenesis have yet to be fully delineated, our data showed that both the archetypal and rearranged forms can be detected in both the brain and kidney. We describe novel detection of the I-S, II-S, and I-R types of RRs in the spleens of patients in all categories. Overall, the HIV-negative group had only one I-R variant and one II-S variant, while the HIV-positive group without PML had three I-R variants, three II-S variants, and one II-R variant, and the HIV-positive group with PML had three I-R variants and two II-S variants. These results suggest that active replication of JCV in immunosuppressed patients contributed to the multiple forms of the RR present in all organs. These results invite us to reappraise the classic assignment of the rearranged I-R type of RR of JCV in the brain and the archetype II-S type in the kidney. Multiple types of RRs can be detected in all organs in PML patients as well as in HIV-positive and HIV-negative patients without PML. However, HIV-negative patients had fewer RR variations detected in only two organs, indicating that immunosuppression most likely enhanced the rearrangements in the RR variations detected in multiple organs in the HIV-positive groups both with and without PML.

Our results confirm and expand the results of previous studies showing the presence of JCV DNA in the brains of individuals without PML (4, 8, 25, 27). We have performed a comprehensive study of a large number of HIV-positive PML patients as well as HIV-positive and -negative individuals using several techniques to detect the presence of JCV DNA and protein in several organs. The JCV RRs in the brains of HIV-negative patients are of the I-S and I-R types, while spleens had the II-S type. Therefore, it is possible that primary infection with JCV is carried out with a mixture of virions harboring a variety of RR types. Thereafter, JCV with the II-S type of RR may preferentially establish latency in kidney epithelium cells, while JCV with the I-R and II-R RR types establishes latency in the brain. In the context of immunosuppression, JCV reactivates both in the brain and in the kidney, producing multiple forms of RRs in all organs.

Our findings of both JCV large T DNA and regulatory region DNA in the brains of individuals without PML demonstrate that JCV is latent in the brains of patients without HIV or PML. In these people, the large T Ag is sometimes expressed but the viral capsid protein VP1 is not. It is not clear if JCV first enters the central nervous system during primary infection. Further studies are needed to show whether the latent JCV strains present in the brain can reactivate under immunosuppression and cause PML. Alternatively, PML may also result from reactivated extraneural JCV strains, which then cross the blood-brain barrier. In conclusion, by demonstrating the presence of JCV DNA in the brains of patients without PML, we have gained new insights into JCV latency, compartmentalization, and reactivation. A better understanding of JCV latency in the brain will help in devising strategies to prevent its reactivation in HIV-infected patients and those treated with immunomodulatory medications.

ACKNOWLEDGMENTS

We are grateful to Susan Morgello, Benjamin B. Gelman, H. Aaron Aronow, Elyse Singer, and Deborah Commins for providing PML samples through the National NeuroAIDS Tissue Consortium (NNTC).

The NNTC is supported by grants R24MH59724, R24NS38841, R24MH59745, and R24MH59656 from the NIH. We acknowledge NIH grants R01 NS 041198, R01 NS 047029, and K24 NS 060950 to I.J.K., the Harvard Medical School Center for AIDS Research (CFAR), an NIH-funded program (grant P30 AI60354), NIH grant K08 NS 064215-01A1 to C.S.T., and NIH grants T32 AI007245-26 and -27 to L.C.E.

REFERENCES

1. Reference deleted.
2. **Atwood, W. J., K. Amemiya, R. Traub, J. Harms, and E. O. Major.** 1992. Interaction of the human polyomavirus, JCV, with human B-lymphocytes. Virology **190:**716–723.
3. **Buckle, G. J., M. S. Godec, J. U. Rubi, C. Tornatore, E. O. Major, C. J. Gibbs, Jr., D. C. Gajdusek, and D. M. Asher.** 1992. Lack of JC viral genomic sequences in multiple sclerosis brain tissue by polymerase chain reaction. Ann. Neurol. **32:**829–831.
4. **Caldarelli-Stefano, R., L. Vago, E. Omodeo-Zorini, M. Mediati, L. Losciale, M. Nebuloni, G. Costanzi, and P. Ferrante.** 1999. Detection and typing of JC virus in autopsy brains and extraneural organs of AIDS patients and non-immunocompromised individuals. J. Neurovirol. **5:**125–133.
5. **Carson, K. R., A. M. Evens, E. A. Richey, T. M. Habermann, D. Focosi, J. F. Seymour, J. Laubach, S. D. Bawn, L. I. Gordon, J. N. Winter, R. R. Furman, J. M. Vose, A. D. Zelenetz, R. Mamtani, D. W. Raisch, G. W. Dorshimer, S. T. Rosen, K. Muro, N. R. Gottardi-Littell, R. L. Talley, O. Sartor, D. Green, E. O. Major, and C. L. Bennett.** 2009. Progressive multifocal leukoencephalopathy after rituximab therapy in HIV-negative patients: a report of 57 cases from the Research on Adverse Drug Events and Reports project. Blood **113:**4834–4840.
6. **Chesters, P. M., J. Heritage, and D. J. McCance.** 1983. Persistence of DNA sequences of BK virus and JC virus in normal human tissues and in diseased tissues. J. Infect. Dis. **147:**676–684.
7. **Delbue, S., E. Branchetti, R. Boldorini, L. Vago, P. Zerbi, C. Veggiani, S. Tremolada, and P. Ferrante.** 2008. Presence and expression of JCV early gene large T antigen in the brains of immunocompromised and immunocompetent individuals. J. Med. Virol. **80:**2147–2152.
8. **Elsner, C., and K. Dorries.** 1992. Evidence of human polyomavirus BK and JC infection in normal brain tissue. Virology **191:**72–80.
9. **Gheuens, S., G. Pierone, P. Peeters, and I. J. Koralnik.** 2010. Progressive multifocal leukoencephalopathy in individuals with minimal or occult immunosuppression. J. Neurol. Neurosurg. Psychiatry **81:**247–254.
10. **Grinnell, B. W., B. L. Padgett, and D. L. Walker.** 1983. Distribution of nonintegrated DNA from JC papovavirus in organs of patients with progressive multifocal leukoencephalopathy. J. Infect. Dis. **147:**669–675.
11. **Jensen, P. N., and E. O. Major.** 2001. A classification scheme for human polyomavirus JCV variants based on the nucleotide sequence of the noncoding regulatory region. J. Neurovirol. **7:**280–287.
12. **Kitamura, T., Y. Aso, N. Kuniyoshi, K. Hara, and Y. Yogo.** 1990. High incidence of urinary JC virus excretion in nonimmunosuppressed older patients. J. Infect. Dis. **161:**1128–1133.
13. **Kleinschmidt-DeMasters, B. K., and K. L. Tyler.** 2005. Progressive multifocal leukoencephalopathy complicating treatment with natalizumab and interferon beta-1a for multiple sclerosis. N. Engl. J. Med. **353:**369–374.
14. **Koralnik, I. J.** 2006. Progressive multifocal leukoencephalopathy revisited: has the disease outgrown its name? Ann. Neurol. **60:**162–173.
15. **Koralnik, I. J., D. Boden, V. X. Mai, C. I. Lord, and N. L. Letvin.** 1999. JC virus DNA load in patients with and without progressive multifocal leukoencephalopathy. Neurology **52:**253–260.
16. **Korman, B. D., K. L. Tyler, and N. J. Korman.** 2009. Progressive multifocal leukoencephalopathy, efalizumab, and immunosuppression: a cautionary tale for dermatologists. Arch. Dermatol. **145:**937–942.
17. **Langer-Gould, A., S. W. Atlas, A. J. Green, A. W. Bollen, and D. Pelletier.** 2005. Progressive multifocal leukoencephalopathy in a patient treated with natalizumab. N. Engl. J. Med. **353:**375–381.
18. **Markowitz, R. B., H. C. Thompson, J. F. Mueller, J. A. Cohen, and W. S. Dynan.** 1993. Incidence of BK virus and JC virus viruria in human immunodeficiency virus-infected and -uninfected subjects. J. Infect. Dis. **167:**13–20.
19. **Marzocchetti, A., M. Sanguinetti, S. D. Giambenedetto, A. Cingolani, G. Fadda, R. Cauda, and A. De Luca.** 2007. Characterization of JC virus in

cerebrospinal fluid from HIV-1 infected patients with progressive multifocal leukoencephalopathy: insights into viral pathogenesis and disease prognosis. J. Neurovirol. **13:**338–346.

19a. **Molloy, E. S., and L. H. Calabrese.** 2009. Therapy: targeted but not trouble-free: efalizumab and PML. Nat. Rev. Rheumatol. **5:**418–419.

20. **Perez-Liz, G., L. Del Valle, A. Gentilella, S. Croul, and K. Khalili.** 2008. Detection of JC virus DNA fragments but not proteins in normal brain tissue. Ann. Neurol. **64:**379–387.

21. **Randhawa, P., R. Shapiro, and A. Vats.** 2005. Quantitation of DNA of polyomaviruses BK and JC in human kidneys. J. Infect. Dis. **192:**504–509.

22. **Ryschkewitsch, C., P. Jensen, J. Hou, G. Fahle, S. Fischer, and E. O. Major.** 2004. Comparison of PCR-Southern hybridization and quantitative real-time PCR for the detection of JC and BK viral nucleotide sequences in urine and cerebrospinal fluid. J. Virol. Methods **121:**217–221.

23. **Stoner, G. L., C. F. Ryschkewitsch, D. L. Walker, D. Soffer, and H. D. Webster.** 1986. Immunocytochemical search for JC papovavirus large T-antigen in multiple sclerosis brain tissue. Acta Neuropathol. **70:**345–347.

23a. **Tan, C. S., and I. J. Koralnik.** 2010. Progressive multifocal leukoencephalopathy and other disorders caused by JC virus: clinical features and pathogenesis. Lancet Neurol. **9:**425–437.

24. **Tan, C. S., B. J. Dezube, P. Bhargava, P. Autissier, C. Wuthrich, J. Miller, and I. J. Koralnik.** 2009. Detection of JC virus DNA and proteins in the bone marrow of HIV-positive and HIV-negative patients: implications for viral latency and neurotropic transformation. J. Infect. Dis. **199:**881–888.

25. **Vago, L., P. Cinque, E. Sala, M. Nebuloni, R. Caldarelli, S. Racca, P. Ferrante, G. Trabottoni, and G. Costanzi.** 1996. JCV-DNA and BKV-DNA in the CNS tissue and CSF of AIDS patients and normal subjects. Study of 41 cases and review of the literature. J. Acquir. Immune Defic. Syndr. Hum. Retrovirol. **12:**139–146.

26. **Van Assche, G., M. Van Ranst, R. Sciot, B. Dubois, S. Vermeire, M. Noman, J. Verbeeck, K. Geboes, W. Robberecht, and P. Rutgeerts.** 2005. Progressive multifocal leukoencephalopathy after natalizumab therapy for Crohn's disease. N. Engl. J. Med. **353:**362–368.

27. **White, F. A., III, M. Ishaq, G. L. Stoner, and R. J. Frisque.** 1992. JC virus DNA is present in many human brain samples from patients without progressive multifocal leukoencephalopathy. J. Virol. **66:**5726–5734.

28. **Wuthrich, C., X. Dang, S. Westmoreland, J. McKay, A. Maheshwari, M. P. Anderson, A. H. Ropper, R. P. Viscidi, and I. J. Koralnik.** 2009. Fulminant JC virus encephalopathy with productive infection of cortical pyramidal neurons. Ann. Neurol. **65:**742–748.

29. **Wuthrich, C., S. Kesari, W. K. Kim, K. Williams, R. Gelman, D. Elmeric, U. De Girolami, J. T. Joseph, T. Hedley-Whyte, and I. J. Koralnik.** 2006. Characterization of lymphocytic infiltrates in progressive multifocal leukoencephalopathy: co-localization of CD8(+) T cells with JCV-infected glial cells. J. Neurovirol. **12:**116–128.

30. **Yogo, Y., T. Iida, F. Taguchi, T. Kitamura, and Y. Aso.** 1991. Typing of human polyomavirus JC virus on the basis of restriction fragment length polymorphisms. J. Clin. Microbiol. **29:**2130–2138.